GAS PHASE CHEMISTRY MECHANISMS FOR AIR QUALITY MODELING: GENERATION AND APPLICATION TO CASE STUDIES

THÈSE N^{O} 2936 (2004)

PRÉSENTÉE À LA FACULTÉ ENVIRONNEMENT NATUREL, ARCHITECTURAL ET CONSTRUIT

Institut des sciences et technologies de l'environnement

SECTION DES SCIENCES ET INGÉNIERIE DE L'ENVIRONNEMENT

ÉCOLE POLYTECHNIQUE FÉDÉRALE DE LAUSANNE

POUR L'OBTENTION DU GRADE DE DOCTEUR ÈS SCIENCES TECHNIQUES

PAR

Martin JUNIER

ingénieur du génie rural diplômé EPF
de nationalité suisse et originaire de Saint-Aubin-Sauges (NE)

acceptée sur proposition du jury:

Dr A. Clappier, Dr F. Kirchner, directeurs de thèse
Dr B. Aumont, rapporteur
Prof. I. Bey, rapporteur
Dr R. Vautard, rapporteur

Lausanne, EPFL
2004

Résumé

Dès la deuxième moitié du XX^{ième} siècle, la pollution de l'air devient un problème majeur de santé publique et de protection de l'environnement dans toutes les grandes villes de la planète. Les polluants photochimiques comme l'ozone — qui est aujourd'hui l'un des principaux polluants de l'air dans la troposphère — sont formés dans l'atmosphère par réaction de deux précurseurs émis (par les activités humaines ou de façon naturelle): les Composés Organiques Volatiles (COV) et les NO_x ($NO + NO_2$). La formation d'ozone nécessite de nombreuses réactions qui en font un processus hautement non linéaire. La réduction de la concentration d'ozone consécutive à une diminution des émissions de l'un de ces précurseurs n'est donc pas prévisible sans l'aide d'un modèle numérique de pollution photochimique. La simulation de la pollution photochimique nécessite un système chimique détaillé et beaucoup de temps de calcul. Le nombre d'espèces chimiques dans un mécanisme doit donc être réduit au strict minimum afin d'optimiser le temps de calcul. Une solution consiste à regrouper le très grand nombre de COV impliqués dans la pollution atmosphérique en un petit nombre d'espèces dans le système chimique, tout en gardant suffisamment de détails pour générer des résultats précis dans un temps raisonnable. Le calcul de toutes les données cinétiques d'un système chimique est une tâche immense qui doit être accompli par un programme informatique. CHEMATA, présenté dans ce travail, est un programme de génération de mécanismes chimiques pour la chimie atmosphérique en phase gazeuse. Sur la base du mécanisme RACM (mécanisme de chimie atmosphérique en troposphère pour des conditions propres ou polluées), CHEMATA a généré un système étendu pour tester la paramétrisation des carbonyles dans RACM et deux mécanismes plus petits pour en comparer les méthodes de regroupement des espèces chimiques (le mécanisme réduit et le petit mécanisme). Les trois nouveaux systèmes et RACM ont été implémentés dans un *box model* et dans le modèle eulérien tridimensionnel de qualité de l'air TAPOM, aussi présenté dans ce travail. TAPOM a tourné avec les quatre mécanismes chimiques sur trois domaines (Mexico City, Milan et Bogota) présentant différentes émissions et des conditions météorologiques différentes. Les comparaisons entre les quatre systèmes, avec le *box model* ou en 3D, avec ou sans réduction d'émission ont mené aux conclusions suivantes:

- La comparaison du mécanisme étendu et de RACM montre que le traitement des carbonyles dans RACM n'induit pas d'erreur significative à mésoéchelle. L'utilisation du mécanisme étendu devrait être confiné aux cas où une précision accrue des COV est nécessaire ou pour des simulations dépassant 2 ou 3 jours.

- Le mécanisme réduit est le meilleur compromis entre le temps de calcul et la précision des résultats. Ce mécanisme peut faire gagner beaucoup de temps lors de simulations de pollution photochimique ou de scénarios de réduction d'émissions.
- Le petit mécanisme présente une tendance claire à produire des résultats plus « sensibles aux COV », ce qui peut conduire à de graves surestimations des concentrations d'ozone. Il devrait être gardé pour des simulations qualitatives, quand le temps de calcul est un facteur déterminant.

Abstract

During the last few decades, air pollution has become one of the major environmental and public health issue in every important cities over the world. Photochemical pollutants, like ozone which play a central role in today's air pollution problems, are formed in the atmosphere by reaction of two emitted precursors: Volatile Organic Carbons (VOCs) and NO_x ($NO + NO_2$). Ozone is a highly non linear process because its formation is driven by complex chain reactions. The decrease of ozone concentration produced by a reduction of its emitted precursors is therefore unpredictable, unless calculated by numerical photochemical models. The simulation of photochemical air pollution requires detailed chemical mechanisms and a lot computer resources. The number of chemical species within the chemical mechanism has to be confined to the strict minimum in order to minimise the CPU time. A solution is to lump the immense number of VOC species involved in atmospheric pollution in a convenient smaller number of mechanism species, keeping enough details to generate accurate results in reasonable calculations times. The calculation of all kinetic data of a lumped mechanism is a tremendous work unless carried out by a generation programme. CHEMATA, presented in this work, is a chemical mechanisms generation programme designed to create lumped and explicit tropospheric gas phase chemical mechanisms. Based on the widely used mechanism RACM, CHEMATA generated an extended mechanism to test the carbonyl species parameterisation of RACM and two smaller mechanisms to compare two lumping methods (the reduced mechanism and the small mechanism). The new mechanisms have been implemented in a box model and in the 3D eulerian air quality model TAPOM, also presented in this work. TAPOM have been run with the four chemical mechanisms on three simulations domains (Mexico City, Milan and Bogota) presenting different emissions strengths and meteorological conditions. The comparisons between the different mechanisms, in a box or 3D model and with or without emission reductions lead to the following conclusions:

- The comparison between the extended mechanism and RACM shows that the treatment of the carbonyl species in RACM does not induce notable errors in mesoscale modelling. The use of the extended mechanism should be kept for special simulations when enhanced precision in VOCs is required or for time periods longer than 2 or 3 days.
- The reduced mechanism is the best compromise between CPU time and accuracy. When calculating photochemical pollution, or emission reduction scenarios, this mechanism can save a lot of time.

- The small mechanism presents a clear tendency to produce more "VOC sensitive" results, which can lead to severe ozone overestimations. It should only be used for qualitative simulation when CPU time is a critical issue.

Acknowledgements

I would like to thank here Prof. Hubert van den Bergh for his excellent lectures in air pollution which, made me choose his laboratory for my diploma work and to carry on with this PhD. I am also grateful to Dr. Alain Clappier and Dr. Frank Kirchner for their scientific support and encouragements. My thanks go as well to the jury for taking the time to read this work, and for their numerous comments.

Funding

This work has been funded by the
Swiss National Science Foundation,
Project No.: 2169-063989

Table of contents

Chapter One

Chapter Two

Chapter Three

Chapter Four

Chapter Five

Chapter Six

Appendix

Chapter One

Introduction

During the 20th century, atmospheric pollution grew with the increase of industrialisation, and soon became one of the most important environmental and public health concern. Air pollutants are of two important classes, the primary pollutants (directly emitted by human activities or natural processes) and the secondary pollutants (formed in the atmosphere by various chemical reactions). The accumulation of primary pollutants can lead to very dangerous pollution peaks. The Great London Smog in December 1952 (leading to over 4'000 deaths) is one of the most impressive instance of air pollution episode. Although measures have been adopted to avoid such peaks of primary pollution, the background concentrations have continued to grow with human activity.

The emitted pollutants can react in the atmosphere forming secondary pollutants. During the day, the light is a key element of the atmospheric chemistry. High concentrations of such secondary mixture are called photochemical smog, in order to be distinguished from primary pollutant peaks like the Great London Smog. Among photochemical pollutants, ozone is an important representative, formed by a very complex reaction chain beginning with two general precursors: volatile organic compounds and two nitrogen oxides: NO and NO_2. (VOCs and NO_x). Both precursors are emitted by human activities (industries, traffic, heating etc.). Air quality management must therefore be focused on emissions abatement strategies. A good understanding of the processes leading to secondary photochemical pollutants is the key to efficient emissions control, requiring appropriate tools such as numerical air quality models.

The modelling of atmospheric pollution needs the calculation of many physical atmospheric parameters (temperature, humidity, wind speed and direction...) and of lots of chemical reactions. There are hundreds of reactive chemical species in the atmosphere, a comprehensive simulation would involve thousands of reactions. A calculation including all the reactions would also imply the exact knowledge of all the atmospheric chemistry, which one does not have. The simulations are therefore based on chemical mechanisms that are simplified representations of the atmospheric chemistry. A typical chemical mechanism simulating the photochemical smog includes 50-100 species and 100-200 equations.

Ozone is one of the main constituent of the photochemical smog. Because of its effects on health and crop yields, it has been intensively studied and is still of primary concern. In the early 1970s, the first mechanisms were optimised to simulate reasonably the evolution of ozone concentrations in urban areas. For example, Reynolds et al. (1973, 1974) designed a model for the study of the Los Angeles air basin. The gas phase chemical mechanism included 11 species involved in 15 equations. At this time, the model performance were severely restricted by the lack of observational data (for emissions inventories and model evaluation) and of computer power and memory.

Nowadays, storage devices with tens of gigabytes are available and affordable so memory is not a problem any more. But if today's computers are much faster, efficiency is still an everyday struggle for air pollution model designers. Models include more complete treatment of physical and chemical atmospheric processes (like chemical mechanisms with over 70 species and 200 equations). The spatial scale has also grown from the urban to the regional area, which implies bigger domains of simulation, more grid cells and therefore more computational requirement. Moreover, the need of new features like aerosol dynamics, high resolution modelling or fast response forecasting requires even more computer power. An efficient way to spare computer time is to confine to the strict minimum the number of chemical species within the chemical

mechanism. Simplification of the chemistry is focused on the huge number of reactive organic compounds. Different types of chemical mechanisms have been developed.

- In *lumped* mechanisms, species are grouped into classes of similar structure and reactivity. For example all alkanes (C_nH_{2n+2}) react with OH in a similar way to form alkyl radicals (C_nH_{2n+1}). By lumping the alkanes into a single group, the several tens of compounds and several hundreds of reactions involved can be reduced to one reaction and two organic species. This represents an immense saving of computational time.
- The *carbon bond* mechanism splits each molecule into functional groups, assuming that the reactivity of a molecule is driven by its functional groups.
- *Surrogate* mechanisms uses one or two compounds in each group to represent the chemistry of the group.

Lumping VOC species into a mechanism of reasonable size is a balance between chemical detail and computational time. For every species and reaction a large number of data must be available: reaction rate constants, product yields, emission rates and reactivity. This implies that a lumped chemical mechanism should be regenerated for each new case and for every different emission inventory. The CHEmical Mechanism Adaptation to Tropospheric Application program is able to generate explicit and lumped gas phase mechanisms, given a list of species and their sources, kinetic data and lumping group definition.

This work investigates the dependence of air quality model's results on the level of detail of various chemical mechanisms generated by CHEMATA. The mechanisms are implemented in the mesoscale eulerian air quality model TAPOM (Transport and Atmospheric POllution Model). Both programmes are detailed in Chapter Two.

RACM, a widely used mechanism, is the base for the generation by CHEMATA of three new chemical mechanisms of different sizes. Chapter Three presents the new chemical mechanisms and a box model study on the differences they generate on simulation results.

The four mechanisms are implemented in TAPOM. The chemical results and the time needed by the computer to complete the calculation are compared in Chapter Four, in order to find the best compromise between time and mechanism detail.

Because of the complexity of the chemical process leading to photochemical pollution, it is not clear if using less detailed mechanisms for abatement strategies studies would give reliable information. Moreover, the reaction of the chemical mechanisms can vary when used on different calculation domains. Chapter Five presents a study of the reaction of the four mechanisms to emissions reduction strategies on three different domains.

Finally, Chapter Six will conclude and propose further work.

Chapter Two

TAPOM and CHEMATA

1. TAPOM

The Transport and Air POllution Model (TAPOM) simulates the evolution of the pollutants in the atmosphere. It is based on the resolution of the mass balance equation for several atmospheric substances. This equation take into account the advection by the mean wind (Adv), the vertical diffusion by the turbulence (Dif), the chemical transformation by several reactions (Chem), the dry deposition (DD) and the emissions (Emi). The mass balance equations solved in TAPOM is the following :

$$\frac{\partial \rho Q_P}{\partial t} + Adv = Dif + Chem + DD + Emi$$

where Q_P is the mixing ratio of the pollutant P, ϱ is the air density, and Adv, Dif, Chem, DD and Emi are the contributions of the advection, diffusion, chemistry, dry deposition and emissions.

1.1. Time discretisation.

The mass conservation equation is solved using the time splitting method of Marchuk (1975). With this method each contribution is treated independently:

$$\rho Q_P^{I} - \rho Q_P^{n} = -\Delta t \cdot Adv$$
$$\rho Q_P^{II} - \rho Q_P^{I} = \Delta t \cdot Dif$$
$$\rho Q_P^{III} - \rho Q_P^{II} = \Delta t \cdot DD$$
$$\rho Q_P^{IV} - \rho Q_P^{III} = \Delta t \cdot Emi$$
$$\rho Q_P^{V} - \rho Q_P^{IV} = 2\Delta t \cdot Chem$$
$$\rho Q_P^{VI} - \rho Q_P^{V} = \Delta t \cdot Emi$$
$$\rho Q_P^{VII} - \rho Q_P^{VI} = \Delta t \cdot DD$$
$$\rho Q_P^{VIII} - \rho Q_P^{VII} = \Delta t \cdot Dif$$
$$\rho Q_P^{n+1} - \rho Q_P^{VIII} = -\Delta t \cdot Adv$$

where Q_P^{n} and Q_P^{n+1} are the mixing ratios at time n and n+1, Δt is the time step and Q_P^{I}, Q_P^{II}, …, Q_P^{VIII} are intermediate calculation steps.

1.2. Spatial discretisation.

1.2.1. Mesh

The spatial discretisation is treated using the finite volume method. With this method the simulation domain is divided in elementary volumes. In TAPOM each volume has 6 sides and is based on 8 corner points. These points can be chosen by the users in order to produce any kind of mesh. The mesh which is currently use for mesoscale air quality simulation follows the topography at ground level and has a flat surface at the top (see Figure 1).

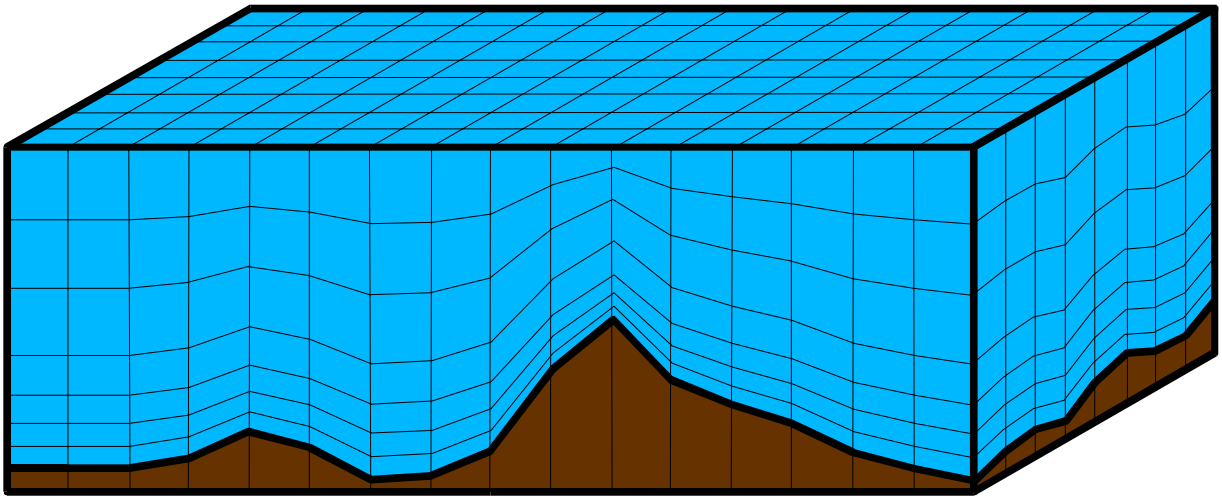

Figure 1: Schematic representation of the most commonly used mesh in TAPOM.

1.2.2. Diffusion

The diffusion and the advection steps are solved by descritisation on the mesh.

The equation for the diffusion contribution is :

$$Dif = \vec{\nabla}\left(K\vec{\nabla}Q\right)$$ where K is the turbulent diffusion coefficient.

With the finite volume method the discretisation is obtained by integration of equation on each mesh cell. The diffusion contribution term becomes :

$$Dif = \frac{1}{V}\int_V \vec{\nabla}\left(K\vec{\nabla}Q\right)dV$$ where V is the volume of the cell.

Using the Gauss formula the diffusion contribution term can be calculated with the mass fluxes crossing the volume surfaces, it gives :

$$Dif = \frac{1}{V}\int_S K\vec{\nabla}Q\cdot\vec{n}\,dS$$ where S the cell surfaces and $\vec{n}$ the surface normal.

For mesoscale air quality simulation the horizontal cell dimension are usually much larger (few km) than the vertical one. Consequently, in TAPOM, the horizontal component of the gradient are neglected. Finally, the discretisation of the diffusion contribution is as follow:

$$Dif = \frac{1}{V_k}\left[K_{k+1/2}S^3_{k+1/2}\frac{\left(Q_{k+1}-Q_k\right)}{\Delta z_{k+1/2}} - K_{k-1/2}S^3_{k-1/2}\frac{\left(Q_k-Q_{k-1}\right)}{\Delta z_{k-1/2}}\right]$$

where Q_k , Q_{k-1} and Q_{k+1} are average mixing ratio at levels k, k-1 and k+1.

V_k is the cell volume at the level k.

$S^3_{k-1/2} = S_{k-1/2}.n^3_{k-1/2}$ with $n^3_{k-1/2}$ the vertical component of the normal to the horizontal cell surfaces k-1/2 (likewise for k+1/2)

$K_{k-1/2}$ is the turbulent diffusion coefficient at the side k-1/2.

$\Delta z_{k-1/2}$ is the distance between the cell centre k and k-1.

1.2.3. Advection

The advection term is treated in a similar way than the diffusion term. The equation for the advection term is :

$Adv = \vec{\nabla}\,\vec{U}\,\rho Q$ where $\vec{U}$ is the average wind velocity.

The advection term is integrated on each cell :

$$Adv = \frac{1}{V}\int_V \vec{\nabla}\,\vec{U}\,\rho Q dV$$

And the fluxes crossing the cell sides are obtained using the Gauss formula :

$$Adv = \frac{1}{V}\int_S \vec{U}\cdot\vec{n}\,\rho Q dS$$

The advection is solved in the three directions, each direction being treated independently using the time splitting method of Marchuck (1975). In one direction the discretisation of the advection term gives :

$$Adv = \frac{1}{V_i}\left[\left(S\rho\,\vec{U}\cdot\vec{n}\right)_{i+1/2}\cdot Q_{i+1/2} - \left(S\rho\,\vec{U}\cdot\vec{n}\right)_{i-1/2}\cdot Q_{i-1/2}\right]$$

where $\left(S\rho\,\vec{U}\cdot\vec{n}\right)_{i+1/2}$ is the air mass flux in kgs^{-1} crossing the side i+1/2 and $Q_{i-1/2}$ is the mixing ratio at the cell sides i-1/2.

The mixing ratio at the cell sides, $Q_{i-1/2}$ and $Q_{i+1/2}$ are interpolated from the mixing ratio at the cell centres Q_i, Q_{i-1} and Q_{i+1}, using the Piecewise Parabolic Method (PPM) developed by Collela and Woodward (1984).

1.2.4. Dry deposition

The dry deposition is calculated in the lowest layer (k=1).

$$DD = v\frac{S_{k=1}\cdot Q_{k=1}}{V_{k=1}}$$

where $S_{k=1}$ is the horizontal surface of the cells at the ground level,
$Q_{k=1}$ is the mixing ratio at ground level,
$V_{k=1}$ is the cell volume,
ν is the dry deposition velocity.

The dry deposition velocity is calculated with the resistance analogy and is the inverse value of the three resistances in series, the aerodynamic resistance (Ra), the boundary layer resistance (Rb), and the surface resistance (Rc). Ra and Rb depend only on meteorological parameters. They are expressed as a function of the wind velocity, friction velocity and the Monin-Obukhov length according to Bussinger et al. (1971) and Wesely and Hicks (1977). Rc depends on the chemical species and on the surface on which they deposit (landuse and roughness).

1.3. Chemical solver

The chemical step $\varrho Q_P^V - \varrho Q_P^{IV} = 2\Delta t \cdot \mathrm{Chem}$ is treated in a specific module for the simulation of homogeneous reactions of atmospheric gaseous constituents. The chemical reaction equations can be defined in a text file and read by a chemical interpreter. The outputs of the chemical mechanisms generation programme CHEMATA (presented in § 2) can directly be read by this interpreter. Chemical reaction schemes therefore can be changed rapidly by creating or editing this text file. The module uses the method of Gong and Cho (1993) for solving the chemical system. This method distinguishes between slow and rapid species. The slow species are integrated using an explicit integration step and the fast ones are integrated by a fully implicit integration procedure. The solving procedure is as follows:

1. Calculate the mixing ratio of the slow species at time t+1 with an explicit time step:

   $$Q_S^* = Q_S^{IV} + \mathrm{Chem}\left(Q_S^{IV}, Q_F^{IV}\right) \cdot 2\,\Delta t$$

   where Q_S^{IV} is the vector of the slow species mixing ratio at step IV and Q_F^{IV} is the vector of the fast species mixing ratio at step IV.

2. Calculate the mixing ratio of the fast species fully implicitly (involving an iterative procedure), using the mixing ratio in step (1).

   The equation $Q_F^V = Q_F^{IV} + \mathrm{Chem}\left(Q_S^*, Q_F^V\right)$ can be solved with an iterative Newton-Raphson procedure :

$$Q^{V}_{Fk+1} = Q^{V}_{Fk} - \left[\mathbf{1} - \frac{\partial\, Chem\left(Q^{*}_{S}, Q^{V}_{Fk}\right)}{\partial\, Q^{V}_{Fk}} \right]^{-1} \cdot \left[Q^{V}_{Fk} - Q^{IV} - Chem\left(Q^{*}_{S}, Q^{V}_{Fk}\right) \right]$$

where Q^{V}_{Fk+1} is the k[th] estimation of the mixing ratio vector of fast species at step V and **1** is the unity matrix.

3. Recalculate the mixing ratio of the slow species using the mixing ratio of the fast ones obtained by step (2):

$$Q^{*}_{S} = Q_{S\,IV} + Chem\left(Q^{IV}_{S}, Q^{V}_{F}\right) \cdot 2\,\Delta t$$

1.4. Required parameters

Boundary and initial conditions for each chemical species have to be specified by the user as input to TAPOM. These data can come from *in situ* measurements or from a larger scale model. A number of meteorological parameters have to be calculated by a meteorological simulation. The mean wind velocity and turbulent diffusion coefficient are used for the advection and diffusion calculation, the friction velocity and Monin-Obukhov length for the dry deposition calculation, the temperature and pressure for the chemical reaction rate constant. The photolysis rate constants needed in the photochemical reactions, are calculated with the TUV solar radiation module by Madronich and Flocke (1999).

2. CHEMATA

Chemical mechanisms for calculation of atmospheric chemistry exist since the 1970's in numerous photochemical models. A lot of such mechanisms have been developed and their results are not always similar. Comparing various gas phase chemical mechanisms is not simple because of their different structures. Differences between mechanisms can generate errors that are likely to compensate each other, making them impossible to be detected by a simple comparison. Inorganic chemistry is always treated explicitly and do not vary so much from one

mechanism to another, but organic chemistry can not be treated explicitly in 3D models. A complete explicit mechanism would need thousands of equations and the calculation time would be prohibitive for 3D calculations. The differences between various mechanisms come from the way the number of the volatile organic compounds is reduced. Listed below are examples of solutions for reducing chemical mechanisms:

- Use of only the most important VOC species for the studied region and specific case. All other species are not taken into account (Carslaw, 1999a, 1999b).
- Choice of surrogate species for each class of VOC, as in EMEP (Simpson et al. 1993).
- Split of the VOC compounds by carbon bond and functional group, as in the carbon bond mechanism (Gery et al., 1989).
- Grouping of one VOC class' molecules into one lumped species using as kinetic data and product yield a weighted average of the data of the molecules in that class (RACM, Stockwell et al., 1997, SAPRC, Carter, 2000).

Grouping VOCs into lumped species allows to keep more information in the lumped mechanism than with the other approaches. But the available lumped mechanisms are calculated with average VOC splits which most of the time differ from the local split of the calculated domain. Recalculating all kinetic data and production yields for the local conditions is an enormous task if not accomplished with a mechanism generation programme. The chemical mechanism generation programme CHEMATA (CHEmical Mechanism Adaptation to Tropospheric Applications) presented hereafter also allows the user to make quick updates when new kinetic data is available and to investigate the sensitivity of the generated mechanisms to different lumping choices.

This ability to generate lumped mechanisms which only differ by the number of VOC species (the manner in which the lumping is defined), has made possible the comparison of the four mechanisms presented in the following chapters.

2.1. Generating lumped mechanisms.

Generating lumped mechanism consists of defining groups of *real species* (really existing in the atmosphere) which will be considered as one *mechanism species*. Every mechanism species will react with the same reactants as the real species do in the atmosphere. VOC species' reactions lead to the formation of various products, following the general equation:

$$VOC_i + X \xrightarrow{k_i^x} \alpha_i^1 P^1 + \alpha_i^2 P^2 + \ldots + \alpha_i^j P^j + \ldots + \alpha_i^J P^J$$

where VOC_i is a real species, X is a reactant (often OH radical), k_i^x is the rate constant of the reaction of VOC_i with X, the α_i^j are the yield coefficients of the products P^j.

Following this notation, the reaction of a group of VOC lumped into the mechanism species L can be described by the equation:

$$L + X \xrightarrow{k_L^x} a_L^1 P^1 + a_L^2 P^2 + \ldots + a_L^j P^j + \ldots + a_L^J P^J$$

where the rate constant k_L^x is calculated by

$$k_L^X = \frac{\sum_{i=1}^{I(L)} \left(VOC_i \cdot k_i^X \right)}{\sum_{i=1}^{I(L)} VOC_i}$$

where I(L) is the number of real VOC species lumped in the mechanism species L. k_L^x is an average of the k_i^x weighted by the strength of the sources of the real species. Sources of real species can be emissions or production in the atmosphere.

The product yields are calculated in a similar way:

$$a_L^i = \frac{\sum_{i=1}^{I(L)} \left(Agg_i \cdot VOC_i \cdot \alpha_i^j \right)}{\sum_{i=1}^{I(L)} \left(Agg_i \cdot VOC_i \right)}$$

with

$$Agg_i = \frac{1 - \exp\left(-k_i^X \cdot \int_0^t [X]dt\right)}{1 - \exp\left(-k_L^X \cdot \int_0^t [X]dt\right)}$$

Agg_i is the aggregation factor of VOC_i. It is used as a weighting factor for the reactivity of the real species.

It comes out of these equations that the rate constant and the product yields of a lumped reaction depends on the sources strengths of the real species, the integrated concentration of the reactant X, and on the rate constants of the real species with X, which can be temperature and pressure dependent. These data obviously change from an area to an other. For the RACM mechanism (Stockwell et al., 1997), the sources strengths were taken from emissions inventories, the product yields were calculated using kinetic data for 298 K and 1.013 x 10^5 Pa and the integrated reactant concentration were calculated for OH with 2-3 days model simulations. If the conditions of the modelling domain are really different from those used to generate the chemical mechanism, it should be recalculated.

In order to generate the lumped equations, CHEMATA calculates the following data:

- kinetic data for all considered real species (rate constants k_i and product yields α_i),
- the correct lumping group for all reactant and products,
- the amount of secondary VOC that will be considered as reactants, following its degradation process.

The programme therefore needs the following input data:

- the list of real species to be considered in the mechanism,
- the temperature, pressure and the integrated OH concentration of the modelling area (which must be estimated, being unknown before modelling),
- emission data.

2.2. What does CHEMATA do ?

2.2.1. Calculation of real species' reactions

Structure of organic molecules

To describe the chemical structures of the input species, the user gives a list of emitted species. For each chemical compound, the list contains its name, its chemical structure, and the kinetic data associated to OH, NO_3 and O_3.

CHEMATA converts the species' structure into a code. For each molecule, code numbers are given to every atom or group of atom. It contains information about the atom itself and the way it is bonded to its neighbours. This code also allows to describe the relationships between every atom with all other atoms in the molecule. Two atoms are considered chemically equivalent if their relations to all other atoms in the molecule are the same. The data once calculated for one atom will be assigned to all atoms that will be found chemically equivalent.

Calculation of the products' structure

CHEMATA calculates the reactions of VOC with OH, NO_3 and O_3, the photolysis reactions and, for peroxy nitrates, the thermal decomposition. For instance, the reaction with OH can abstract a hydrogen atom or add to a double bond, finally resulting, under atmospheric condition, in a peroxy radical (by subsequent addition of an oxygen):

$$VOC + OH \rightarrow RO_2$$

To take these transformations into account, the code number of the affected atoms are modified accordingly to the reaction. RO_2 produced by reactions with VOCs continue to react. CHEMATA calculates the reactions of peroxy radicals with NO, NO_2, NO_3, HO_2 and other peroxy radicals. These reactions give various products that need the calculation of branching ratios ζ:

$$RO_2 + NO \rightarrow \zeta_1(RO + NO_2) + (1 - \zeta_1)RONO_2$$

$$RO_2 + NO_2 \rightarrow RO_2NO_2$$

$$RO_2 + NO_3 \rightarrow \zeta_2(RO + NO_2) + (1-\zeta_2)RONO_2 + O_2$$

$$RO_2 + HO_2 \rightarrow \zeta_3(ROOH + O_2) + (1-\zeta_3)(ROH + O_3)$$

$$RO_2 + R'CH_2O_2 \rightarrow \zeta_4(RO + R'CH_2O) + (1-\zeta_4)(ROH + R'CHO) + O_2$$

All the products' structures and branching ratios are calculated by CHEMATA. R and RO radicals are not treated as mechanism species. They are represented by the products of their reactions.

2.2.2. Kinetic parameters

Kinetic parameters like reaction rate constants, branching ratios and product yields are given to CHEMATA by the way of an input file. This file can easily be modified to update the mechanism or perform sensitivity analysis. If there is no data available for a molecule or radical, it is calculated from structure-reactivity relationships (Atkinson, 1994, Kwok and Atkinson, 1995, Aschmann and Atkinson, 1995, Kirchner and Stockwell, 1996, Neeb, 2000). The structure related rate constants, branching ratios and product yields are provided by another input file. Both methods can be mixed, for example if experimental data is not available for all temperatures.

2.2.3. Generating lumped species

Real species can be lumped using functional groups, chain length and reactivity. CHEMATA compares the definitions of the mechanism species with the code numbers of the real species and determines the correct lumping group. Then the lumped mechanism is generated considering the sources strengths (emission rates and atmospheric formation) of all real species. Lumped species may contain one or several VOC species. For example in RACM, formaldehyde is the only compound in the mechanism species HCHO. Species that have a group for themselves are of course excluded from other lumping groups. This means that despite its aldehyde function,

formaldehyde will not be added in the ALD mechanism species which contains real species with R-CHO functional groups.

A problem arises with multi functional species: in which mechanism species should be lumped a compound like HC(O)-CH_2-C(O)-CH(OH)-C(O)OH which contains an aldehyde function and a ketone function, is an hydroxy ketone and a higher acid? The proper lumping actually depends on the user's needs. From a chemical point of view, the aldehyde function is the most reactive and thus the molecule should be lumped into the ALD species. But if the user is more interested in the amount of formed acids, a grouping with other carboxylic acids may be a better choice.

The user can therefore define a priority lumping order for the different functional groups, reactivity and chain length. Moreover, a personal lumping scheme can also be defined with user preferences like, for example, the distance between two functional groups.

2.2.4. Source strength of primary VOC

Source strengths of primary VOC are given by emission rates. Emission inventories for 3D modelling usually do not contain all needed primary species for chemical mechanism generation. In addition, emission inventories usually give emission rates for groups of real species when rates for every species are needed. In order to complete the local emission inventory, a more detailed emission inventory can be used, which includes data for all real species but is compiled for another region (like the US-NAPAP inventory, Middleton et al., 1990). Missing emission rates are estimated with the following formula:

$$E_i^{local} = E_i^{global} \cdot \frac{E_G^{local}}{\sum_{i \in G} E_i^{global}}$$

where E are emission rates and G is the emission group of the local inventory to which the real species i belongs. The user must therefore provide both inventories as well as the definitions of the local inventory's emission groups.

2.2.5. Secondary VOC

Secondary VOC are formed in the atmosphere by chemical reactions of the emitted VOC. Secondary species are included in the mechanism if explicitly specified as input in the reactant list or if their production yields exceed a given threshold (in which case, they are added by CHEMATA to the reactant list).

The source strength of secondary VOC are calculated from the strength of the precursors (emission rates or already calculated secondary VOC), the product yields and the integrated radical concentration. The integrated radical concentration allows to consider the correct amount of reacting precursors for the integration time interval. Thus, the two sources of atmospheric VOC are consistent.

2.2.6. Explicit mechanisms

Species which are to be treated explicitly must be listed as one-element groups. The list can be given as input or can be made by the programme itself. All products which yields exceed a dedicated threshold are excluded from the lumping process and treated explicitly. In this case, the calculated products are also added to the reactant list. The thresholds defined for adding species in the one-element group list and the reactant list are independent.

2.2.7. Outputs

The main output of CHEMATA is the lumped or explicit chemical mechanism. The output format can be specified in order to fit with the user's need. A second output file collects the entire set of calculated data for all real species: rate constants, branching ratios, product yields, structure of reactant and products, lumping and emission group.

2.3. Restrictions and future work

CHEMATA is currently restricted to gas phase chemistry and to molecules including only C, H, O and N. The reactions are limited to photolysis, thermal decomposition and reactions with OH,

NO_3 and O_3. Development continues at the present time to make CHEMATA able to deal with all atoms and other phases than gas phase.

References

Aschmann, S. M. and Atkinson, R., 1995, Rate constants for the reactions of the NO_3 radical with alkanes at 296 ± 2 K, Atmospheric Environment, 29, pp. 2311-2316.

Atkinson R., 1994, Gas-phase tropospheric chemistry of organic compounds: a review, Journal of Physical Chemistry, Ref. Data, Monogr. 2, pp. 1-216.

Businger, J. A., Wyngaard J. C., Izumi Y., Bradley E. F., 1971, Flux-profile relationships in the atmospheric surface layer. Journal of the Atmospheric Sciences, Vol. 28, No. 2, pp. 181-189.

Carter, W. P. L., 2000, Documentation of the SAPRC-99 Chemical Mechanism for VOC Reactivity Assessment. Final Report to California Air Resources Board Contract No. 92-329 and 95-308.

Carslaw, N., Creasey, D. J., Heard, D. E., Lewis, A. C., McQuaid, J. B., Pilling, M. J., Monks, P. S., Bandy, B. J., Penkett, S. A., 1999a, Modeling OH, HO_2, and RO_2 radicals in the marine boundary layer - 1. Model construction and comparison with field measurements. Journal of Geophysical Research, Vol. 104, No. D23, pp. 30241-30255.

Carslaw, N., Jacobs, P. J., Pilling, M. J., 1999b, Modeling OH, HO_2, and RO_2 radicals in the marine boundary layer - 2. Mechanism reduction and uncertainty analysis. Journal of Geophysical Research, Vol. 104, No. D23, pp. 30257-30273.

Collella, P., Woodward P., 1984, The piece-wise parabolic method (PPM) for gas dynamical simulations. Journal of Computational Physics, 54, pp. 174-201.

Kirchner F., Stockwell W. R., 1996, Effect of peroxy radical reactions on the predicted concentrations of ozone, nitrogenous compounds, and radicals. Journal of Geophysical Research, 101, pp. 21007-21022.

Kwok, E. S. C., Atkinson R., 1995, Estimation of hydroxyl radical rate constants for gas phase organic compounds using a structure-reactivity relationship: An update. Atmospheric Environment, 29, pp. 1685-1695.

Madronich, S., Flocke, S., 1999, The role of solar radiation in atmospheric chemistry. Handbook of Environmental Chemistry (P. Boule, ed.), Springer-Verlag, Heidelberg, pp. 1-26.

Marchuk, G. I., 1975, Method of Numerical Mathematics,.Springer-Verlag, 316 pp.

Middleton P., Stockwell, W. R.., Carter, W. P. L., 1990, Aggregation and analysis of volatile organic compound emissions for regional Modelling. Atmospheric Environment, 24A, pp. 1107-1133.

Neeb P., 2000, Structure-reactivity based estimation of the rate constants for hydroxyl radical reactions with hydrocarbons, Journal of Atmospheric Chemistry, 35, pp. 295-315.

Simpson, D. , Andersson-Sköld, Y. , and Jenkin, M. E. , 1993, Updating the chemical scheme for the EMEP MSC-W oxidant model: current status, Norwegian Meteorological Institute, EMEP MSC-W Note 2/93.

Stockwell W. R., Kirchner, F., Kuhn, M., Seefled, A., 1997, A new mechanism for regional atmospheric chemistry modelling. Journal of Geophysical Research, Vol. 102, No. D22, pp. 25847-25879.

Wesely, M. L., Hicks B. B., 1977, Some factors that affect the deposition rates of sulfur dioxide and similar gases on vegetation. Journal Air Pollution Control Association, 27, pp. 1110-1116.

Chapter Three

Influence of species lumping and new kinetic data on simulation results: a box model study

Abstract

A sensitivity study about the influence of species lumping and of updated kinetic data in chemical gas phase mechanisms on the simulation results is presented. Using the "Regional Atmospheric Chemistry Mechanism" (RACM) as a starting point, the mechanism has been extended in order to investigate whether the treatment of carbonyl species in RACM may lead to an underestimation of the ozone concentrations. For simulation times of three or more days under polluted conditions, higher ozone values were found by using a more detailed carbonyl scheme. Investigations on further reductions of the mechanism showed that reducing the number of peroxy radicals by a new parameterisation influences the simulation results much less than reducing the number of VOC lumping groups. An update of the kinetic of oxy radical reactions leads to somewhat higher ozone concentrations in the model. In our scenarios the update of the structure activity relations for VOC+OH reactions show nearly no influence on the results. All tested mechanisms were generated by programme CHEMATA (CHEmical Mechanism Adaptation to Tropospheric Applications).

Keywords: Tropospheric chemistry; VOC lumping; box model; Carbonyl species parameterisation; Peroxy radical parameterisation.

1. Introduction

Explicit mechanisms are far too large for application in 3D models. Smaller mechanisms can be obtained by lumping the real species into a smaller number of mechanism species. For reasons of CPU time it is favourable to obtain a gas phase mechanism as small as possible, especially if this mechanism is to be used for air pollution forecasting or if it is to be coupled to a multi-phase model where more CPU time is needed to calculate the chemistry inside other phases and of phase-to-phase interactions. But the mechanism reduction is restricted by the requirement that the results obtained by the smaller mechanism should not differ too much from the results of the more explicit mechanism. That means that the errors introduced by the lumping process should be as small as possible. The aim is to find the best compromise between minimisation of CPU-time and minimisation of inexactness.

Validation of a lumped mechanism can be done against experiments and against a more explicit mechanism. It is favourable to combine these both approaches because the information they give are different: Validation against a more explicit mechanism will tell whether the lumping process itself introduces errors into the mechanism. It will not tell whether the lumped mechanism describes well the chemistry (because the more explicit mechanism may already fail) and in the case of large differences it is not even sure which mechanism is better (because errors introduced by the lumping process may compensate errors in the kinetic data base or in the concept of the larger mechanism). But if the differences between the two mechanisms are small, it can be concluded that the lumping process does not introduce additional errors into the mechanism. Validation against experiments will tell whether the mechanism works well for the experimental conditions. But for experimental reasons these conditions may differ from atmospheric conditions. Validation against environmental chamber studies as done for many lumped mechanisms like the RACM mechanism (Stockwell at al., 1997) suffer from two main experimental restrictions: high precursor concentrations and short reaction times of only a few

hours. Because of the short reaction times the results are not much influenced by the chemistry of secondary VOCs, meaning that the chemistry of secondary VOCs is not really validated by the environmental chamber experiments.

This work investigates the sensitivity of model results to the method of lumping by comparing differently extended mechanisms. Starting point for all studies will be the RACM mechanism, which was already validated against smog chamber data (Stockwell et al., 1997). Because of the above mentioned problems in the application of smog chambers for validating the chemistry of secondary VOCs, this chapter first investigates whether the simple approach of the treatment of secondary VOCs in RACM may be a source of errors by comparing RACM to a mechanism with a more extended carbonyl chemistry module. In a second step is tested in which way further reductions of the mechanism will affect the results.

The mechanism generation programme CHEMATA (CHEmical Mechanism Adaptation to Tropospheric Applications) will be applied to generate these mechanisms. CHEMATA which was described in Chapter One is able to reproduce the RACM mechanism with very small differences to the original version. For most species the differences between the original RACM and the mechanism produced by CHEMATA are less than a few percent. Larger differences are found for glyoxal (where the products in RACM were not mathematically correct but chosen for reasons explained in detail in Stockwell et al. (1997), butadiene (which was too much based on isoprene in RACM, not sufficiently considering the special behaviour of butadiene) and for the treatment of the RO_2 radicals resulting from the organic nitrates (ONIT) and hydro peroxides (OP2) which are treated in RACM as HC3P for reasons of analogies in the products resulting from these peroxy radicals. CHEMATA does not use those analogies but calculates all individual species and lumps them.

In a sensitivity study on the influence of new kinetic data CHEMATA will be applied to introduce updated kinetic data into the RACM mechanism. Introducing the most recent

laboratory results or review recommendation for rate constants or product yields is easy if the corresponding reaction is explicitly treated in the mechanism. More difficult is their introduction into reactions of lumped mechanism species because the lumping procedure must be repeated with the new data. Most difficult is the replacement of kinetic data estimated by structure-activity relations (SAR) in the case of new SAR estimation because that means that hundreds or thousands of rate constants or product yields must be revised in the kinetic database of the mechanism. With CHEMATA new SAR estimations can be introduced in a very easy way, just by introducing the new recommendations into the structure-reactivity input file and running the programme. This work presents two examples: the introduction of new kinetic data for the reactions of oxy radicals and the replacement of the SAR estimations by Kwok and Atkinson (1995) which were used in RACM by the new SAR estimations of Neeb (2000). These two examples were chosen in order to illustrate the capability of CHEMATA to handle those issues. They are not assumed to be the most important updates for RACM. A complete update will be done in the future.

2. Investigation of species lumping

2.1. Extending the carbonyl groups in the mechanism

The most common secondary products from atmospheric VOC degradation are carbonyl species like aldehydes and ketones. They undergo subsequent reactions; aldehydes can for example react with OH in the following way:

$$R\text{-}CH_2CHO + OH\ (+O_2) \rightarrow R\text{-}CH_2C(O)OO^* + H_2O \quad (1)$$

$$R\text{-}CH_2C(O)OO^* + NO \rightarrow R\text{-}CH_2^* + CO_2 + NO_2 \quad (2)$$

$$R\text{-}CH_2^* + O_2 \rightarrow R\text{-}CH_2OO^* \quad (3)$$

$$R\text{-}CH_2OO^* + NO\ (+O_2) \rightarrow R\text{-}CHO + HO_2 + NO_2 \qquad (4)$$

The resulting aldehyde in equation (4) has one C atom less than the aldehyde in equation (1) and can react again with OH in the same way as its higher homologue. Therefore aldehydes with long carbon chains can pass several times through the reaction sequences of equation (1) to (4) until R becomes equal to H and HCHO is produced. Representing all higher aldehydes by acetaldehyde (CH_3CHO) as it is done in RACM and in several other mechanisms means that the reaction chain equation (1)-(4) can be passed through only once. Considering the fact that aldehydes are very reactive species, this treatment might lead to an underestimation of the system's reactivity.

Two mechanism species describe ketones in RACM: HKET and KET. HKET is treated as $CH_3C(O)CH_2OH$ and KET is treated as a mixture of acetone and methylethylketone. In reality ketones often have more carbon atoms. This underestimation of the real average C atom number may reduce the degradation sequences (as explained above for the aldehydes), which can be passed through. In addition, this treatment underestimates the reactivity of ketones because it depends largely on the number of carbon atoms (compare Atkinson, 1994).

In order to investigate whether these simplifications of the carbonyl chemistry in the mechanism are justified or whether they will introduce errors, an *extended mechanism* was generated by replacing the lumping groups for aldehydes (ALD) and ketones (KET and HKET) of RACM by several new lumping groups. The higher aldehydes are split into 7 groups: CH_3CHO, C_2H_5CHO, n-C_3H_7CHO, i-C_3H_7CHO, R'-CHO, R"CHO, R'"CHO (with: R' for a chain ≤ 4 C atoms, R" for a chain = 5 C atoms, R'" for a chain ≥ 6 C atoms). In order to maintain this additional information during the calculations it was necessary to split also the acyl peroxy radicals (R-C(O)OO*, called ACO3 in RACM) into the 7 corresponding groups. The acyl peroxy nitrates (PAN in RACM) were also split into several groups: $CH_3C(O)OONO_2$, $C_2H_5C(O)OONO_2$ and $ROONO_2$ with 4 or more C atoms. The ketones are split into 7 groups: acetone, hydroxy acetone and ketones with 4, 5, 6, 7, and more than 7 carbon atoms. Whereas hydroxy acetone (HKET in RACM) is

assumed to react completely to $CH_3C(O)CH_2O^*$ and therefore not to produce peroxy radicals, the other ketones react under formation of peroxy radicals (KETP in RACM) which are split into 6 corresponding groups.

CHEMATA has been run to create the lumped mechanism with these new carbonyl lumping groups. In the new mechanism, all degradation products of non-aromatic VOC species being emitted by more than 100 ty^{-1} in the USA according to the emission inventory of Middleton et al. (1990) have been summed up, all carbonyl products which exceed a yield of 0.1 $Mmoly^{-1}$ were lumped into the above-mentioned lumping groups for aldehydes and ketones, and their primary RO_2 products were lumped into the above mentioned new RO_2 groups. Table 1 shows these compounds and the corresponding lumping group in the extended mechanism.

Species name	***Definition***	***Species on which the lumping is based***
ALD2	aldehydes with chain length = 2	CH_3CHO
ALD3	aldehydes with chain length = 3	C_2H_5CHO
ALDn4	aldehydes with chain length = 4	n-C_3H_7CHO and 4 other aldehydes with chain length = 4
ALDi4	iso-C_3H_7CHO	iso-C_3H_7CHO
ALD5	aldehydes with chain length = 5	3 aldehydes with chain lengths = 5
ALD6	aldehydes with chain length = 6	3 aldehydes with chain length = 6
ALD7	aldehydes with chain length = 7	$CH_3C(O)CH_2CH(OH)CH_2CH_2CHO$
KET3	$CH_3C(O)CH_3$	$CH_3C(O)CH_3$
KET4	$C_2H_5C(O)CH_3$	$C_2H_5C(O)CH_3$
KET5	ketones with chain length = 5	9 ketones with chain lengths = 5
KET6	ketones with chain length = 6	4 ketones with chain lengths = 6
KET7	ketones with chain length = 7	3 ketones with chain lengths = 7
KET8	ketones with chain length ≥ 8	21 ketones with chain lengths ≥ 8 (between 8 and 15)

Table 1: New carbonyl species in the extended mechanism.

2.2. Mechanism reduction

RACM contains 77 species, within which 22 are inorganic species, 56 are organic species (32 VOCs, 20 organic peroxy radicals and 4 other organic radicals). In order to obtain a smaller mechanism the number of mechanism species can be reduced by further lumping of the organic species, combining several existing mechanism species into new lumping groups. In the logic of RACM where most of the VOC species have their own RO_2 lumping group, a reduction of the VOC lumping groups leads automatically to a reduction of the RO_2 species. On the other hand one can also try to reduce the number of RO_2 groups without changing the number of the VOC species, just by changing the parameterisation of the RO_2 chemistry. Therefore the reduction of the mechanism was performed in two steps. In a first step the number of radical lumping groups has been reduced, generating a new mechanism here after called the *reduced mechanism*, and in a second step a smaller mechanism has been generated, referred to as the *small mechanism*, by reducing the number of VOC lumping groups.

2.2.1. The reduced mechanism

The RACM mechanism was condensed by a new parameterisation of the RO_2 chemistry. Only the RO_2 species CH_3O_2 (MO2) and $CH_3C(O)O_2$ (ACO3) were kept, all other RO_2 species of RACM were replaced by the species XO2 and XO2N. In this way the number of RO_2 radicals in the mechanism was reduced from 20 to 4 species. The number of RO_2 reactions was reduced from 110 to 23. The parameterisation was made in a way that the products of the RO_2 reactions were formed at the same time as RO_2. In RACM the formation of a peroxy radical from the reaction of a VOC species with OH and its reaction with NO was parameterised in the following way:

$$VOC_x + OH \rightarrow RO2_x \quad (5)$$

$$RO2_x + NO \rightarrow \alpha_{nit} ONIT + (1-\alpha_{nit})(\alpha_1 PROD_1 + \alpha_2 PROD_2 + \cdots + \alpha_n PROD_n + NO2) \quad (6)$$

α_i represents the product yield, α_{nit} is the yield of organic nitrates (ONIT), $(1-\alpha_{nit})$ is therefore the yield of the product channel leading to the oxy radical RO and NO_2. In RACM oxy radicals are not represented by individual mechanism species but always by their reactions products $PROD_i$ which are secondary VOCs, organic peroxy radicals or HO_2. For some reactions, RACM already included another parameterisation which is based on the idea that one can separate the two main attributes of peroxy radicals: the fact of being a radical interacting with other radicals and the fact of being a precursor of oxy radicals and their products $PROD_i$. This approach is now further developed by splitting the RACM species XO2 into the new species XO2 and XO2N leading to the following parameterisation for the same reactions:

$$VOC_x + OH \rightarrow \alpha_{nit} XO2N + (1-\alpha_{nit}) XO2 + \beta(\alpha_1 PROD_1 + \alpha_2 PROD_2 + \cdots + \alpha_n PROD_n) \quad (7)$$

$$XO2 + NO \rightarrow NO2 \quad (8)$$

$$XO2N + NO \rightarrow ONIT \quad (9)$$

β is the product yield for the intermediate product RO which may differ from $(1-\alpha_{nit})$ because in addition to the reaction with NO the peroxy radicals can also react with NO_2, NO_3, HO_2, and $R'O_2$ with various RO yields. The reaction with NO_3 is very similar to the reaction with NO only differing in the nitrate yield:

$$RO2 + NO3 \rightarrow \alpha_{nit2} ONIT + (1-\alpha_{nit2})(RO + NO2) \quad (10)$$

In agreement with the RACM mechanism where $\alpha_{nit2} = 0$, the same value were chosen, parameterising the reactions as

$$XO2 + NO3 \rightarrow NO2 \quad (11)$$

$$XO2N + NO3 \rightarrow 0.971\,HO2 + 0.584\,XO2 + 0.131\,HCHO + 0.029\,MO2 + 0.165\,MACR + 0.200\,ALD + 0.656\,KET + 0.002\,HKET + 0.076\,OLT \quad (12)$$

The products result from calculating the average products from all peroxy radicals from all VOCs. This treatment is consistent with $\beta = (1-\alpha_{nit})$, but one has to consider that with increasing α_{nit} values, the individual products of each VOC described by equation (7) are more and more replaced by the average products from equation (12).

The reaction

$$RO_2 + NO_2 \rightarrow ROONO_2 \qquad (13)$$

leads to very unstable peroxy nitrates $ROONO_2$ if R is an alkyl group and to relatively stable peroxy nitrates of the PAN type if R is an acyl group (Kirchner et al., 1999). Therefore, alkyl peroxy radicals and acyl peroxy radicals have to be distinguished. Because of the relatively stable intermediate PAN, there is often a long time difference between the formation of the acyl radical and the formation of its products $PROD_i$. Therefore acyl peroxy radicals are represented by the old RACM parameterisation style but grouping the old RACM species ACO3 (saturated acyl peroxy radicals) and TCO3 (unsaturated acyl peroxy radicals) into one mechanism species. As in RACM, the reactions of alkyl peroxy radicals with NO_2 are not included because of the very fast decomposition reaction of the formed alkyl peroxy nitrate.

The reaction with HO_2

$$RO_2 + HO_2 \rightarrow ROOH + O_2 \qquad (14)$$

is parameterised as

$$XO2 + HO2 \rightarrow OP2 \qquad (15)$$

$$XO2N + HO2 \rightarrow OP2 \qquad (16)$$

where OP2 represents as in RACM hydroperoxides other than CH3OOH and CH3C(O)OOH. Because no other products $PROD_i$ are formed, the value of β must decrease with increasing importance of the $RO_2 + HO_2$ reaction as RO_2 loss reaction.

The peroxy radical - peroxy radical reactions

$$\begin{aligned} R\text{-}CHX\text{-}O_2 + R'\text{-}CHX\text{-}O_2 \rightarrow\ & \gamma(R\text{-}CHX\text{-}O + R'\text{-}CHX\text{-}O) \\ & + (1-\gamma)\{\delta(R\text{-}CXO + R'\text{-}CHX\text{-}OH) \\ & + (1-\delta)(R\text{-}CHX\text{-}OH + R'\text{-}CXO)\} \end{aligned} \quad (17)$$

are parameterised as

$$XO2 + XO2 \rightarrow (\text{no products}) \quad (18)$$

$$XO2 + XO2N \rightarrow (\text{no products}) \quad (19)$$

$$XO2N + XO2N \rightarrow (\text{no products}) \quad (20)$$

All products $PROD_i$ are formed with a yield of at least γ, some of them (the carbonyl species) with a yield of $\gamma + (1-\gamma)\,\delta$. The less reactive alcohol type products are ignored in agreement with their treatment in the RO2 + RO2 reactions of the RACM mechanism.

For polluted air masses the reaction with NO is the most important reaction, β was therefore chosen to be equal to $(1-\alpha_{nit})$. At night-time the reaction with NO_3 becomes especially important (Kirchner and Stockwell, 1996). As explained above this reaction is also well described if β is equal to $(1-\alpha_{nit})$. Only in the case of a large contribution of the HO_2 reaction to the overall RO_2 reactions, β and therefore the products resulting from RO will be overestimated.

The rate constants for the reactions of alkyl peroxy radicals with NO, NO_3, and HO_2 do not depend much on the group R. The rate constant of peroxy radical - peroxy radical reactions depend largely on the group R (Kirchner and Stockwell, 1996), meaning that the single rate constant may differ largely from the average value of 3×10^{-12} for 298 K which was applied in the mechanism.

2.2.2. The small mechanism

The RO_2 parameterisation was the same as in the reduced mechanism. The number of different VOC classes was lowered from 34 to 10 (CH_4, alkanes, alkenes, aromatics, HCHO, 3 classes of higher aldehydes, ONIT, PAN). The lumping was based on the average emission values in the

VOC species	*Extended mechanism*	*RACM Reduced mechanisms*	*Small mechanism*
methane	CH4	CH4	CH4
alkanes, alcohols, esters, ethers	ETH, HC3, HC5, HC8	ETH, HC3, HC5, HC8	ALKA
alkenes	ETE, OLT, OLI, ISO, API, LIM, DIEN	ETE, OLT, OLI, ISO, API, LIM, DIEN	OLE
aromatics	TOL, XYL, CSL	TOL, XYL, CSL	ARO
saturated aldehydes (low photolysis)	HCHO ALD2, ALD3, ALDn4, ALDi4, ALD5, ALD6, ALD7	HCHO ALD	HCHO ALD
saturated aldehydes (high photolysis)	GLY, MGLY	GLY, MGLY	ALDR
unsaturated aldehydes (low photolysis)	MACR	MACR	ALD, OLE
unsaturated aldehydes (high photolysis)	DCB	DCB	DCB
ketones	KET3, KET4, KET5, KET6, KET7, KET8 HKET	KET HKET	-
RO_2 species	***Extended mechanism***	***RACM***	***Reduced & small mechanisms***
CH_3OO*	MO2	MO2	MO2
R-C(O)OO*	ACO2, ACO3, ACOn4, ACOi4, ACO5, ACO6, ACO7 TCO3	ACO3 TCO3	ACO3
RO_2 from ketones	KET3P, KET4P, KET5P, KET6P, KET7P, KET8P	KETP	-
other RO_2	ETHP, HC3P, HC5P, HC8P, ETEP, OLTP, OLIP, ISOP, APIP, LIMP, TOLP, XYLP, CSLP, OLNN, OLND, XO2	ETHP, HC3P, HC5P, HC8P, ETEP, OLTP, OLIP, ISOP, APIP, LIMP, TOLP, XYLP, CSLP, OLNN, OLND, XO2	XO2, XO2N

Table 2: List of organic species in RACM, the extended mechanism, the reduced mechanism, and the small mechanism. The species names of the RACM mechanism are defined in Stockwell et al. (1997), the species names of the extended mechanism which are different from RACM's names are explained in Table 1.

box model run Case 1 (see below) and is therefore adapted to this special situation. The inorganic chemistry of RACM was adopted without any changes except excluding the species H_2. Table 2 details the species of the four mechanisms.

2.3. Box model studies

Four scenarios were used to test these mechanisms in a box model. Cases 1 to 3 are calculated for a 5 days period and case 4 is calculated for 24 hours.

- Case 1 (Moderately polluted case with constant emissions): The emissions and conditions are taken from Kirchner and Stockwell (1996) which was identical with the "plume2" case of Kuhn et al. (1998) except that the temperature was set to 298 K. The simulation starts at noon and ends the 6th day at noon.
- Case 2 (Highly polluted case with constant emissions): In Case 2 ten times higher VOC emissions and 30 times higher NO_x emissions than in Case 1 are applied.
- Case 3 (Highly polluted case, but no emissions): No emissions are considered in Case 3. The initial concentrations are equal to the concentrations of the RACM mechanism of Case 2 at noon of the third day.
- Case 4: Extremely polluted: 300 times more NO_x and 1000 times more VOC than in Case 1. Conditions like this do not exist for a whole day in reality, but in the morning before the mixing layer increases this kind of concentrations can be found downtown very polluted cities. For this reason, it is run only for 24 hours.

2.4. Results

Results of the comparison of different kinds of lumping in a box model are shown in Figure 1, 2 and 3. Comparing the results of RACM and the extended mechanism for higher aldehydes

(RACM species ALD and equivalent species in the extended mechanism according to Table 2) shows that the errors made by restricting to small products (as it is done in RACM) lead to lower aldehyde mixing ratios in comparison with the extensive carbonyl treatment in the extended mechanism (Figure 3). For Case 2 and 3 these lower aldehyde values correspond to a lower ozone production (Figure 1). This underestimation is small during the first 2 days and becomes more important for longer time scales. For Case 1 the effect on the ozone mixing ratios is very small because in this case, the ozone production is less sensitive to VOC concentrations and more sensitive to NO_x.

The differences between RACM and the reduced mechanism are very small in Cases 1-3 for ozone, aldehydes and OH, suggesting that introducing this RO_2 parameterisation is a good way to reduce the size of a mechanism. Nevertheless Case 4 shows a faster increase of ozone in the morning. Therefore at 10 a.m. the reduced mechanism yields 30% more ozone than RACM. This

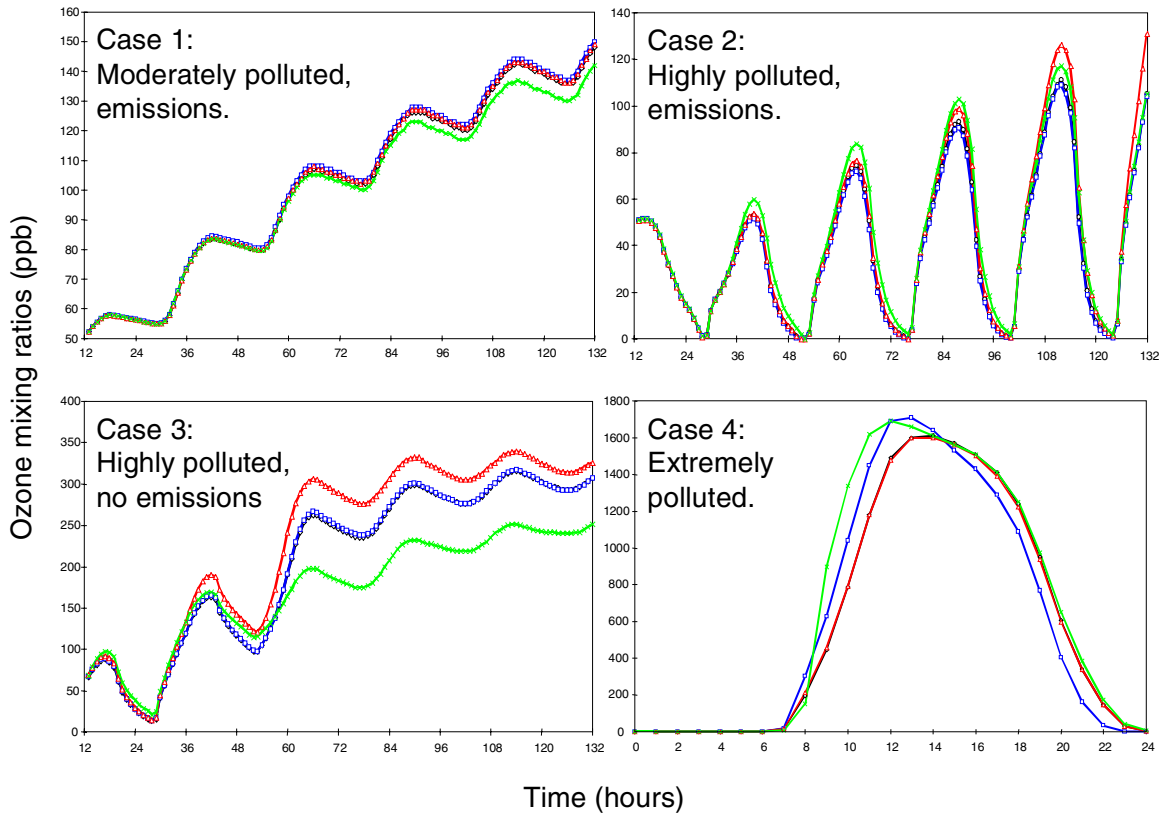

Figure 1: Changing the lumping method: effect on ozone mixing ratios (ppb). RACM: black line with diamonds; extended mechanism: triangles; reduced mechanism: squares; small mechanism: crosses.

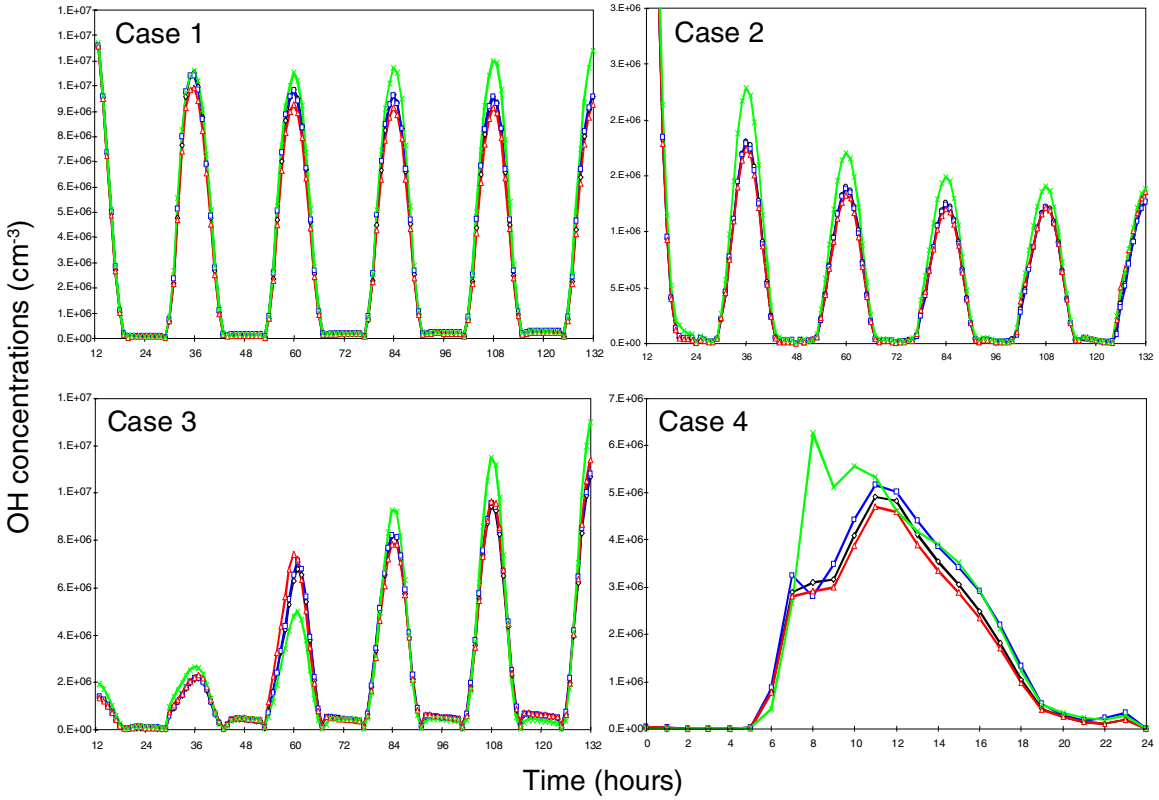

Figure 2: Changing the lumping method: effect on OH concentrations (cm^{-3}). RACM: black line with diamonds; extended mechanism: triangles; reduced mechanism: squares; small mechanism: crosses.

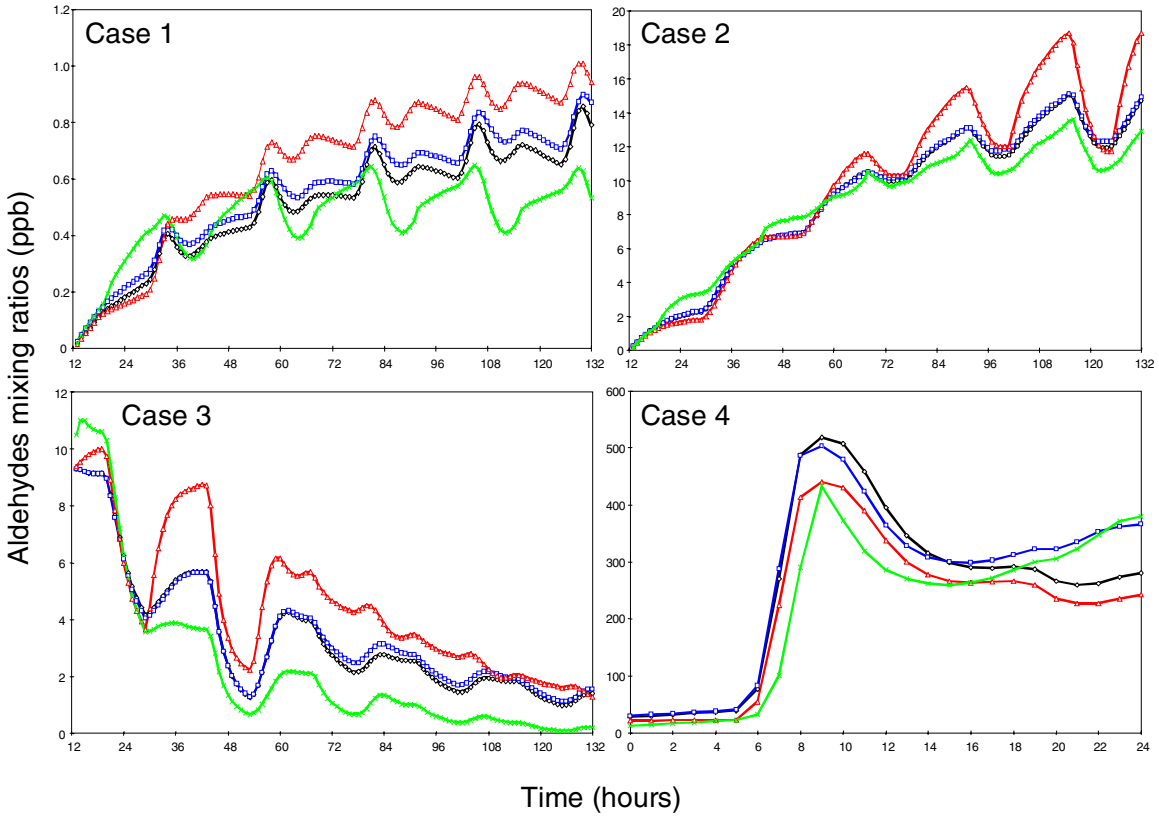

Figure 3: Changing the lumping method: effect on Aldehydes mixing rations (ppb). RACM: black line with diamonds; extended mechanism: triangles; reduced mechanism: squares; small mechanism: crosses.

is due to the fact that with the new RO_2 parameterisation products are formed in the first reaction step (reaction 7) instead of the second step (reaction 6) in RACM. Especially the fact that the radicals formed in reality in the degradation process of the RO radicals are formed earlier with the new parameterisation leads to a faster ozone formation.

The differences between the small mechanism and the reduced mechanism are much larger than the differences between the reduced mechanism and RACM showing that reducing the RO_2 groups by the new RO_2 parameterisation is a better way for reducing the mechanism than a reduction of the VOC lumping groups by lumping more species into the same lumping group. Nevertheless the ozone values of the small mechanism differ not very much from the other mechanisms for Case 1 and 2. But in Case 3 the small mechanism fails calculating the ozone values for longer simulation times. Summing up all the rates for VOC+OH reactions shows that the VOC split in the small mechanism becomes with the time less and less reactive compared to the other mechanisms in the Cases 1-3. In Case 4 an even faster ozone increase is found leading at 10 a.m. to 70% more ozone than in RACM.

3. Sensitivity study on the influence of new kinetic data

Depending on the branching ratios of the reactions of oxy radicals (RO*), the reactivity of secondary VOCs' mixture can vary. RO radicals can react in three different ways: by abstraction, isomerisation or decomposition reaction. For secondary oxy radicals theses reactions lead to the following products:

The abstraction reaction leads to ketones:

$$R\text{-}CH(O^*)\text{-}R' + O_2 \rightarrow R\text{-}C(O)\text{-}R' + HO_2 \qquad (21)$$

Abstraction[a]			$k_{(298K)} * [O_2]$ s^{-1}	
Abstraction from C(prim)			$4.90 \times 10^{+4}$	
Abstraction from C(sec)			$3.96 \times 10^{+4}$	
Abstraction from C(tert)			Not possible	
Isomerisation[a]			k(298K) s^{-1}	$k/(k_{O2}[O_2] + k)$
Abstraction from C(prim)			$6.71 \times 10^{+4}$	0.578
Abstraction from C(sec)			$8.44 \times 10^{+6}$	0.994
Abstraction from C(tert)			$4.14 \times 10^{+6}$	0.988
Abstraction from CH_2OH			$3.41 \times 10^{+5}$	0.875
Abstraction from CHROH			$3.15 \times 10^{+7}$	0.998
Decomposition[b]			k(298K) s^{-1}	$k/(k_{O2}[O_2] + k)$
R(prim)CH_2O	→ CH_3	+ HCHO	1.50×10^{-1}	0.0
R(sec)CH_2O	→ R(prim)	+ HCHO	$2.38 \times 10^{+1}$	0.001
R(tert)CH_2O	→ R(sec)	+ HCHO	$4.67 \times 10^{+1}$	0.001
R(quar)CH_2O	→ R(tert)	+ HCHO	$3.54 \times 10^{+2}$	0.007
$ROCH_2O$	→ RO	+ HCHO	1.00×10^{-1}	0.0
R(prim)CRHO	→ CH_3	+ ALD	$2.82 \times 10^{+1}$	0.070
R(sec)CRHO	→ R(prim)	+ ALD	$4.46 \times 10^{+3}$	0.101
R(tert)CRHO	→ R(sec)	+ ALD	$8.79 \times 10^{+3}$	0.182
R(quar)CRHO	→ R(tert)	+ ALD	$5.62 \times 10^{+4}$	0.587
ROCRHO	→ RO	+ ALD	$2.00 \times 10^{+7}$	0.998
R(prim)CR_2O	→ CH_3	+ KET	$4.97 \times 10^{+2}$	0.0
R(sec)CR_2O	→ R(prim)	+ KET	$7.89 \times 10^{+4}$	0.0
R(tert)CR_2O	→ R(sec)	+ KET	$1.31 \times 10^{+5}$	0.0
R(quar)CR_2O	→ R(tert)	+ KET	$9.94 \times 10^{+5}$	0.0
$ROCR_2O$	→ RO	+ KET	$2.00 \times 10^{+7}$	0.0

Table 3: RO reaction rate constants in the RACM mechanism. [a] Atkinson (1990), [b] Atkinson (1994).

RO	***reaction***	***k / k_{O2}***	***k(298K) s^{-1}***	***k(298K) s^{-1} RACM***	***Factor***
2-butoxy	decomp.	$2.90 \times 10^{+18}$ [a]	$2.30 \times 10^{+04}$	$4.46 \times 10^{+03}$ [c]	5.2
i-butoxy	decomp.	$6.2 \times 10^{+18}$ [b]	$5.87 \times 10^{+04}$	0.10 [c]	1258.0
3-pentoxy	decomp.	$3.6 \times 10^{+18}$ [b]	2.76 x 10+04	$2x4.46 \times 10^{+03}$ [c]	3.1
1-butoxy	isom.	$1.50 \times 10^{+19}$ [b]	$1.71 \times 10^{+05}$	$6.71 \times 10^{+04}$ [d]	2.5

Table 4: Comparison to experimental values. [a] Libuda et al. (2002), [b] Geiger et al. (2002), [c] Atkinson (1990), [d] Atkinson (1994).

The isomerisation reaction produces in a first step an alkyl radical:

$$R\text{-}CH_2\text{-}CH_2\text{-}CH_2\text{-}CH(O^*)\text{-}R' \rightarrow R\text{-}C(^*)H\text{-}CH_2\text{-}CH_2\text{-}CH(OH)\text{-}R' \quad (22)$$

This alkyl radical will be transformed to a peroxy radical by adding oxygen. In a second step it may react with NO forming an oxy radical and NO_2. If the original oxy radical was secondary, the new oxy radical will react in the following way:

$$R\text{-}C(O^*)H\text{-}CH_2\text{-}CH_2\text{-}CH(OH)\text{-}R' \rightarrow R\text{-}C(OH)H\text{-}CH_2\text{-}CH_2\text{-}C(^*)(OH)\text{-}R' \quad (23)$$

$$R\text{-}C(OH)H\text{-}CH_2\text{-}CH_2\text{-}C(^*)(OH)\text{-}R' + O_2 \rightarrow R\text{-}C(OH)H\text{-}CH_2\text{-}CH_2\text{-}C(O)\text{-}R' + HO_2 \quad (24)$$

Finally the isomerisation reaction also leads to ketones. The decomposition reaction of a secondary oxy radical leads to the much more reactive aldehyde:

$$R\text{-}CH(O^*)\text{-}R' \rightarrow R\text{-}CHO + R'^* \quad (25)$$

The branching ratios of the oxy radical reaction are therefore crucial for the reactivity of the formed carbonyl products. In RACM, branching ratios were estimated according to recommendations from Atkinson (1990) and Atkinson (1994). The values are listed in Table 3. New experimental data from Geiger et al. (2002) and Libuda et al. (2002) show considerable differences to these recommendations (see Table 4). The product yields are especially sensitive to uncertainties in rate constants if two rate constants are very similar – i.e. if $k/(k+k_{O2}[O_2])$ is close to 0.5 with k being the rate constant of the isomerisation or decomposition reaction and k_{O2} being the rate constant for the H abstraction by O_2 –. Table 3 shows that this is the case for the decomposition of secondary oxy radicals. The new experimental data are implemented and, according to these new measurements, the old decomposition rate constants are increased by a factor of 5 and the old isomerisation rate constants are increased by a factor of 2 for all RO radicals for which no experimental kinetic data are available.

The results are shown in Figure 4 and 5. For the Cases 1, 2 and 3, higher daytime aldehyde mixing ratios are found with the updated oxy radical kinetic. In the NO_x saturated test Cases 2 and 3 this increase in the aldehydes leads to higher ozone mixing ratios. Especially in Case 2, where the ozone increase is large for long simulation times, these higher ozone produces more NO_3 at night-time and therefore a larger night-time loss of aldehydes by the aldehyde + NO_3 reaction. For Case 3 the largest difference in ozone is found the third day. Later, the difference becomes smaller because of the lack of emissions and the low ozone production during the last days. In Case 1 the increase in the aldehyde mixing ratios has only small effects on ozone because the ozone production is mainly NO_x limited. For the short simulation time in Case 4, no differences are found.

Replacing the structure-reactivity relations of Kwok and Atkinson (1995) which are used in RACM by new SAR estimations of Neeb (2000) leads to very small changes in the mixing ratios

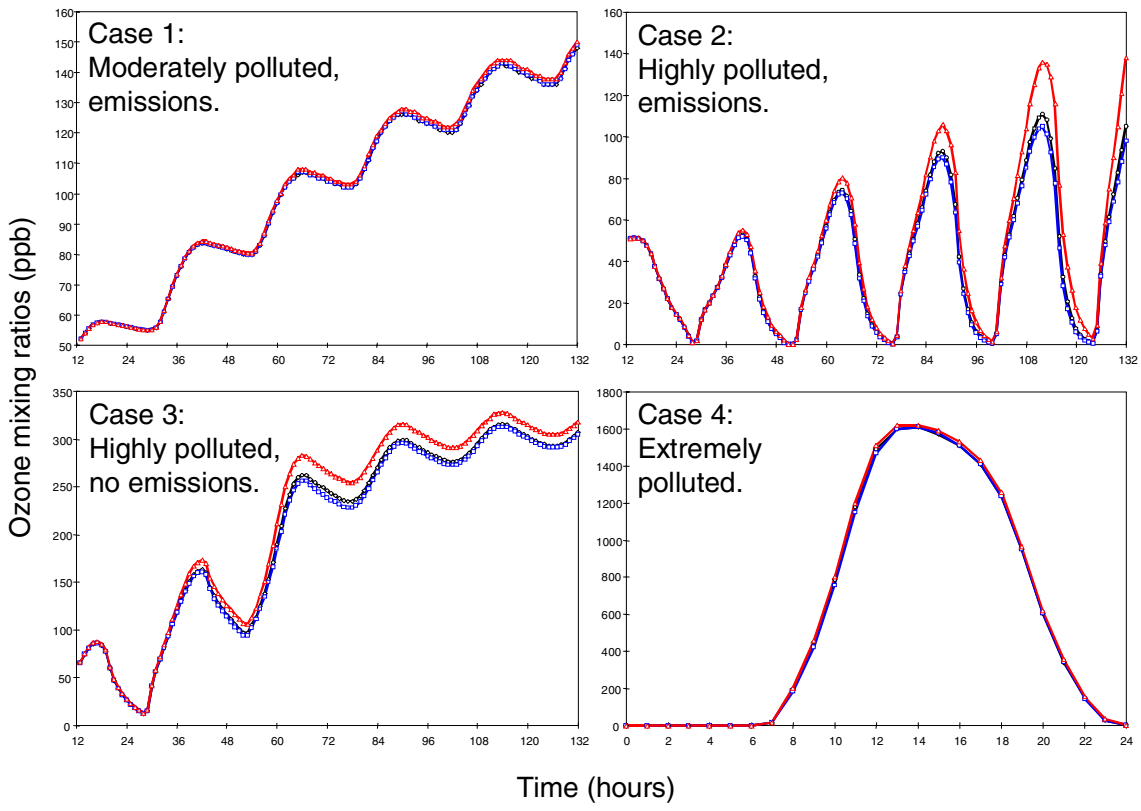

Figure 4: Updating the kinetic data: effect on ozone mixing ratios (ppb). RACM: black line with diamonds; updated RO chemistry: triangles; updated SAR for VOC+OH: squares.

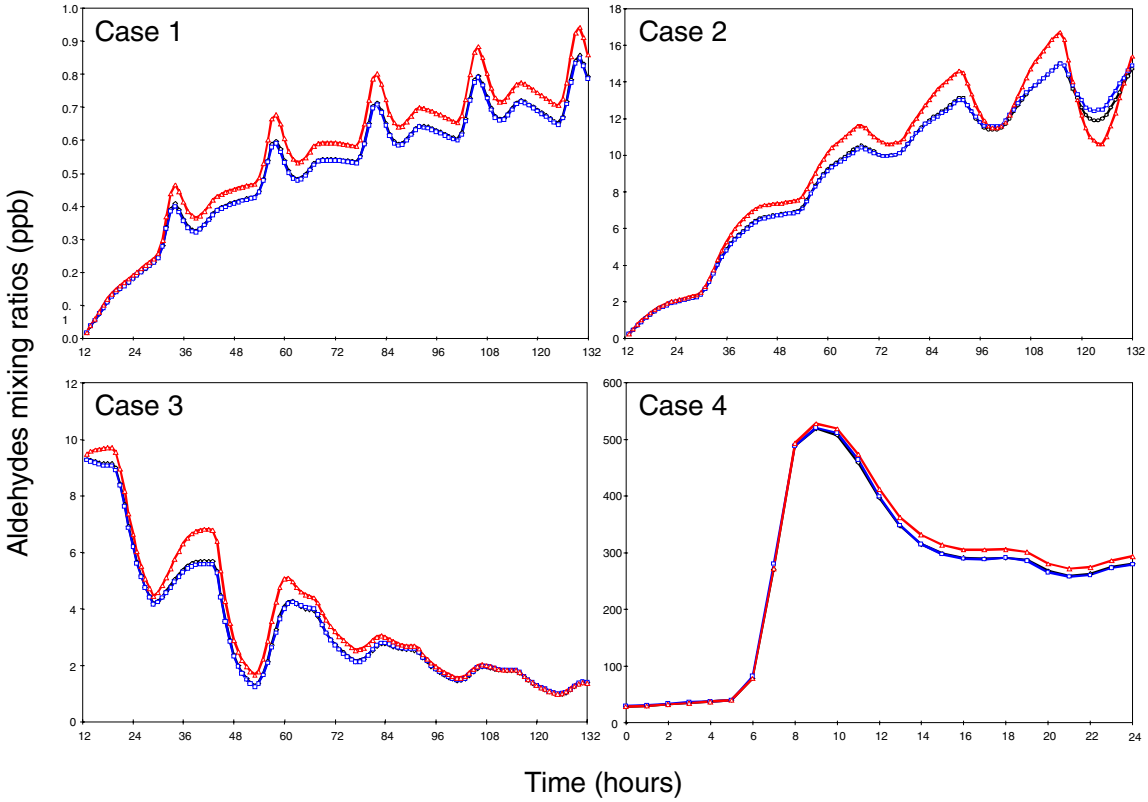

Figure 5: Updating the kinetic data: effect on aldehydes mixing ratios (ppb). RACM: black line with diamonds; updated RO chemistry: triangles; updated SAR for VOC+OH: squares.

of species like ozone for all test cases (Figures 4 and 5). But it should be noted that the largest differences for these two SAR estimations are found for oxygenated VOC which are emitted only in low quantities in our test cases but probably will have increased importance in the future.

4. Conclusion

The calculations show that the error made by treating the higher carbonyl species like smaller carbonyls in RACM is small for simulating ozone episodes up to two days but may be important for longer time scales. From this box model study it seems that it is not necessary to extend the carbonyl chemistry in RACM for normal regional modelling applications where the pollutants stay only 1 or 2 days inside the modelling area. But it also shows that implementing a mechanism

with this simplified carbonyl species treatment into a global model where the pollutants stay much longer in the modelling area may cause problems.

Further mechanism reduction is possible by changing the parameterisation of the RO_2 reactions which may lead to a small ozone overestimation in the morning in very polluted areas. Reducing the VOC groups can severely affect the morning values in very polluted areas and can lead to wrong results for simulation times of three or more days. For less polluted conditions where the ozone formation is limited by NO_x, the reduction of the VOC groups did not generate any considerable deviations in ozone values compared to the more detailed VOC representation in RACM. For these less pollutant conditions the differences between all mechanisms investigated in this work are much smaller than the differences found by Kuhn et al. (1998) for comparing different standard mechanisms. Updating the kinetic data base for reactions of oxy radicals leads to higher aldehyde mixing ratios which generate higher ozone mixing ratios in the case of NO_x saturated conditions, especially for episodes of three or more days. The old kinetic data and the simplified treatment of carbonyl species in the RACM mechanism therefore lead both to an ozone underestimation for longer simulation times. For 1 or 2 day episodes the error in ozone seems to be small.

References

Atkinson, R., 1990, Gas-phase tropospheric chemistry of organic compounds: a review. Atmospheric Environment, 24A, pp. 1-41.

Atkinson, R., 1994, Gas-phase tropospheric chemistry of organic compounds: a review. Journal of Physical Chemistry, Ref. Data, Monogr. 2, pp. 1-216.

Atkinson, R., 2000, Atmospheric chemistry of VOCs and NO_x. Atmospheric Environment, 34, pp. 2063-2101.

Gery, M. W., Whitten G. Z., Killus J. P., Dodge M. C., 1989, A photochemical kinetics mechanism for urban and regional scale computer modelling. Journal of Geophysical Research, Vol. 94, pp. 12925-12956.

Kirchner, F., Stockwell W. R., 1996, Effect of peroxy radical reactions on the predicted concentrations of ozone, nitrogeneous compounds and radicals. Journal of Geophysical Research, Vol. 101, pp. 21007-210022.

Kirchner, F., Mayer-Figge A., Zabel F., Becker K. H., 1999, Thermal stability of peroxynitrates. International Journal of Chemical Kinetics, 31, pp. 127-144.

Kuhn, M., Builtjes P. J. H., Poppe D., Simpson D., Stockwell W. R., Andersson-Sköld Y., Baart A., Das M., Fiedler F., Hov Ø., Kirchner F., Makar P.A., Milford J. B., Roemer M. G. M., Ruhnke R., Strand A., Vogel B., Vogel H., 1998, Intercomparison of the gas-phase chemistry in several chemistry and transport models. Atmospheric Environment, 32, pp. 693-709.

Kwok, E. S. C., Atkinson R., 1995, Estimation of hydroxyl radical rate constants for gas phase organic compounds using a structure-reactivity relationship: An update. Atmospheric Environment, 29, pp.1685-1695.

Middleton, P., Stockwell W. R., Carter W. P. L., 1990, Aggregation and analysis of volatile organic compound emissions for regional modeling. Atmospheric Environment, 24A, pp. 1107-1133.

Neeb, P., 2000, Structure-reactivity based estimation of the rate constants for hydroxyl radical reactions with hydrocarbons. Journal of Atmospheric Chemistry, 35, pp. 295-315.

Stockwell, W. R., Kirchner F., Kuhn M., Seefeld S., 1997, A new mechanism for regional atmospheric chemistry modeling. Journal of Geophysical Research, Vol. 102, No. D22, pp. 25847-25879.

Geiger, H., Barnes I., Becker K. H., Bohn B., Brauers T., Donner B., Dorn H. P., Elend M., Freitas Dinis C. M., Grossmann D., Hass H., Hein H., Hoffmann A., Hoppe L., Hülsemann F., Kley D., Klotz B., Libuda H. G., Maurer T., Mihelcic D., Moortgat G. K., Olariu R., Neeb P., Poppe D., Ruppert L., Sauer C. G., Shestakov O., Somnitz H., Stockwell W. R., Thüner L. P., Wahner A., Wiesen P., Zabel F., Zellner R., Zetzsch C., 2002, Chemical mechanism development: Laboratory studies and model applications. Journal Atmospheric Chemistry, 42, pp. 323-357.

Libuda, H.G., Shestakov O., Theloke J., Zabel F., 2002, Relative-rate study of thermal decomposition of the 2-butoxyl radical in the temperature range 280-313 K. Physical Chemistry Chemical Physics, 4, pp. 2579-2586.

Chapter Four

Comparison of four chemical mechanisms

Abstract

In order to assess the possibility to increase the speed of atmospheric air quality models, a comparison of four chemical mechanisms of different sizes is presented. Using CHEMATA, three new mechanisms are generated, based on the RACM mechanism (one bigger and two smaller). The *extended* one has a more precise aldehydes and ketones parametrisation. It will be used to test the accuracy of RACM itself. In the two smaller mechanisms (the *reduced* and the *small*) the RO_2 chemistry of RACM is condensed (4 species instead of 22), the small one keeping only 10 VOC groups instead of 34. All four mechanisms are implemented in a three dimensional mesoscale air quality model. The comparison of ozone results shows that there is no significant difference between RACM and the extended mechanism. The reduced mechanism and RACM give very similar results, while the small mechanism present some differences. The analysis of these results shows that the reduced mechanism is a very good compromise between speed and accuracy. The extended mechanism should be kept for special use when enhanced precision is needed in aldehydes and ketones, while the small one will be useful when quick response is important. The comparison between the extended and RACM shows that the aldehydes and ketones parametrisation in RACM do not induce significant errors.

Keywords: Mesoscale modelling; Air quality modelling; Tropospheric chemistry; VOC lumping;

1. Introduction

Because of the huge number of chemical species and the complexity of the processes involved, the formation of secondary photochemical pollutants is highly non-linear. A three dimensional air quality model is therefore a useful tool to simulate the chemical processes occurring in the atmosphere. These models can be used for different purposes needing different chemical mechanisms. For emission abatement strategies assessment (Kuebler et al., 1996) a very detailed chemical mechanism is required, which consumes a lot of time. For daily ozone forecasting (Vautard et al., 2001), very quick simulation is needed with less accurate mechanisms. When more calculation time is needed for other processes like aerosol chemistry or heterogeneous processes, an optimal chemical mechanism will be desirable. In any case, finding the best compromise between needed detail and calculation time is always interesting.

As chemistry calculation is the most time consuming part of three dimensional photochemical models,decreasing the time needed for its calculation will efficiently decrease the overall calculation time. In order to reduce the chemistry calculation time, the number of species in the chemical mechanism can be reduced. But this can also have an impact on the accuracy of the simulation's results.

The first goal of this work is to investigate the possibility to increase the calculation speed by reducing the chemical mechanism but keeping enough precision. The reduction of the chemical mechanisms is carried out by lumping the huge amount of VOC species involved in atmospheric chemistry into a smaller number of new species. To investigate the impact of mechanism reduction, two small mechanisms have been generated, based on a widely used chemical mechanism, the RACM mechanism by Stockwell et al. (1997). In these two mechanisms (hereafter respectively called the *reduced* and the *small* mechanisms), the RO_2 chemistry is condensed, and the smaller one has even less VOC species. These two mechanisms will be faster than RACM but are expected to be less accurate.

The second goal is to test the lumping process of carbonyl species in RACM. For this purpose, RACM has been extended to a more complete mechanism. This mechanism (called the *extended* mechanism) has a more precise parametrisation of aldehydes and ketones (larger number of lumping groups). The difference between the outputs of this two mechanisms will give the opportunity to testRACM's simplifications.

All four mechanisms have been implemented in a three-dimensional air quality model and tested against pollution measurements in the Milan air basin. The chemical results of the four mechanisms and the consumed CPU time have been compared. Finally, in order to find the most efficient mechanism, the speed/accuracy relation has been investigated.

2. Model description

The four chemical mechanisms have been implemented in the three-dimensional eulerian air quality model TAPOM (Transport and Air POllution Model). The model calculates gas phase chemistry, transport, diffusion, solar radiation and dry deposition. Since TAPOM does not calculate any atmospheric dynamics, the meteorological data are given as input (wind speed, wind direction, temperature, humidity, pressure, air density, turbulent coefficient). The advection is solved with the third order scheme PPM (parabolic piecewise method) by Collela and Woodward (1984).

The co-ordinates of each grid cell can be given to TAPOM as input. This gives to the user the ability to define any suitable grid. TAPOM also allows the user to change easily its main modules, including the chemical mechanism. This feature allows the modification of the whole chemical mechanism, leaving all the other parts of the code unchanged and ensuring, for this work, that the chemistry calculation is the only difference between the four versions. The solver for gas phase chemistry is the one by Gong and Cho (1993).

3. Simulation description and validation

3.1. Description

TAPOM, with the four different chemistry mechanisms, was used to simulate an ozone episode in the Northern Po Valley, Italy, on may 13th 1998. Different models, such as TVM (Martilli et al., 2002), have already simulated this episode and their results have been successfully validated using the measurements of the PIPAPO campaign (Pianura Padana Produzione di Ozono).

This episode shows the formation of a photochemical pollution plume growing from Milan to the northern direction. Two main polluted areas are found in this domain:

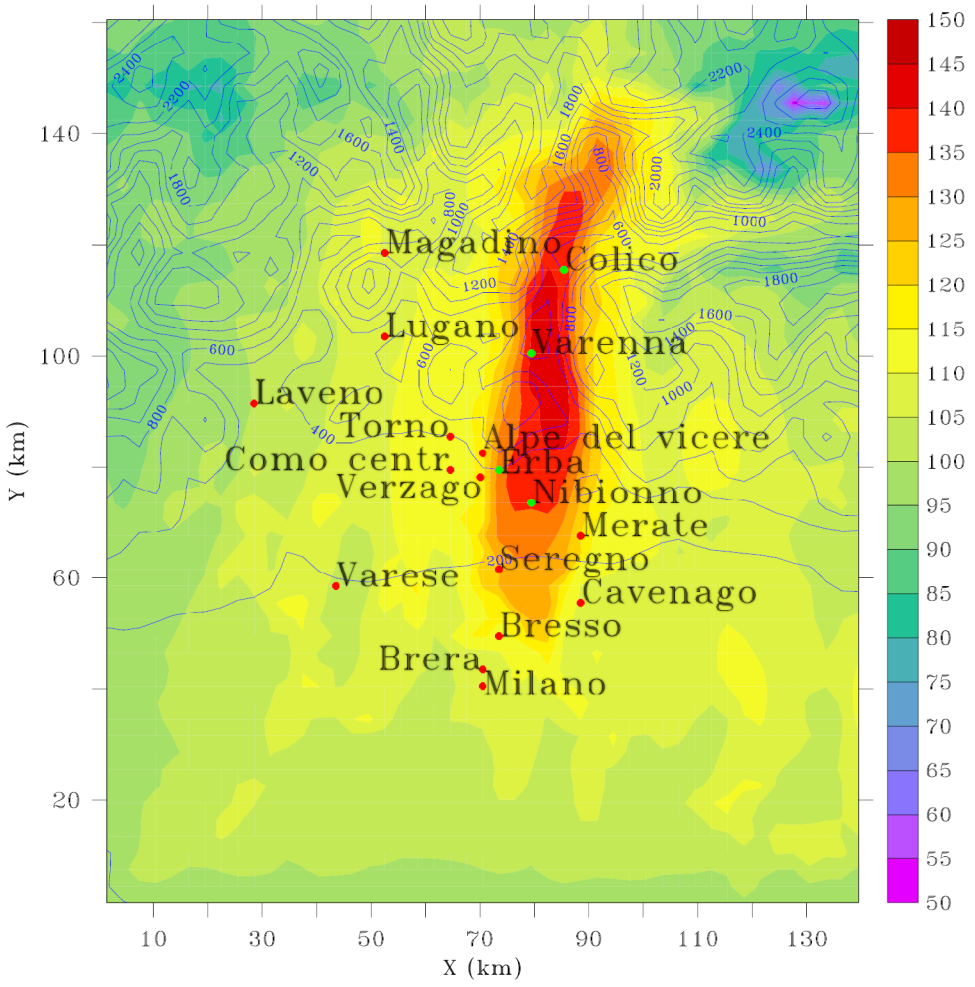

Figure 1: Calculation domain over Milan (47 x 54 square cells of 3 km), measurements stations (colour dots), ozone plume at6 pm (colour filled contour, unit is ppb) and topography contour.

- The Milan area is a typical urban zone with a large amount of primary pollutants.
- The plume area grows north; emissions of the Milan urban area are pushed in this part of the domain by slope winds. This is where secondary pollutants are mainly formed.

The maximum of ozone (~180 ppb) appears about 100 km north of the urban area around 3 pm.

The grid has been chosen terrain-following (keeping flat the top of the mesh, see Chapter Two, Figure 1), with 3 km square cells (horizontally). The domain has a horizontal resolution of 47 by 54 cells(141 x 162 km, see Figure 1) and 12 unevenly spaced vertical levels with maximum heights from 30 (ground cell) to 2000 m. The top of the domain reaches 7300 m.

3.2. Validation of the TAPOM model

For this paper, the whole set of meteorological data calculated by TVM (Thermal Vorticity Model) and validated by Martilli et al. (2002) were given as input to the TAPOM model. The results from TAPOM, using the RACM chemical mechanism, have been compared to the same measurements and validated using the same methodology: the measurements stations have been classified in three categories, using the average night ozone concentration and the maximum daytime concentration.

In the first category the stations are located where important NO_x emissions occur. NO_x reacts with ozone during the night, driving ozone concentration down to zero (see Milan and Brera, Figure 2).

The stations in the third category are far from the sources, in Milan's ozone plume. The night value is rather high because of the low level of emission. The pollution is not produced locally but is transported from the southern urban area (see Erba and Varenna, Figure 2).

Stations in the second category are between category 1 and 3 (see Colico and Varese, Figure 2).

TAPOM generally succeeded in reproducing the low levels during the night in category 1 sites, and the afternoon's peak of the stations of the 3rd category, although it is slightly underestimated.

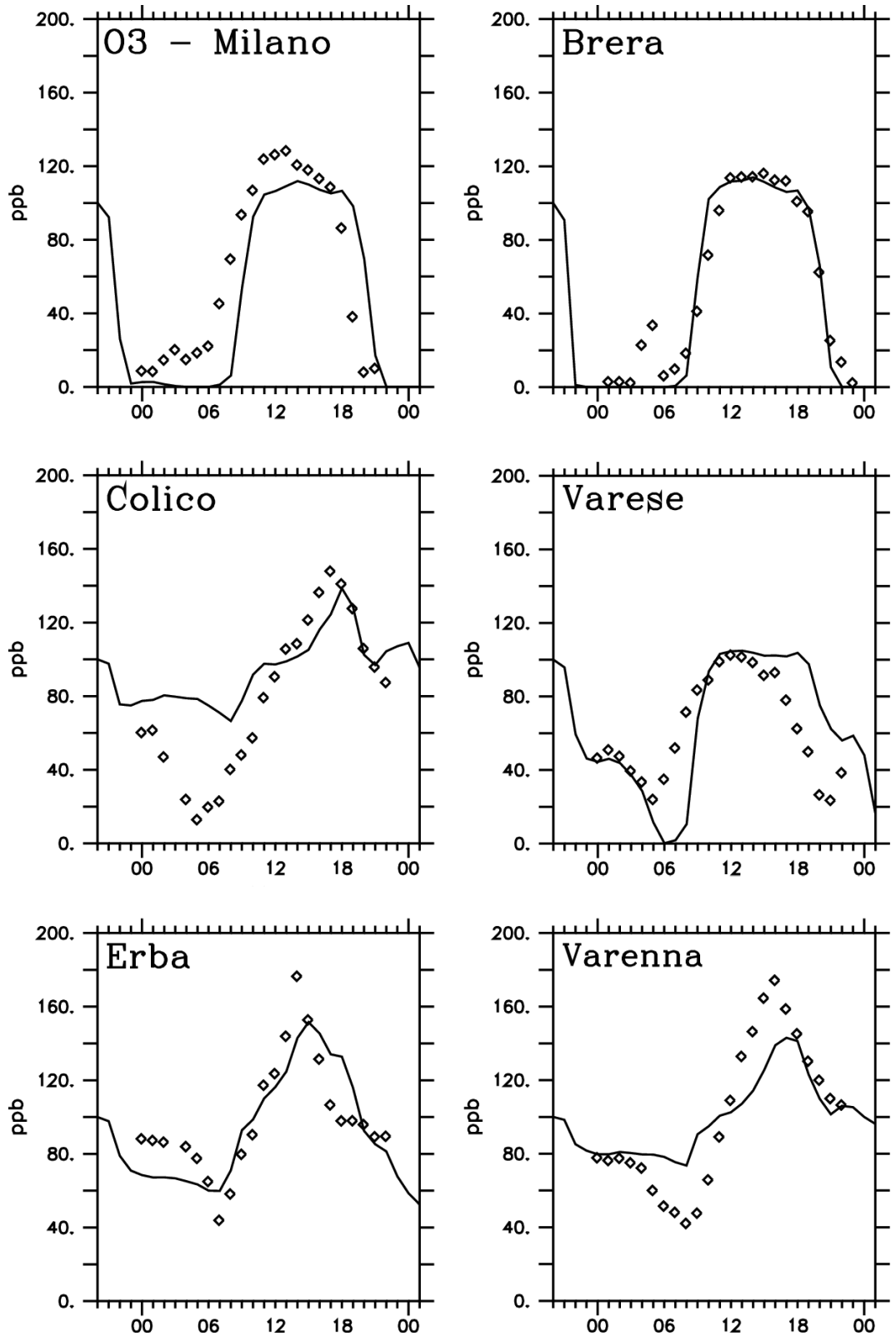

Figure 2: Comparisons between ozone measurements (diamonds) and model results (solid line) for stations in the three categories. Milan and Brera for category 1 (near the emission sources, low ozone during the night and quick grow in the morning), Erba and Varenna for category 3 (far from the sources, in the plume of Milan) and Colico and Varese for category 2 (between categories 1 and 3).

4. Mechanisms description

Four mechanisms are compared. The RACM (Regional Atmospheric Chemistry Mechanism) mechanism (Stockwell et al., 1997) is chosen as reference mechanism. To check whether RACM's precision can be efficiently enhanced, its number of species is increased in the first new mechanism. Increasing the number of species will lead to a more detailed but slower mechanism. Both smaller mechanisms are also based on RACM, in order to see if it can be reduced without losing to much accuracy, increasing the calculation speed. The main characteristics of the four mechanisms are presented in .

Mechanism	*Number of species*	*Number of equations*	*Remarks*
RACM	77	237	Reference mechanism.
Extended	98	367	Aldehydes and ketones are splitin new species.
Reduced	54	142	RO_2 chemistry is reduced.
Small	29	94	Same as above + further reduction of VOCs.

Table 1: The four mechanisms main characteristic

Following are short descriptions of the four mechanisms. For more detailed presentations, please refer to Chapter Three.

4.1. The base mechanism: RACM

RACM includes 77 species and 237 equations. The chemical species are made of 13 stable inorganic species, 4 abundant stable species, 4 inorganic intermediates, 32 stable organic species and 24 organic intermediates. It is designed to be valid for simulations of tropospheric remote to polluted conditions.

4.2. The extended mechanism

The extended mechanism includes 98 species and 367 equations. The RACM species ALD (higher aldehydes) and KET (ketones) are split into several new lumping groups. Higher

aldehydes are divided into 7 groups: CH_2CHO, C_2H_5CHO, a-C_3H_7CHO, i-C_3H_7CHO, R'-CHO, R''-CHO, R'''-CHO, with R' representing a chain of 4 or less C atoms, R'' a chain of 5 C atoms and R''' a chain of 6 or more C atoms. The ketones are split in 6 new groups depending on the number of C atoms (ketones with 3, 4, 5, 6, 7 and more than 7 C atoms). The corresponding short-lived intermediates are added too: RACM's ACO_3 (acetyl peroxy and higher saturated acyl peroxy radicals) and KETP (peroxy radical formed from KET) are split respectively in 7 and 6 new species. This mechanism has therefore a better representation of the reactivity of the aldehydes and the ketones.

4.3. The reduced mechanism

The reduced mechanism is made by condensing the RACM RO_2 chemistry. Only two RO_2 groups are kept (MO_2 -methyl peroxy radical- and ACO_3 -acetyl peroxy radicals lumped together with the unsaturated acyl peroxy radicals, the former TCO3-). All other peroxy radicals (20 species) are lumped into two new groups: XO2 and XO2N.

In the RACM mechanism, when some VOC reacts forming an RO_2, the produced RO_2 depends on the reacting VOC:

$$\begin{aligned}
&VOC_x + HO \rightarrow RO2_x \\
&RO2_x + NO \rightarrow \alpha_{nit} ONIT \\
&\quad + (1-\alpha_{nit})(\alpha_1 PROD_1 + \alpha_2 PROD_2 + \cdots + \alpha_n PROD_n + NO2)
\end{aligned}$$

where ONIT are organic nitrates, and α are product yields. This ensures that the species produced afterward when the RO_2 reacts also depend on the reacting VOC. But with this parametrisation the mechanism has to count as many RO2 as it counts reacting VOC species.

With the new parametrisation, the products of RO_2 reactions appear at the same time as RO_2:

$$\begin{aligned}
&VOC_x + HO \rightarrow \alpha_{nit} XO2N + (1-\alpha_{nit}) XO2 \\
&\quad + \beta(\alpha_1 PROD_1 + \alpha_2 PROD_2 + \cdots + \alpha_n PROD_n) \\
&XO2 + NO \rightarrow NO2 \\
&XO2N + NO \rightarrow ONIT
\end{aligned}$$

with β between (1-α_{nit}) and 1. This allows to generate correct products depending on which VOC reacts and keeps RO_2's in the two new groups. But the products of the RO_2's reactions may appear too early.

4.4. The small mechanism

The small mechanism takes the same RO_2 parametrisation as the reduced mechanism, but other VOCs are more condensed. Only 10 groups are kept on the 34 original species: methane (CH4), alkanes (ALK), alkenes (OLE), aromatics (ARO), formaldehyde (HCHO), higher aldehydes (ALD), unsaturated dicarbonyls (DCB), α-carbonyl aldehydes (ALDR), organic nitrates (ONIT) and peroxyacetylnitrates (PAN).

5. Results

As the extended mechanism is more detailed than the other three mechanisms, the results will be presented with respect to this one. The following comparisons will show the differences between the extended mechanism and the three smaller mechanisms, RACM, the reduced mechanism and the small mechanism. In this way, all comparisons will refer to the largest mechanism and consistent rankings can be made.

5.1. Comparison of the NO_xresults

The chemistry of NO and NO_2 in the model is driven by the following equilibrium:

$$NO_2 + O_2 \underset{h\nu}{\rightleftharpoons} NO + O_3$$

This equilibrium has no effect on the NO_x concentration (NO + NO_2). And as most of the other reactions affecting NO and NO_2 are rather slow during the day, the chemistry has almost no impact on NO_x concentrations near the emission sources. In this situation, NO_x behaves like a passive tracer. Therefore, very few difference between the four mechanisms are expected for the NO_x results.

part a) presents the maximum differences in NO_x concentration for the three station categories. As expected, the differences are very small. The small mechanism produces unsurprisingly the largest differences. The average values on the whole domain are showed in part b). These values are very low, staying under 0.4 ppb. This emphasise the very low mean differences between the four mechanisms for the NO_x.

a)		***RACM***	***Reduced***	***Small***
Cat. 1	Milan	0.21	1.41	-2.71
	Brera	-0.44	2.53	2.79
Cat. 2	Colico	-0.07	0.26	-0.55
	Varese	0.14	0.38	1.40
Cat. 3	Erba	-0.21	0.78	3.76
	Varenna	-0.10	0.24	0.34
b)	Average	0.024	0.142	0.352

Table 2: a) Maximum NO_x concentration differences between the extended and the other mechanisms for the three measurement station categories. Differences are in ppb. b) Average NO_x concentration differences on the whole domain.

5.2. Comparison of the O_3 results

Ozone is a secondary pollutant formed by a complex non linear reaction pathway involving VOC and NO_x as main precursors. Since the lumping of the VOC species, the parametrisation of aldehydes and ketones and/or the RO_2 chemistry differ in the four tested mechanisms, their ozone results are expected not to be exactly the same.

The results of the three bigger mechanisms are very similar. The most important differences appear in the results of the small mechanism (see Figure 3). In every station, the small mechanism consumes more ozone during the night. In polluted areas, the small mechanism's results present a peak of ozone in the morning (see Milan and Brera, Figure 3).

The low ozone concentration during the night is explained by the way the lumped species' rate constants are calculated.

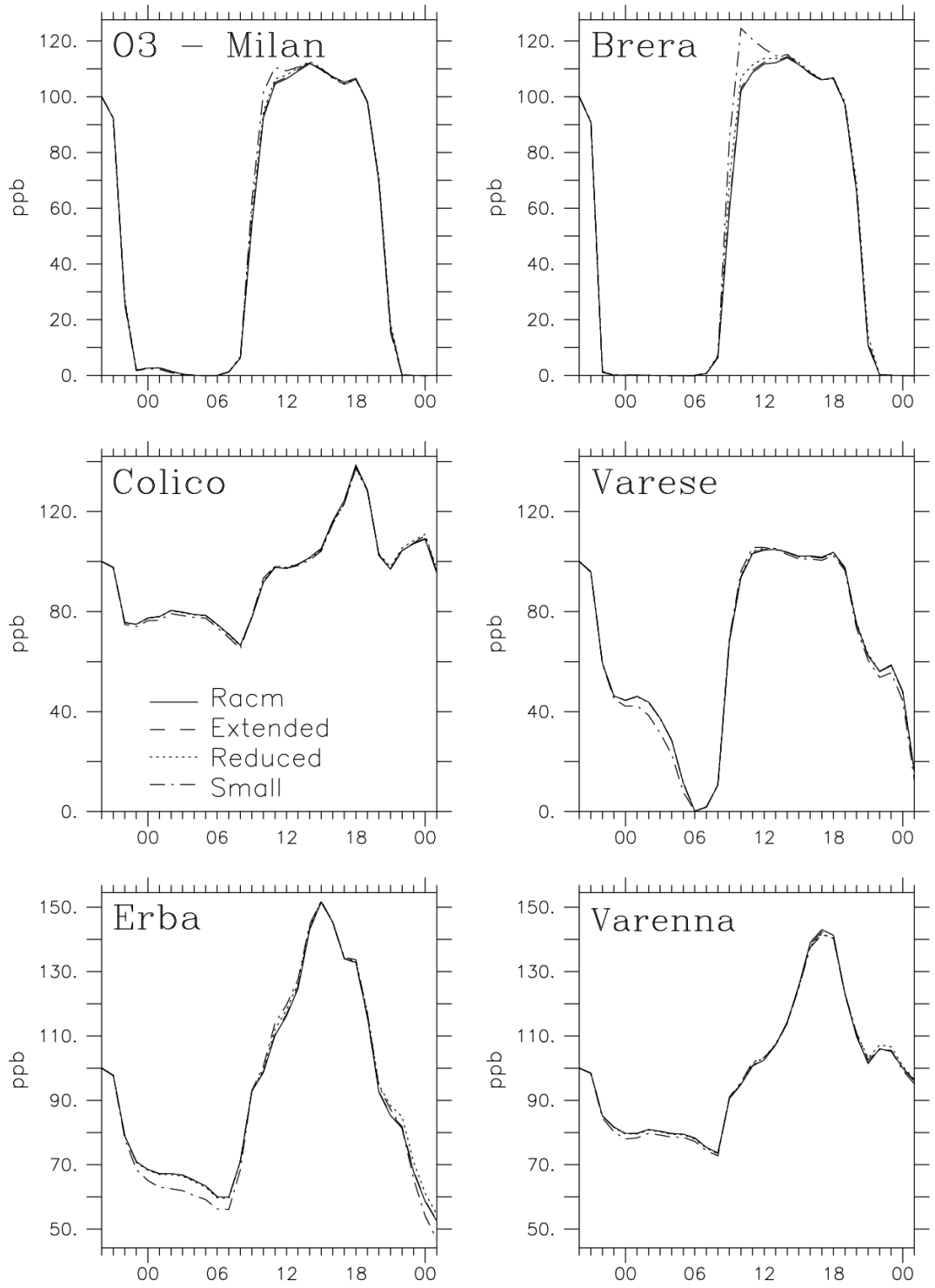

Figure 3: Ozone results for the four mechanisms for the three measurements stations categories. Milan and Brera, cat. 1, Colico and Varese, cat. 3, Erba and Varenna cat. 2. RACM is thesolid black line, extended the dashed black line, reduced is the solid grey line and small is dash-dotted black line. Only the small mechanism gives significantly different results.

The chemical mechanisms are defined by chemical equations of the form:

$$L + x \xrightarrow{k_L^x} \sum_j a_L^j P^j$$

where L is the lumped species. L stands for a number n of real species. The equation above represents all the real equations of these n real species with the species x (real or lumped). P^j are the products formed by the reactions. The rate constant k_L^x and the production coefficient a_L^j are weighted averages of the constants in the real equations (see Chapter Two). A high variability is observed between individual rate constants of the real species. Differences can reach more than two orders of magnitude. The lumped rate constant may therefore be a rough approximation if the lumped species integrates real species with high rate constant variability. Moreover, lumped rate constants are optimised for the reactions with OH. This means that a real species with low reactivity can be considered as very quicker in the mechanism when integrated in a lumped species. An example is given by the reaction of alkenes (OLE) with ozone giving products like formaldehyde (HCHO). The small mechanism shows almost two third less OLE than the other three mechanisms during the night and almost one third more HCHO (Figure 4). OLE is over reacting with ozone during the night, leading to an over production of formaldehyde.

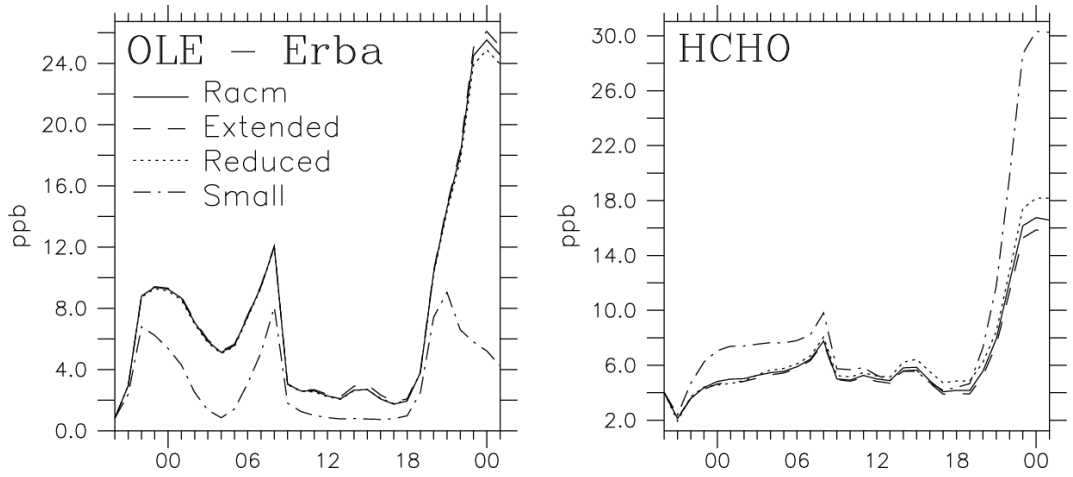

Figure 4: OLE (alkenes) and HCHO in Erba. Alkenes react with O_3 giving HCHO. The small mechanism (dash-dotted line) consumes too much OLE, over generating HCHO.

This over production of secondary hydrocarbons which accumulates during the night causes the morning peak of ozone in polluted areas (Milan and Brera, Figure 3). As soon as the sun has raised, NO_2 is photo-dissociated in NO and O·, the latter reacting with O_2 to produce ozone. In presence of enough VOC and NO_x, RO_2 is reduced by NO, regenerating NO_2. This cycle leads to a huge amount of ozone released in a short time in the morning.

Ozone comparison over the whole domain

To compare the ozone concentrations over the whole domain, two criteria have been used:

- The mean difference $\frac{1}{N_{hour} \cdot N_{cell}} \sum \left| O_3^{ext} - O_3^{mech} \right|$
- The maximum difference $\max \left| O_3^{ext} - O_3^{mech} \right|$

"ext" in superscript is for the extended mechanism and "mech" is for RACM, the reduced mechanism or the small mechanism. In both cases, the absolute value of the differences is used in order to avoid a neutralisation of the positive and negative differences. The results, in ppb, are presented in :

	RACM	***Reduced***	***Small***
Mean ozone difference	0.12	0.23	0.63
Maximum ozone difference	2.37	13.07	37.53

Table 3: Mean and maximum ozone differences (ppb) between the extended mechanism and the other three mechanisms over the whole domain.

The mean differences stay very low (the bigger value is lower than 0.7 ppb) for the three comparisons, but there is a notable increase in the maximum differences from RACM to the small mechanism. This means that the differences are generally not important, but locally, bigger differences occur. The maximum difference between RACM and the extended mechanism is very small, meaning that the tow mechanisms are very close to each other.

5.3. Comparison of secondary VOCs

The reduced mechanism produces too much secondary hydrocarbons in less polluted areas. This is due to the new chemistry parametrisation of the RO_2 species. The products of the reactions of RO_2 with NO are formed at the same time as the RO_2 themselves:

$$VOC + OH \rightarrow XO2 + \text{Secondary VOC}$$
$$XO2 + NO \rightarrow NO2$$

In RACM we have:

$$VOC + OH \rightarrow RO2$$
$$RO2 + NO \rightarrow NO2 + \text{Secondary VOC}$$
$$RO2 + HO2 \rightarrow ROOH$$
$$RO2 + RO2 \rightarrow \text{Products including secondary VOCs}$$

This means that these secondary VOCs are overestimated in the reduced mechanism under low NO_x concentration conditions. Example is given with HCHO (Figure 5).

Brera is in the Milan neighborhood and has high NO_x concentrations. At this station, the HCHO concentrations given by the reduced mechanism are very close to the RACM results. On the contrary, in Varenna, NO_x is rather low, and the reduced mechanism overestimates the HCHO concentration.

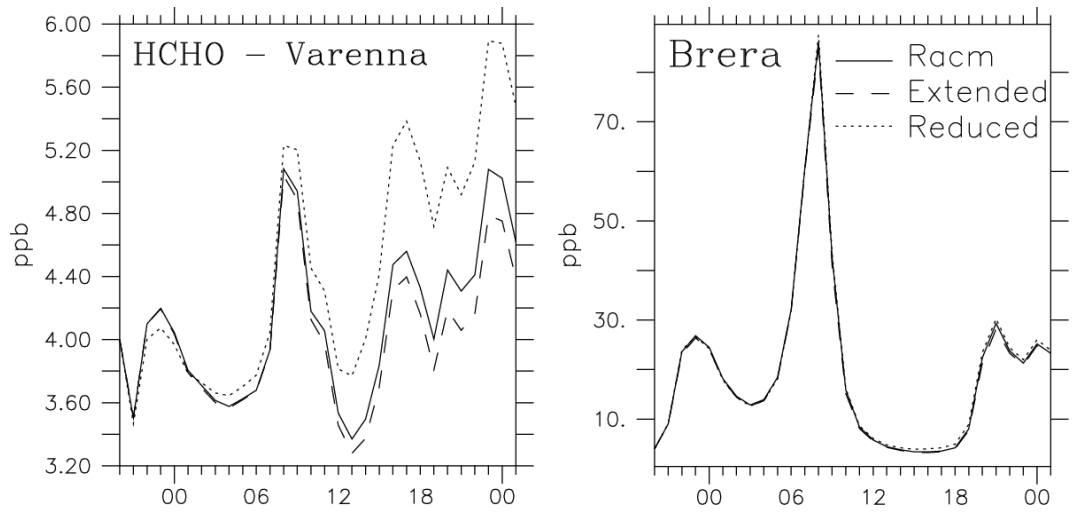

Figure 5: HCHO results at Varenna and Brera. The reduced mechanism produces too much HCHO in less polluted areas (Varenna).

5.4. Testing RACM's parametrisation of carbonyl species

RACM uses less carbonyl species than the extended mechanism (see § 4.2). A comparison of the results of these two mechanisms will point out the errors which may be induced by this parametristion. If the RACM parametrisation is good, there will be only little difference between both mechanisms' results.

Considering the ozone results, the two mechanisms are very similar. There is actually no significant difference in ozone concentrations. Looking at the species that differ in the two mechanisms, it is seen that ketones are lower in the extend mechanism. The reactivity of ketones is lower in RACM because it is calculated from the least reactive ketones. They are therefore more consumed, explaining this difference. Consequently the species formed by these reactions (like RO_2 for instance) are expectedly higher in the extended mechanism.

5.5. General comparison

In order to have a general overview of the comparison of the four mechanisms, the Average of the Absolute Value (AAV) of the relative differences between the extended and the three other mechanisms are calulated:

$$AAV = \frac{\sum_{i=1,n} |X_i|}{n} \quad \text{with} \quad X_i = \frac{R_i^{ext} - R_i^{mech}}{\overline{R^{ext}}} \quad \text{and} \quad \overline{R^{ext}} = \frac{\sum_{j=1,n} R_j^{ext}}{n}$$

R is the calculations' results for the variable of interest (O_3, NO_x, RO_2 and aldehydes), “ext” in superscript stands for the simulation with the extended mechanism and “mech” is for RACM, the reduced or the small mechanism. X is therefore the difference between two mechanisms normalised with respect to $\overline{R^{ext}}$, the average result of the extended mechanism. Using relative difference allows to compare species having different ranges of values, and using the mean result $\overline{R^{ext}}$ as reference instead of R_i^{ext} (the actual cell value), avoids finding meaninglessly high results when dealing with very small values. The mean, computed at ground level for the whole domain

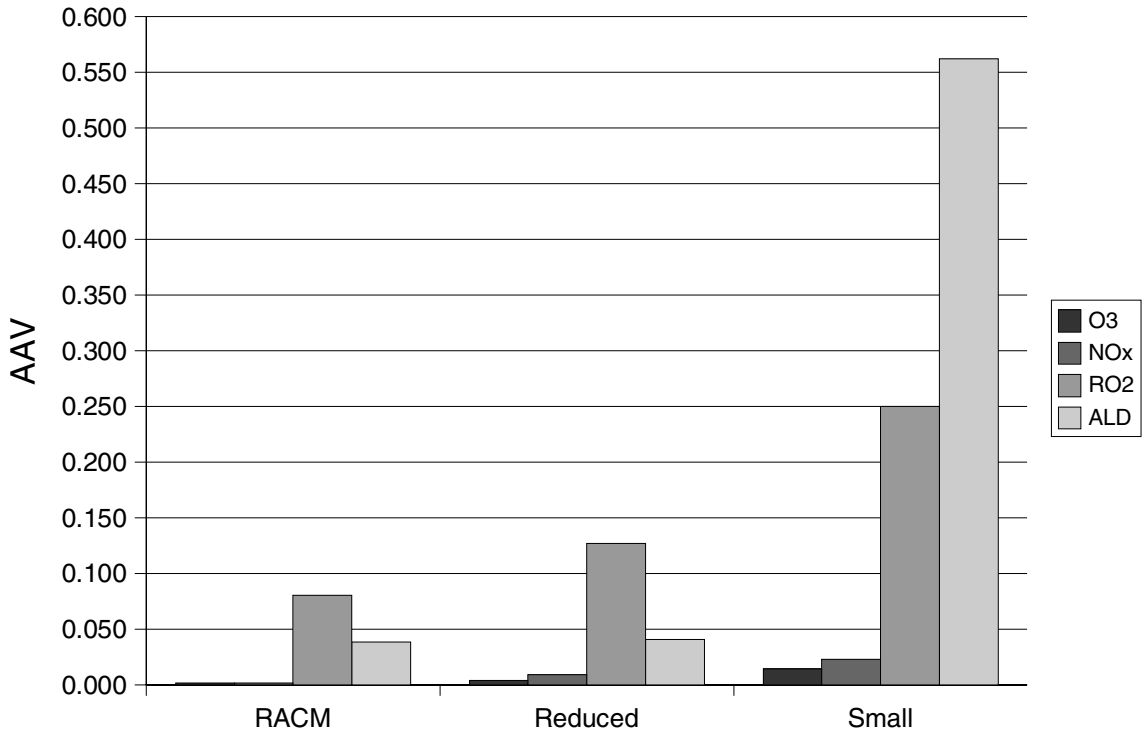

Figure 6: AAV of the relative differences between the extended and the other three mechanisms for O_3, NO_x, RO_2 and aldehydes. For ozone and NO_x, differences are always under 2.5 %. Differences grow from RACM to the small mechanism. Only the small mechanism shows very significant differences for secondary VOC.

and for 24 hours, is performed on the absolute value of X in order to avoid that the positive and negative differences neutralise each other. Results are presented in Figure 6.

It shows that for RACM. the reduced mechanism and the small mechanism, the ozone relative difference stay under 1.5 %. For NO_x, it is always lower than 2.5 %. For RACM, the four differences are under 4 %. This shows again the good behaviour of RACM in comparison with the extended mechanism.

The secondary VOC are in a reasonable range (up to 13 %) for RACM and the reduced mechanism but grow very high for the small mechanism (56 %). This is a strong restriction for the use of this mechanism.

5.6. CPU time

A chemical solver's sensitivity to the number of species (with respect to CPU time) depends on the type of the solver. In a general manner, increasing the number of chemical species with an

explicit and non iterative solver generates a linear increase of CPU time. An implicit or iterative solver needs a matrix inversion which leads to a second order growth of time consumption. The Gong and Cho's solver divides the chemical reactions in two groups (Gong W. and Cho H.-R., 1993): the faster reactions are solved implicitly, and the slower ones explicitly. The growth of CPU time evolves therefore neither linearly nor quadratically but somehow in between.

The simulations have been performed under SUN Solaris 8, on SUN Blade 100 workstations. All calculations simulated 29 hours. The run using RACM took 5 hours and 30 minutes to complete the simulation. Taking this time as reference, the comparison with the other three mechanisms are presented in .

Mechanism	*Number of species*	*CPU time*	*Ratio*
RACM	73	5 h 30	1
Extended	98	10 h 30	1.9
Reduced	54	2 h 30	0.45
Small	29	1 h 30	0.27

Table 4: CPU time needed by the four mechanisms to complete a 29 hours simulation.

The extended mechanism is almost twice slower (1.9 times) than RACM (10 hours and 30 minutes). With a calculation time of 2 and a half hours, the reduced mechanism is more than twice as fast as RACM (0.45). The small mechanism is unsurprisingly the faster (1 and a half hour), with almost a fourth of the RACM CPU time (0.27).

These differences are clearly due to the number of species. To emphasise this, Figure 7 shows the growth of the CPU time with respect to the number of species.

In order to assess the efficiency of the different mechanisms, the following criterion (c) has been defined:

$$c = 1 - \frac{\overline{m}}{\max(\overline{m})} \quad \text{with} \quad \overline{m} = \frac{1}{N_{hour} \cdot N_{cell}} \sum \left| O_3^{ext} - O_3^{mech} \right|$$

The meaning of $\overline{m}$ is the average ozone concentration at ground level over all the cells and all the hours of the absolute value of the differences between the extended and the three others

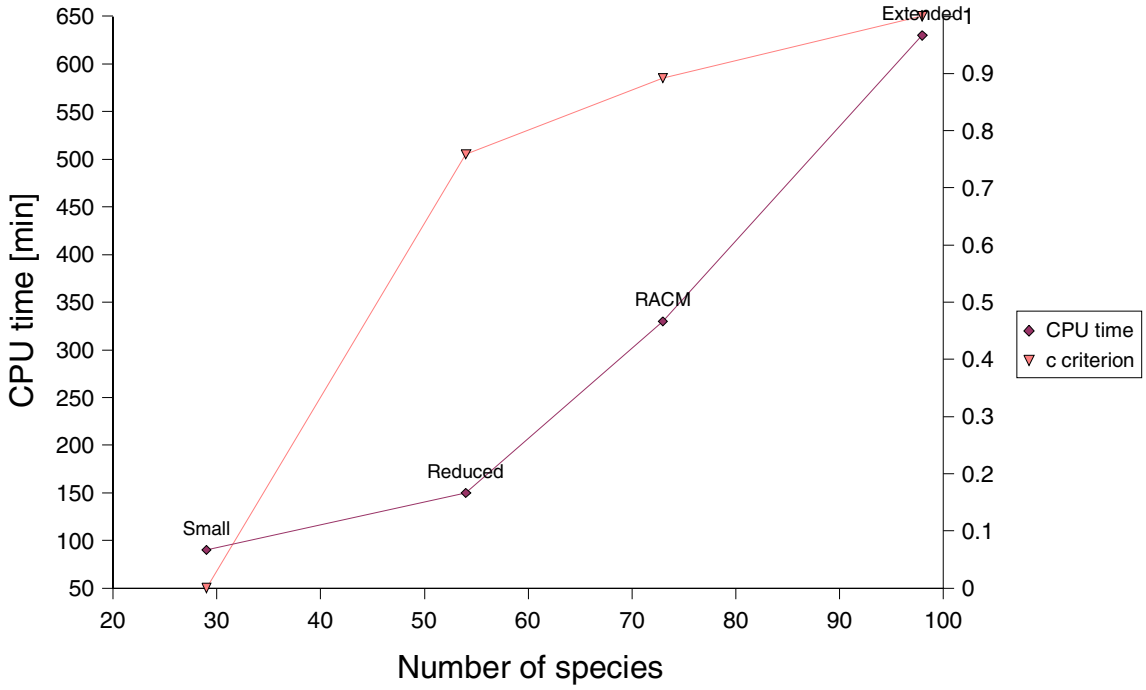

Figure 7: Number of species of the mechanisms versus CPU time. The line with diamonds shows the growth of CPU time with respect to the number of species in the four tested mechanisms. One can clearly see the quadratic tendency due to the part of the equations solved with a matrix inversion. The second line is the c criterion (see definition in text). It emphasises the efficiency of the the reduced mechanism which give very good ozone results with a low calculation time.

mechanisms. It represents the average error resulting of the use of the smaller mechanisms with respect to the extended mechanism. The c criterion is its inverted normalised value. By definition, c is equal to 1 for the extended (no difference) and to 0 for the mechanism with the largest difference.

The plot of the c criterion clearly shows that the reduced mechanism gives the best possible results for a very low cost in calculation time (high value of c).

6. Conclusion

In order to be efficient (fast and accurate), three-dimensional numerical air quality models must include an optimal chemical mechanism. A chemical mechanism gives more accurate results if it has a large number of species but the time needed for the calculation grow fast with the number of species. A comparison of four chemical mechanism has been presented. The three new

mechanisms are based on the RACM mechanism. The so called extended mechanism is an extension of RACM, the reduced mechanism has a different RO_2 chemistry which uses less RO_2 chemical species and the small mechanism has the same reduction as the latter but has additional VOC lumping. The analysis of the results seems to indicate that an optimum exists between speed and accuracy, which is reached with mechanisms of lower size than RACM.

The four mechanisms are implemented in the three-dimensional model TAPOM and run on the domain of Milan. Very few differences have been found between the chemical results of RACM and the extended mechanism, but the latter needs almost twice the CPU time. This justifies the aldehydes and ketones parametrisation in RACM, with all the ketones lumped in one KET species and all the aldehydes lumped in ALD. Compared to the low enhancement of the results with the extended mechanism its high time consumption is prohibitive for its use in a three-dimensional model for usual applications. It should be kept for simulations needing a higher level of accuracy especially in aldehydes and ketones. The reduced mechanism is more than twice as fast as RACM. Its good results (particularly ozone) allows its use for modelling photochemical pollutant plumes, but there are restrictions with secondary VOC. For ozone, the reduced mechanism is the best compromise between accuracy and calculation speed. The small mechanism is almost twice faster than the reduced, but there are significant differences in ozone prediction and VOC. It can still be used for ozone modelling but will be particularly useful for quick preliminary works.

References

Collela P., Woodward, P. R. 1984, The piecewise parabolic method (PPM) for gas-dynamical simulations. Journal of Computational Physics, 54, pp. 174-201.

Gong W., Cho, H.-R. 1993, A numerical scheme for the integration of the gas-phase chemical rate equations in three-dimensional atmospheric models. Atmospheric Environment, Vol. 27A, No. 14, pp. 2147-2160.

Kuebler, J., Giovannoni, J.-M., Russell, A. G., 1996, Eulerian modelling of photochemical pollutants over the swiss plateau and control strategies analysis. Atmospheric Environment, Vol. 30, No. 6, pp. 951-966.

Martilli, A., Neftel, A., Favaro, G., Kirchner, F., Sillman, S., Clappier, A., 2002, Simulation of the ozone formation in the northern part of the Po Valley. Journal of Geophysical Research, Vol. 107, No. D22.

Stockwell W. R., Kirchner, F., Kuhn, M., Seefled, A., 1997, A new mechanism for regional atmospheric chemistry modelling. Journal of Geophysical Research, Vol. 102, No. D22, pp. 25847-25879.

Vautard R., Beekmann, M., Roux, J., Gombert, D., 2001, Validation of a hybrid forecasting system for the ozone concentration over the Paris area. Atmospheric Environment, Vol. 35, No. 14, pp. 2449-2461.

Chapter Five

Response of four chemical mechanisms to emission reduction

Abstract

Because of the high non linearity of the ozone production, the effect of a reduction of the ozone precursors (NO_x and VOCs) on its formation is unpredictable. Numerical simulation with reduced emissions is a convenient way to forecast the regions where a reduction of the NO_x or VOC emissions is more efficient.

Four chemical mechanisms of different size (RACM, an *extended*, a *reduced* and a *small* mechanism), are used to simulate a 35 % reduction of the NO_x or VOC emissions on three domains (Mexico City, Milan and Bogota) presenting different emissions strengths and meteorological conditions. RACM, the extended and the reduced mechanism present very similar ozone results in the three domains. The small mechanism shows a higher variability in ozone results and significant differences on the ozone peak in Mexico City and Bogota.

The response of the four chemical mechanisms to emissions reduction is evaluated by considering the ozone difference between the runs using reduced NO_x and reduced VOC emissions. With respect to the extended mechanism, RACM presents differences under 5 %, the reduced mechanism's differences reach 14 % (both with small variations) and the differences with the small mechanism varies from 19 to 40 %.

Comparing RACM and the reduced mechanism with the extended mechanism on three domains and two emissions reduction scenarios shows little differences. The three larger mechanisms give similar results on the ozone reduction forecast. The small mechanism is likely to give very overestimated ozone reductions, but the four mechanisms agree on the generated NO_x and VOC sensitive areas.

Keywords: Mesoscale modelling, Tropospheric chemistry, Chemical mechanism generation, VOC lumping, Emissions reduction strategies.

1. Introduction

One of the most important feature of 3D mesoscale air pollution models is their ability to simulate emission abatement strategies. To investigate the better way of reducing pollutant emissions, numerous simulations have to be performed with various scenarios of emission reductions. Since chemistry resolution requires a long calculation, being able to use fast chemical mechanisms can save a lot of time.

Although reduced chemical mechanisms and more detailed mechanisms give similar ozone results, see Chapter Four (Junier et al., 2004), the behaviour of the different mechanisms may be different when the emissions are decreased. Moreover, the differences can vary from a modelling area to another, depending on the emission strengths and the meteorological conditions.

This Chapter presents a comparative study of the response of four chemical mechanisms to emissions abatement strategies in three different cities: Milan, Mexico City and Bogota. Three simulations (one with the whole emissions inventory and two emissions reduction scenarios) are performed for each simulated city and each chemical mechanism.

2. Short description of the chemical mechanisms

This study is based on the four different chemical mechanisms previously described in Chapters Three and Four (Kirchner et al. (2004) and Junier et al. (2004)). The detailed presentation of the process leading to their generation is presented in Chapter Two. The following description is a very short reminder of their main characteristics:

- The reference mechanism for this work is the RACM mechanism (Stockwell et al., 1997). It contains 77 chemical species and 237 equations. The three other mechanisms are based on RACM.
- The extended mechanism has a more precise aldehyde and ketone parametrisation, with 98 species and 367 equations.
- In the reduced mechanism, the 22 RACM RO_2 species are condensed in 4 new species. It consists of 54 species and 142 equations.
- The small mechanism comprises the same RO_2 chemistry as the reduced mechanism with less VOC species (10 instead of 34), finally counting 29 chemical species and 94 equations.

3. Description of the simulation domains.

Simulations have been performed on the urban areas of Milan (Italy), Mexico City (Mexico) and Bogota (Colombia). These cities lie at different latitudes and longitudes and have different topographical characteristics, which leads to different meteorological conditions. The different numbers of inhabitants and population densities result in different kind of pollutant emissions. As air quality depends mainly on emissions and meteorology, theses differences are used to test the robustness of the different chemical mechanisms.

3.1. Emissions

The emissions of primary pollutants are characterised by the amount of emitted NO_x and VOCs (total emissions in mol and density in mol km^{-2}), and the reactivity of the emitted VOCs (total reactivity in cm^3 s^{-1} and density in cm s^{-1}). Emissions depend mostly on human activity (transportation, industries, heating). The number of inhabitants and the population density of an urban area have therefore a very important impact on the amount of emitted pollutants. These characteristics for the three cities of interest are presented in Table 1.

Mexico City is the second most populated urban area in the world (after Tokyo) with about 20 million inhabitants living on a surface of 1476 km^2 (11'700 inhabitant per km^2). The population of Bogota is about 6.8 million inhabitants with a density of 4318 inhabitants per km^2. The build-up area of Milan with 5.5 million people counts less inhabitants than Bogota but the relatively small extent of its urban surface leads to a higher population density (7377 inhabitant per km^2). This concentration of population, coupled with the important industrial activity of Milan leads to high levels of emissions. Milan lies on a plain at 120 m ASL while Bogota and Mexico City were built on high elevated plateaux (2600 and 2200 m ASL respectively). This high altitude situation, because of the lower atmospheric pressure, increases the CO emission (less O_2 causes bad combustion of gas in car engines) and decreases the NO_x emissions (less N_2).

	Inhabitants		***NO_x emissions***		***VOC emissions***		***Emitted VOC reactivity***	
	total	***density*** [km^{-2}]	***total*** [mol]	***density*** [mol km^{-2}]	***total*** [mol]	***density*** [mol km^{-2}]	***total*** [cm^3 s^{-1}]	***density*** [cm s^{-1}]
Mexico	20 mio	11700	$25.3 \cdot 10^4$	32.9	$35.9 \cdot 10^4$	46.7	$3.43 \cdot 10^{15}$	45.0
Milan	5.5 mio	7377	$14.3 \cdot 10^4$	42.2	$24.7 \cdot 10^4$	70.7	$3.19 \cdot 10^{18}$	940.2
Bogota	6.8 mio	4318	$3.4 \cdot 10^4$	3.1	$4.9 \cdot 10^4$	4.4	$1.45 \cdot 10^{14}$	1.3

Table 1: The population density is computed using the surface of the urbanised area and the various emission densities using the surface in which emission occurs: Mexico City: 7695 km2 (380 cells), Milan: 3393 km2 (377 cells), Bogota: 11'120 km2 (695 cells).

3.2. Meteorology and ozone plume.

The concentration of pollutants in the atmosphere is highly dependent on the meteorological conditions. The wind and atmospheric stability in the lower atmosphere influence the pollutant dispersion while the temperature and the solar radiation influence the rate constants of numerous chemical reactions.

The simulated periods for the three cities correspond to three ozone pollution episodes which always appear under high solar radiation and low wind conditions. In such situations, the atmospheric circulation is mainly driven by ground heating, which generates upwards slope winds during the day and downwards slope winds during the night.

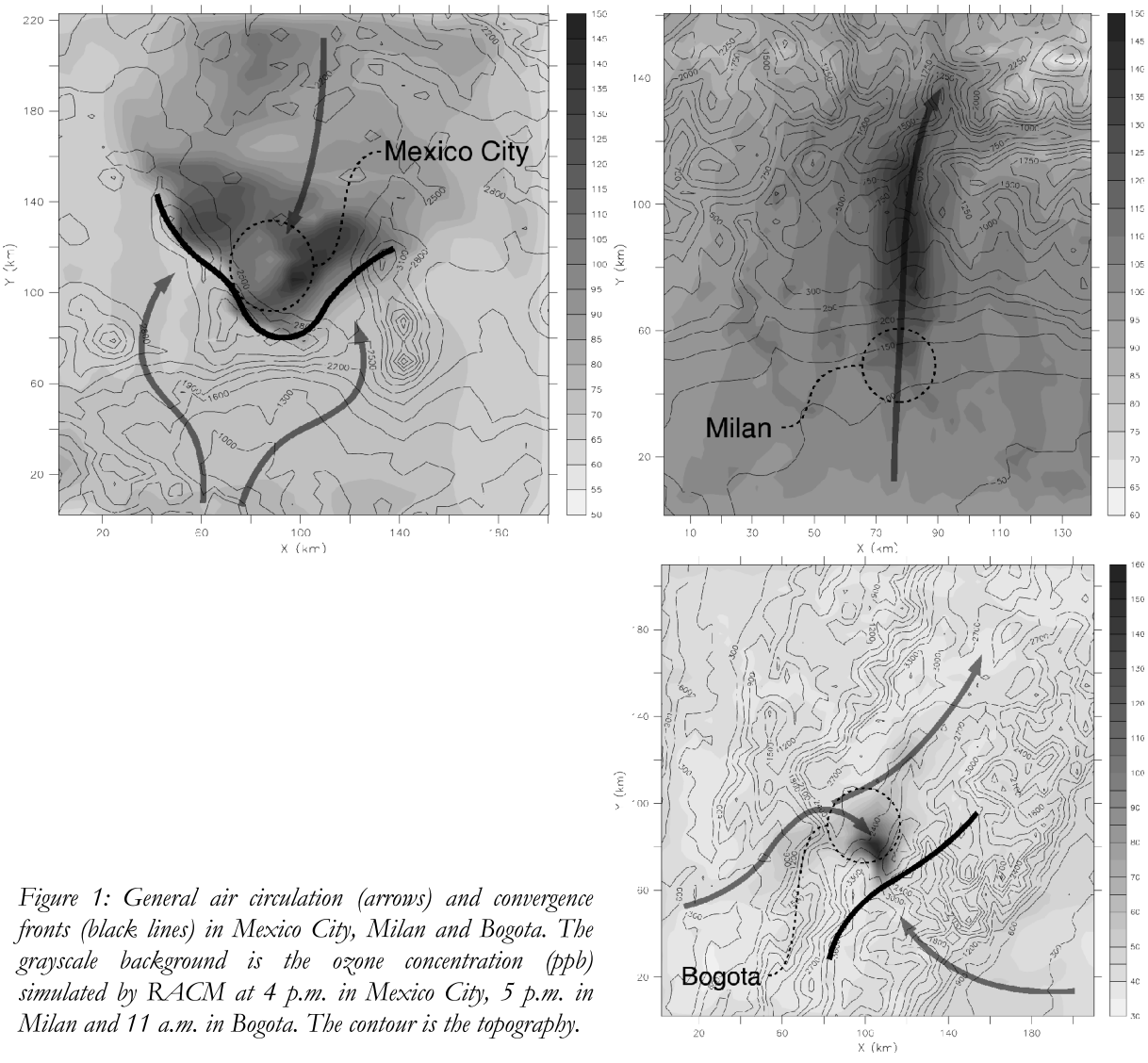

Figure 1: General air circulation (arrows) and convergence fronts (black lines) in Mexico City, Milan and Bogota. The grayscale background is the ozone concentration (ppb) simulated by RACM at 4 p.m. in Mexico City, 5 p.m. in Milan and 11 a.m. in Bogota. The contour is the topography.

Milan is located at 100 m ASL in the Po Valley, about 40 kilometres south of the Alps. Because of the ground cooling, the atmosphere is very stable during the night and the wind is very weak in the Po Valley. The ozone precursors emitted by the city are accumulated in Milan and its surroundings. After sunrise, the ground temperature increases, generating slope winds in the Alps and northwards flows in the Po Valley. These winds transport the pollution accumulated in the plain from Milan to the Alps. Simultaneously, the photochemical processes leading to ozone generation take place in the plume and a maximum of ozone (172 ppb) is found at 1 p.m. outside the city (see Figure 1).

Mexico City and Bogota show some similarities. Both cities lie on high plateaux and are surrounded by mountain. Like in Milan, the winds are weak at night and the ozone precursors are accumulated at ground level. During the day, the situation is different than in Milan, slope winds are generated on both sides of the mountains around the cities and flow convergences appear over the urban area. The ozone maximums are found at the convergence fronts where pollutants accumulates (see Figure 1). In Mexico, the slope winds generate southward and northward flows (Bossert, 1997, Fast, 1998). The convergence line is oriented in the west-east direction and appears in the south of the city. In Bogota, the slope winds blow from the west and east of the city and create a rather south-north oriented convergence line. In Mexico and Bogota, the ozone maximum appears at the convergence lines over the cities rather than over the countryside like in Milan. A major difference between the episode of Mexico and Bogota is that in Mexico the ozone maximum is reached at 4 p.m. (146 ppb) when it appears at 11 a.m. in Bogota (169 ppb).

3.3. Emission reduction with RACM

In order to assess the behaviour of the four mechanisms to emissions reduction, two simulations have been performed, with 35 % reduction of the NO_x or VOC emissions.

The results of the simulations with emissions reductions are presented with plots of the difference in ozone values between the runs with VOC and NO_x reductions (O_3 produced with

65 % VOC – O_3 produced with 65 % NO_x hereafter referred to as ΔO_3). Two regions show up in these plots: if ΔO_3 is positive, the NO_x reduction is more efficient and the region is called NO_x-sensitive. If the VOC reduction happens to be the more efficient, ΔO_3 is negative and the area is named VOC-sensitive.

In each case, regions of high NO_x emission concentration, like in the city centres, are VOC sensitive. During the day, the plume generally moves out of urban areas to regions of less NO_x emissions and the sensitivity switches to NO_x sensitive (Couach et al., 2004, Martilli et al., 2002).

In Mexico City, NO_x sensitive regions appear at 12 a.m. on the north-east of the urban area, growing until 4 p.m. (see Figure 2) and then progressively fading after sunset. The city centre remains VOC sensitive all day long.

In Milan, all the build up area surrounding the city is VOC sensitive until 12 a.m. From 1 to 5 p.m., almost all the domain become NO_x sensitive, except Milan itself which remains slightly VOC sensitive. After 5 p.m., the city and its surroundings progressively become more VOC sensitive. The most significant effect of the NO_x emission reduction is seen in the ozone plume, but it is less important than for both of the other cities (Figure 2).

Bogota is the city where the NO_x reduction produces the largest effect. The only VOC sensitive region is the very centre of the city, from 8 to 10 a.m. (Figure 2). Afterwards, the plume is NO_x sensitive. Outside the city, the domain is rather insensitive to NO_x or VOC emissions reduction.

4. Comparison of the four chemical mechanisms

The results of the four chemical mechanisms will be compared in each city. The comparisons are based on the differences in ozone concentration at ground level between the extended and the other three mechanisms. Please refer to Chapter Four (Junier et al. (2004)) for the reason of the

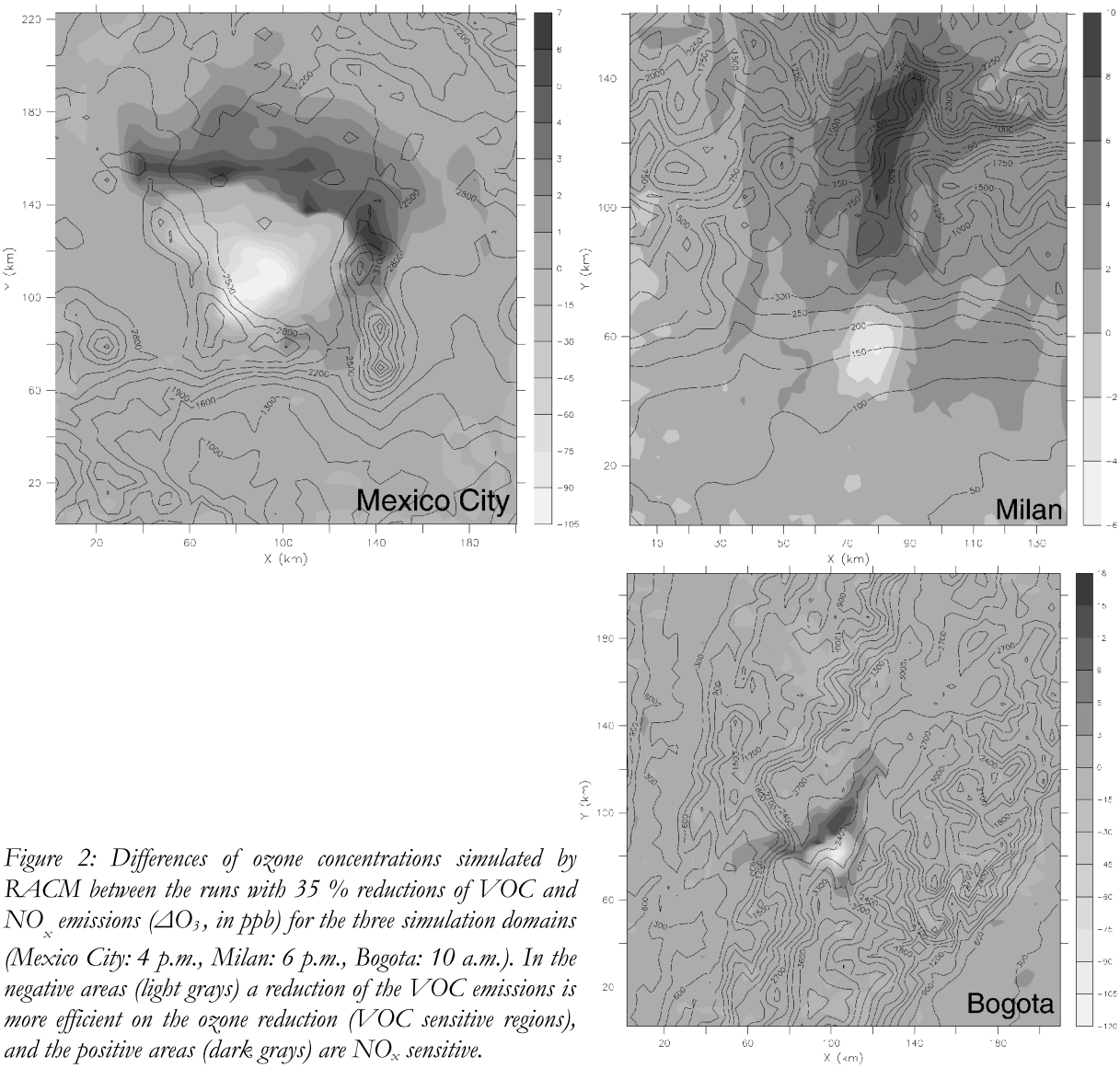

Figure 2: Differences of ozone concentrations simulated by RACM between the runs with 35 % reductions of VOC and NO_x emissions (ΔO_3, in ppb) for the three simulation domains (Mexico City: 4 p.m., Milan: 6 p.m., Bogota: 10 a.m.). In the negative areas (light grays) a reduction of the VOC emissions is more efficient on the ozone reduction (VOC sensitive regions), and the positive areas (dark grays) are NO_x sensitive.

choice of the extended mechanism as reference. The following parameters are used to perform the comparison:

- *The average of the absolute value of the relative difference (AAV)* of ozone between the extended mechanism and the other three mechanisms is used to show the overall difference on 24 hours simulation. It is computed by (see details in Chapter Four):

$$AAV = \frac{\sum_{i=1,n} |X_i|}{n} \quad \text{with} \quad X_i = \frac{R_i^{ext} - R_i^{mech}}{\overline{R^{ext}}} \quad \text{and} \quad \overline{R^{ext}} = \frac{\sum_{j=1,n} R_j^{ext}}{n} \ .$$

  The AAV is calculated for O_3, and ΔO_3.

- *The root-mean-square of the relative difference (RMS)* of ozone between the extended mechanism and the three other mechanisms is calculated with the following formula:

$$RMS = \sqrt{\frac{\sum_{i=1,n} X_i^2}{n}}$$

The RMS is another way to perform a mean of differences providing an always positive result, by squaring the variable. This also gives more importance to values more distant from unity. The RMS are provided as double check for the global tendencies of the differences' growth with respect to the several mechanisms.

- *The ozone peak*. The value of the ozone peak resulting of the runs with the four chemical mechanisms will be compared as well as the place and time of the peak concentration.

4.1. Ozone results

4.1.1. The average of the absolute value of the relative ozone difference

Generally, the average of the absolute value (AAV) of the ozone differences show growing differences from RACM to the small mechanism. Only in Mexico City, the AAV is smaller with the reduced mechanism than with RACM (Figure 3). For the three calculation domains, RACM

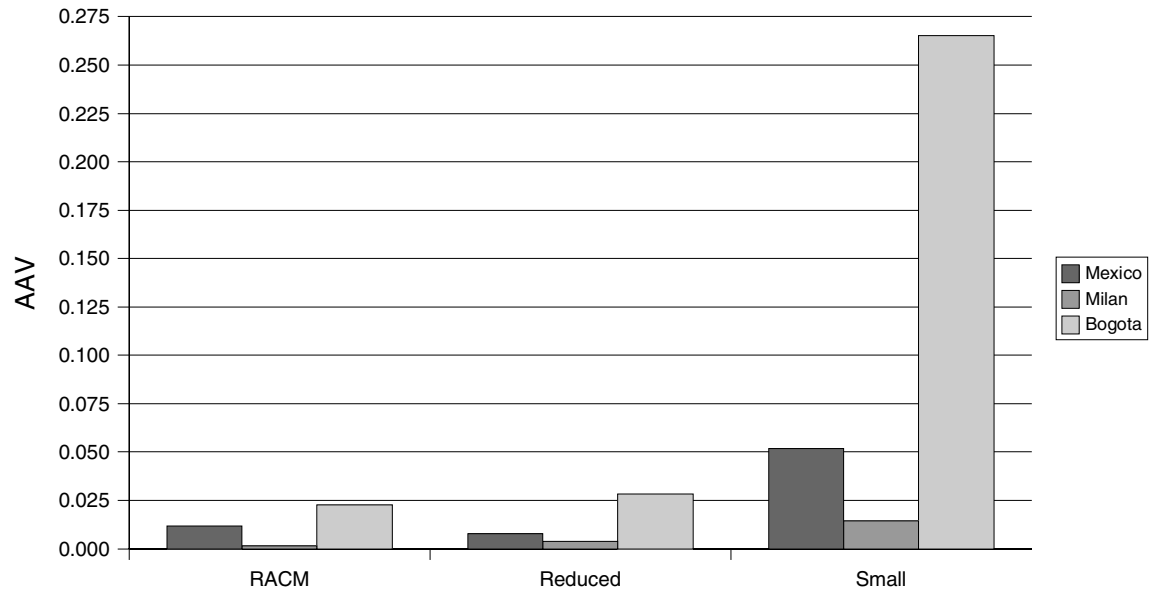

Figure 3: AAV of the ozone differences between the extended mechanism and the three smaller mechanisms for the different cases.

	RACM		*Reduced*		*Small*	
	AAV	***RMS***	***AAV***	***RMS***	***AAV***	***RMS***
Mexico City	0.012	0.013	0.008	0.011	0.052	0.085
Milan	0.002	0.003	0.004	0.007	0.014	0.024
Bogota	0.023	0.024	0.028	0.033	0.265	0.279

Table 2: AAV and RMS of the differences of ozone between the extended mechanism and the three other mechanisms for the three city cases.

and the reduced mechanism are very close to each other. The AAV of the ozone differences are in the order of 2.5 % for RACM and the reduced mechanism. The small mechanism presents a much higher variability. While ozone differences are quite small in Milan (1.4 %), they become significant in Mexico City with 5.2 % and grow up to 26 % in Bogota.

4.1.2. The root-mean-square of the relative difference

The RMS of the relative ozone difference between the extended mechanism and the three smaller mechanism, presented with the AAV in Table 2, are very close to the AAV values. Their values are always a little larger but follow the same pattern.

4.1.3. The ozone peak

The ozone peak is not significantly different for the three larger mechanisms, but the peak generated by the small mechanism is larger for the three cities. Bogota is the only domain where a difference in the time and location of the ozone peak is generated. The peak concentration of ozone generated by the small mechanism appears at 10 a.m. instead of 11 a.m. (Figure 4), and it is located one cell upwind.

	Extended	***RACM***	***Reduced***	***Small***
Mexico City	150	147 (-2 %)	155 (3 %)	226 (51 %)
Milan	174	173 (-0.7 %)	177 (2 %)	183 (5 %)
Bogota	159	160 (1 %)	172 (8 %)	247 (56 %)

Table 3: Peak value of ozone (ppb). In brackets are shown the relative differences with respect to the extended mechanism.

The cell in which the peak occurs in Bogota is inside the urban area with the small mechanism, while with the other mechanisms, the peak is reached an hour later and the air masses are pushed one cell further, out of the city. This explains the difference seen during the night in Figure 4 for Bogota. The ozone concentration for the small mechanism is zero during the night because of the high level of emissions in the urban cell, and the other three mechanisms show a value of about 30 ppb, which is the background value for this domain.

On Bogota and Mexico City, the small mechanism highly overestimates the ozone peak (56 % and 51 % respectively, see Table 3), although on Milan, even if the peak is also too high, it stays in a reasonable range (5 %). As showed in Chapter Four (Junier et al. (2004)), the small

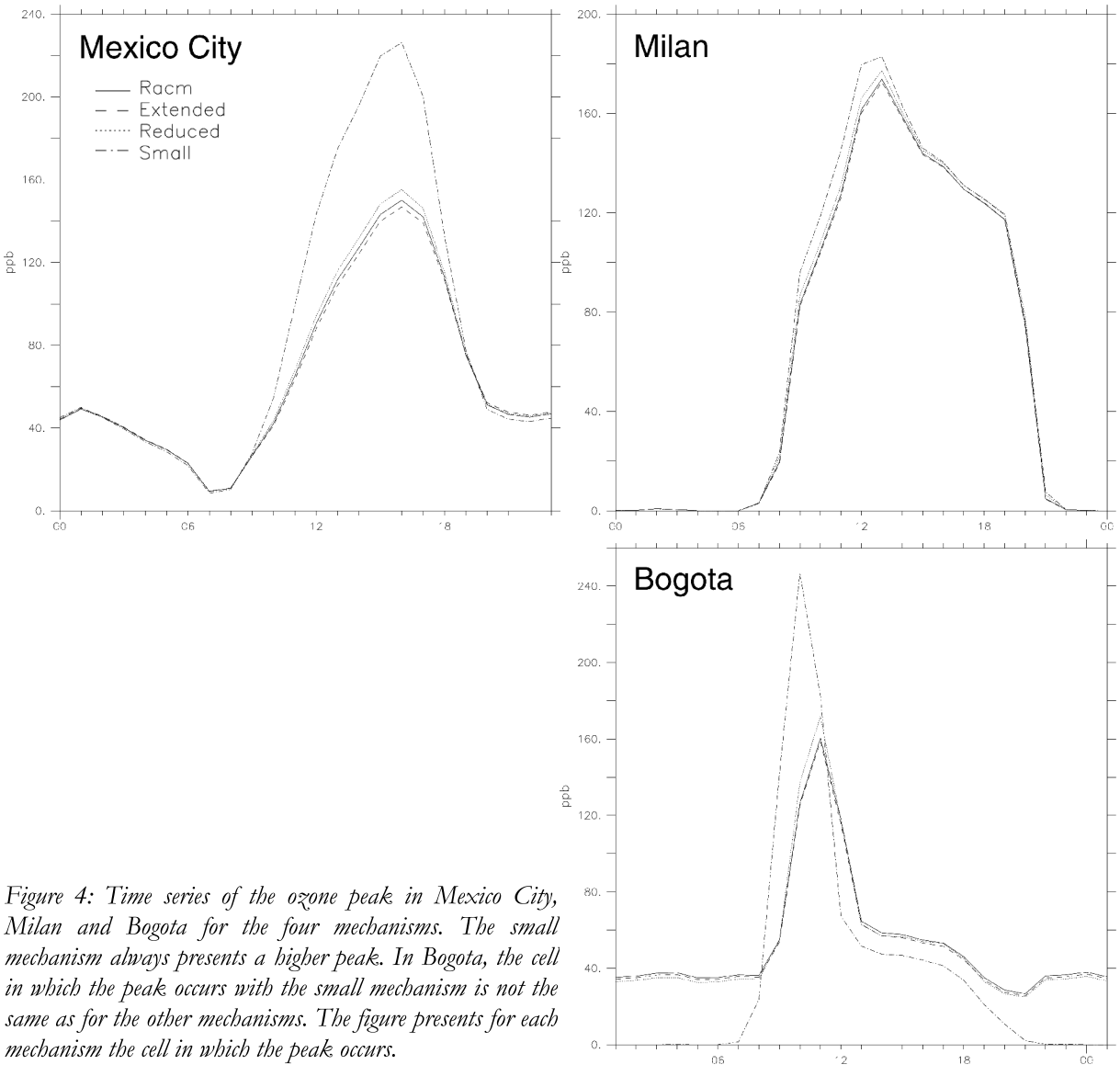

Figure 4: Time series of the ozone peak in Mexico City, Milan and Bogota for the four mechanisms. The small mechanism always presents a higher peak. In Bogota, the cell in which the peak occurs with the small mechanism is not the same as for the other mechanisms. The figure presents for each mechanism the cell in which the peak occurs.

mechanism present a higher reactivity, which is responsible for the higher ozone concentrations. The difference between the small over estimation in Milan and the cases of Mexico City and Bogota lies in the NO_x or VOC sensitivity of the area in which the peak occurs. In Mexico City and Bogota, the peak occurs inside a VOC sensitive region. The higher reactivity of the VOC in the small mechanism therefore generates a very important ozone production. In Milan, the region is NO_x sensitive, which leads to a lower overestimation of the ozone peak.

4.2. Emission reduction for the four mechanisms

The reduction of the emissions points out the two chemical regimes which drive the production of O_3. To compare the sensitivity of the chemical mechanisms to emission reduction, the following comparisons are performed:

- *The AAV of the ΔO_3 differences between the four mechanisms* give a general understanding of the differences generated by the mechanisms when the chemical mechanism is changed (see § 3.3 for the definition of ΔO_3).
- *The cumulated surface of the NO_x sensitive area* is a more precise parameter about the ozone production sensitivity for each mechanism.
- *The minimum and maximum values of ΔO_3* and their location in space and time indicate the amplitude of the maximum ozone reduction and where it take place.

4.2.1. The AAV of the ΔO_3 differences between the four mechanisms

As described in § 3.3, ΔO_3 points out the sensitivity of ozone production to a reduction of NO_x or VOC emissions. A small ΔO_3 difference between the extended mechanism and a smaller mechanism denotes a similar response to emissions reduction. The average of the absolute value of this difference is a summary of the response for the whole domain. Figure 5 presents the AAV of the ΔO_3 difference between the extended mechanism and the other mechanisms for the three simulations cases.

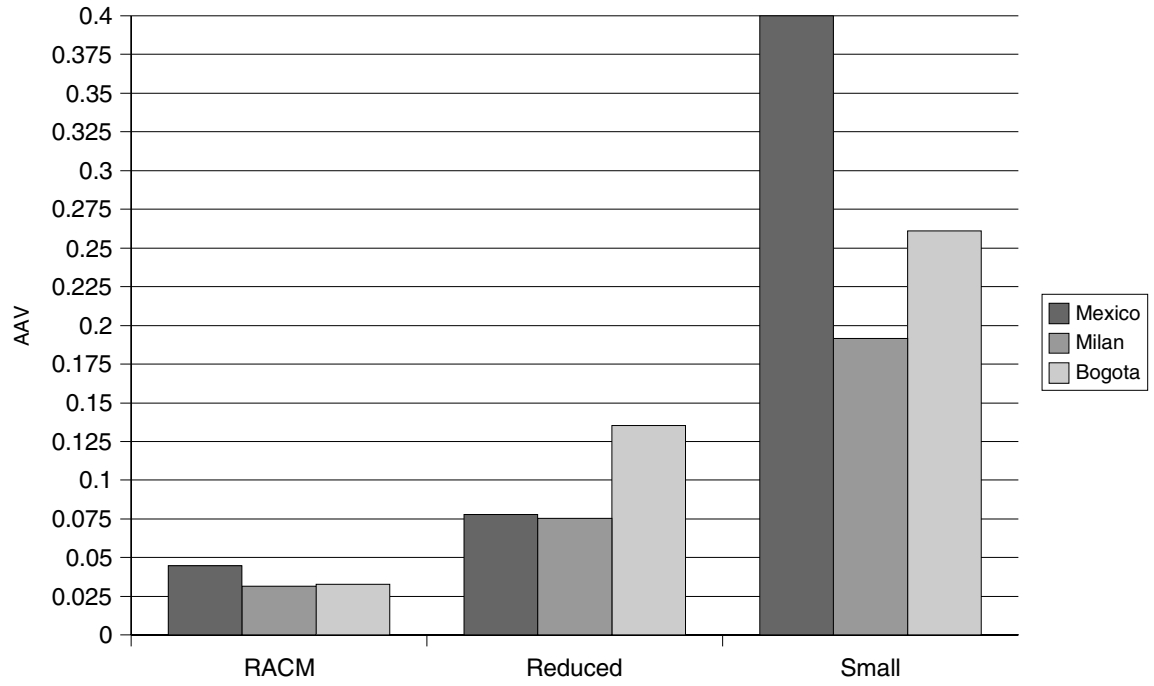

Figure 5: Average of the absolute value of the ΔO_3 (see text for the definition) difference between the extended mechanism and the smaller mechanisms.

RACM shows average differences under 5 % for the three simulation domains. The reduced mechanism reaches 14 % in Bogota but stays lower than 8 % in Milan and Mexico City. Therefore, the three larger mechanisms show similar response to emissions reduction. On the other hand, the differences found by using the small mechanism are larger and present an important variability (19 to 40 %).

The RMS (Table 4) shows the same trend: growing differences from RACM to the small mechanism and higher variability for the small mechanism.

	RACM		***Reduced***		***Small***	
	AAV	***RMS***	***AAV***	***RMS***	***AAV***	***RMS***
Mexico City	0.045	0.196	0.078	0.333	0.400	2.305
Milan	0.032	0.070	0.075	0.179	0.192	0.570
Bogota	0.033	0.123	0.136	0.587	0.261	2.169

Table 4: Average of the absolute value (AAV) and root-mean-square (RMS) of the ΔO_3 (see text for the definition) difference between the extended mechanism and the smaller mechanisms.

4.2.2. The location and value of the ΔO_3 maximum and minimum.

The location of the maximum of ΔO_3 is the place where a reduction of the NO_x emissions is the most efficient. The place where VOC reduction is more efficient is found at the location of the larger negative value (minimum) of ΔO_3. If two mechanisms forecast similar ozone reductions, the ΔO_3 values generated by both mechanisms will be close to each other.

Table 5 presents relative differences of the ΔO_3 maximum and minimum with respect to the extended mechanism and indicates if the peak differences occur in a different cell or at a different time.

	RACM		***Reduced***		***Small***	
	Max	***Min***	***Max***	***Min***	***Max***	***Min***
Mexico City	9.30% [c]	0.47%	-22.09%	-5.35%	-55.81%	-35.96% [c]
Bogota	-1.67%	0.54%	-23.85%	-4.06%	-36.82%	-48.51% [t]
Milan	7.02%	-0.78%	-9.65% [c,t]	-12.31%	-26.32% [c,t]	-62.74%

Table 5: Relative differences of the minimum and maximum values of ΔO_3 with respect to the extended mechanism. In superscript, the letter informs whether the peak occurs at a different place or time: a c *denotes that the peak appears in a different cell, a* t *at a different time.*

In Mexico City, the maximum value of ΔO_3 is not found at the same place with RACM and the extended mechanism. This is actually the same peak, since they appear at the same time and the NO_x sensitive area is rather extended and stable in Mexico City. This is due to the wind pattern which accumulates air masses over the city (see § 3.2). It creates more stable NO_x and VOC sensitive regions than in cases where the wind pushes a plume away. Other variations are quite small, the minimum value of ΔO_3 (largest negative difference) with the small mechanism is located one cell beside on Mexico City or one hour earlier on Bogota. On the Milan domain, time and location of the peaks are closely bound together due to the regular northwards wind. With the small mechanism, the peak is reached earlier. Air masses have less time to be transported and therefore the cell in which the peak is reached is situated a few cells upwind. The reduced mechanism's maximum is one hour late, locating the peak a few cells downwind.

4.2.3. The surface of the NO_x sensitive area

The surface of the NO_x sensitive regions are compared using the proportion of the domain which comes out to be NO_x sensitive along the day. A portion of territory is considered as NO_x sensitive if ΔO_3 is positive. Table 6 presents the percentage of the domains that are NO_x sensitive for the four mechanisms.

	Extended	***RACM***	***Reduced***	***Small***
Mexico City	54.59 %	54.48 % (0.11)	54.57 % (0.02)	60.29 % (-5.70)
Milan	43.70 %	43.25 % (0.45)	44.12 % (-0.42)	44.46 % (-0.76)
Bogota	69.59 %	69.47 % (0.12)	69.43 % (0.16)	70.79 % (-1.20)

Table 6: Percentage of the domains that is NO_x sensitive depending on the chemical mechanism. In brackets are presented the difference with respect to the extended mechanism.

The differences of the NO_x sensitive areas with respect to the extended mechanism (Table 6, in brackets) are generally lower than 1.2 % of the total calculation domain, except with the small mechanism on Mexico City where it is of 5.7 %. The small mechanism presents higher and always negative percentage differences. This denotes generally more VOC sensitive results for this mechanism.

The location and time of the ozone peak as well as the extent of the NO_x sensitive areas are generally the same whichever mechanism is used. On the other hand, the values of the ozone maximum and minimum are higher with the reduced mechanism (10 to 24 %) and even more different with the small mechanism (26 to 63 %).

5. Conclusion

When calculating a large number of emissions scenarios, smaller mechanisms can save a lot of time if they give reliable results. This study compared the response to emissions reductions of four chemical mechanisms of different sizes on three different calculation domains (Mexico City,

Milan and Bogota). The cities vary by their emission concentrations and meteorological conditions.

The comparison of the ozone results on the different domains show very small differences between the extended mechanism, RACM and the reduced mechanism. On the other hand, the small mechanism presents significant differences with respect to the extended mechanism. In addition, the differences vary much more from one case to another with the small mechanism than with the other mechanisms. The ozone peak is generally well reproduced with all mechanism but is overestimated in Mexico City and Bogota with the small mechanism because of the higher reactivity of the VOC in this mechanism. RACM and the reduced mechanism give similar ozone results in comparison with the extended mechanism and can be used for 3D mesoscale air quality simulations, only the small mechanism should be used with caution, for instance for quick qualitative calculations.

Two simulations with reduced emissions (35 % of NO_x or VOC emissions) have been performed on the three domains. The ozone difference between the runs with VOC and NO_x reductions (noted as ΔO_3) shows the regions where VOC or NO_x reductions is more efficient in decreasing the ozone concentration. The three cities showed very different behaviour of their NO_x and VOC sensitive regions.

The ΔO_3 differences between the extended mechanism and the three smaller mechanisms are small for RACM and the reduced mechanism but are important for the small mechanism. The ozone reduction achieved with the NO_x or VOC emissions reduction are almost the same with RACM and the extended mechanism, slightly overestimated with the reduced mechanism and largely overestimated with the small mechanism. The cumulated surfaces of the NO_x sensitive areas calculated for the four chemical mechanisms do not present important differences, but the small mechanism presents generally smaller NO_x sensitive regions.

RACM and the extended mechanism give similar results when the emissions are reduced. When emission reduction scenarios are tested for ozone reduction, the use of the extended mechanism is not recommended, because of its higher requirements in input data and computer resources, unless a high level of detail is needed in chemical species. The reduced mechanism is very efficient, giving really reliable results on ozone reduction and on forecast of the ozone production chemical regimes. This mechanism is recommended for ozone abatement strategies studies. Notable differences appear when the small mechanism is compared to the extended mechanism. The results of this mechanism present large variations from a calculation domain to another. Because of its high VOC reactivity and the high VOC sensitivity of is results, ozone reductions may be unpredictably overestimated.

References

Bossert J. E., 1997, An Investigation of flow regimes affecting the Mexico city region. Journal of Applied Meteorology, 36, pp. 119-140.

Couach O., Kirchner F., Jimenez R., Balin I., Perego S., van den Bergh H., 2004, A Development of Ozone Abatement Strategies for the Grenoble Area using Modelling and Indicators. Atmospheric Environment, in press.

Fast, J. D. and Zhong S., 1998, Meteorological factors associated with inhomogeneous ozone concentrations within the Mexico city basin. Journal of Geophysical Research, Vol. 103, pp. 18927-18946.

Junier M., Kirchner F., Clappier A., van den Bergh H., 2004, The Chemical Mechanism Generation Programme CHEMATA, Part 3: Comparison of Four Chemical Mechanisms for Mesoscale Calculation of Atmospheric Pollution. Submitted to Atmospheric Environment.

Kirchner F., Junier M., Clappier A., 2004, The Chemical Mechanism Generation Programme CHEMATA, Part 2: Boxmodel study about the influence of species lumping and od new kinetic data on the simulation results. Submitted to Atmospheric Environment.

Martilli, A., Neftel, A., Favaro, G., Kirchner, F., Sillman, S., Clappier, A., 2002, Simulation of the ozone formation in the northern part of the Po Valley. Journal of Geophysical Research, Vol. 107, No. D22.

Chapter Six

Conclusion

This work presented a chemical mechanism generation programme and a comparative study of different chemical mechanisms for tropospheric air quality modelling. Four chemical mechanisms have been compared in order to assess the efficiency of two lumping methods against calculation time and accuracy.

Generating different chemical mechanisms for mesoscale air quality numerical simulations has as principal goal to optimise the requirements of computational resources. For instance, sparing calculation time on gas phase chemistry calculation allows its use for new concerns like aerosol dynamics, high resolution modelling or short time scale air pollution forecasting.

Lumping the immense number of VOC species which play a role in atmospheric pollution in a convenient smaller number of mechanisms species provides a solution that keep enough details to generate accurate results in reasonable calculations times. The calculation of all kinetic data of a lumped mechanism is a tremendous work unless carried out by a generation programme. CHEMATA has been designed to generate lumped and explicit tropospheric gas phase chemical mechanisms. In addition, CHEMATA also provides a easy way of updating mechanism when new kinetic data is available or of modifying the lumping method.

CHEMATA was used to generate three new mechanisms of different sizes. They have been first tested in a box model. Using the RACM as base mechanism, an *extended mechanism* was generated to test the lumping process of the carbonyl species in RACM. RACM was found to underestimated the ozone values for simulations of more than three days under polluted

conditions. Two smaller mechanisms were also generated to compare two lumping methods. Reducing the number of VOC lumping groups shows much more influence on the results (using the *small mechanism*) than just reducing the number of peroxy radicals by a new parametrisation (with the *reduced mechanism*).

The four mechanisms have been implemented in the 3D eulerian air quality model TAPOM. The comparisons on 3D simulations had the same goals than the box models studies with the addition of a calculation time comparison. TAPOM have been run with the four chemical mechanisms on three simulations domains (Mexico City, Milan and Bogota) presenting different emissions strengths and meteorological conditions. No significant differences have been found in the chemical results of RACM and the extended mechanism. RACM, the extended and the reduced mechanism present very similar ozone results in the three domains, while the small mechanism present differences which can be very important. The small mechanism presents a higher variability in ozone results and significant differences on the ozone peak in Mexico City and Bogota. The CPU time comparison showed a very important increase of the computational time when the extended mechanism is used. On the other hand, the reduced mechanism showed an interesting gain of time. As expected, the small mechanism was found to be the fastest. The analysis of these results shows that the reduced mechanism is a very good compromise between speed and accuracy.

Because of the high non linearity of the ozone production the effect of a reduction of the precursors on ozone formation may be unpredictable. Numerical simulation with reduced emissions allows to study the NO_x and VOC sensitive behaviour of a photochemical plume. The four chemical mechanisms simulated a 35 % reduction of the NO_x or VOC emissions on the three different domains. Comparing RACM and the reduced mechanism to the extended mechanism on three domains with two emissions reduction scenarios shows little differences. The three larger mechanisms give similar results on the ozone reduction forecast when using

reduced emissions. The small mechanism is likely to give very overestimated ozone reductions, but the four mechanisms agree on the generated NO_x and VOC sensitive areas.

From all these comparisons, it can be concluded that:

- The treatment of the carbonyl species in RACM do not induce notable errors in mesoscale modelling. The use of the extended mechanism should be kept for special simulations when enhanced precision in VOCs is required or for time periods longer than 2 or 3 days.
- The reduced mechanism is the best compromise between CPU time and accuracy. When calculating photochemical pollution, or emission reduction scenarios, this mechanism can save a lot of time.
- The small mechanism present a clear tendency to produce more VOC sensitive results, which can lead to severe ozone overestimations. It should only be used for qualitative simulation when CPU time is a critical issue.

Future work

The reduced mechanism can be used with a daily pollution forecast 3D model. The CPU time saved in chemistry will allow to run emissions abatement strategies and forecast simulations in the same time, facilitating the making of decision. It will also be possible to add aerosol formation processes, which nowadays became a very important issue.

CHEMATA is currently restricted to gas phase chemistry and to compounds including C, H, O and N. The development of CHEMATA is still in progress. The programme will be able to generate mechanisms including aerosol chemistry (gas to aqueous phase transitions and aqueous phase chemistry) without atom restrictions. Like for the present work, it will be interesting to test the robustness of chemical mechanisms which include aerosol chemistry under different chemical or meteorological conditions.

Appendix

The three new mechanisms

In the following pages, the three new mechanisms are detailed by listing the three output files of CHEMATA. These files contain all the chemical equations and the required data for solving the system. With every equation are given the type of the reaction (photolysis, thermal decomposition, troe and troe equilibrium) and the corresponding constants. The calculation of the reaction rates for each type of reaction are presented hereafter:

- **Photolysis reactions** are denoted by: phorat (A, B)

  B is the number of the photolysis reaction (as numbered in RACM) and A is a multiplying factor that takes into account the lumping of the original RACM species. TAPOM attributes to every equation the correct photolysis rate calculated by TUV according to B:

  $$k = A \cdot rate(B)$$

  where rate(B) is the photolysis rate calculated by TUV for equation B:

1. NO2 → O3P + NO
2. O3 → O1D + O2
3. O3 → O3P + O2
4. HONO → HO + NO
5. HNO3 → HO + NO2
6. HNO4 → 0.65 HO2 + 0.65 NO2 + 0.35 HO + 0.35 NO3
7. NO3 → NO + O2
8. NO3 → NO2 + O3P
9. H2O2 → HO + HO
10. HCHO → H2 + CO
11. HCHO → 2 HO2 + CO
12. ALD → NO2 + HO2 + CO
13. OP1 → HCHO + HO2 + HO
14. OP2 → ALD + HO2 + HO
15. PAA → MO2 + HO
16. KET → ETHP + ACO3
17. GYL → 0.13 HCHO + 1.87 CO + 0.87 H2
18. GLY → 0.45 HCHO + 1.55 CO + 0.80 HO2 + 0.15 H2
19. MGLY → CO + HO2 + ACO3
20. DCB → TCO3 + HO2
21. ONIT → 0.20 ALD + 0.80 KET + HO2 +NO2
22. MACR → CO + HCHO + HO2 + ACO3
23. HKET → HCHO + HO2 + ACO3

If B is negative, the attributed rate is calculated by:

-17	GLY → 2 CO + 2 HO2	rate = 0.4 * rate(18)
-18	GLY → CO + HCHO	rate = 0.13 * rate(17) + 0.45 * rate(18)
-24	GLY → 2 CO + H2	rate = 0.87 * rate(17) + 0.15 * rate(18)

- **Thermal decompositions** (second order reactions) are denoted by: thermal(A, E/R)

  k in $cm^3\ s^{-1}$ is calculated by:

$$k = A \cdot \exp\left(\frac{-E/R}{T}\right)$$

  where T is the temperature.

- **Troe reactions** are denoted by: troe (k_0^{300} , n, k_∞^{300} , m)

  k in cm^3 molecule^{-1} s^{-1} is calculated by:

$$k = \left(\frac{k_0(T)\cdot[M]}{1+\frac{k_0(T)\cdot[M]}{k_\infty(T)}}\right)\cdot 0.6^{\left\{1+\left[\log_{10}\left(\frac{k_0(T)\cdot[M]}{k_\infty(T)}\right)\right]^2\right\}^{-1}}$$

  where: $k_0(T) = k_0^{300}\cdot\left(\frac{T}{300}\right)^{-n}$, $k_\infty(T) = k_\infty^{300}\cdot\left(\frac{T}{300}\right)^{-m}$ and [M] is the concentration of air in molecules cm^{-3}.

- **Troe equilibrium reactions** are denoted by: troe-equil (k_0^{300} , n, k_∞^{300} , m, A, B)

  k in s^{-1} is calculated by:

$$k = A\exp\left(\frac{-B}{T}\right)\cdot\left(\frac{k_0(T)\cdot[M]}{1+\frac{k_0(T)\cdot[M]}{k_\infty(T)}}\right)\cdot 0.6^{\left\{1+\left[\log_{10}\left(\frac{k_0(T)\cdot[M]}{k_\infty(T)}\right)\right]^2\right\}^{-1}}$$

  where: $k_0(T) = k_0^{300}\cdot\left(\frac{T}{300}\right)^{-n}$, $k_\infty(T) = k_\infty^{300}\cdot\left(\frac{T}{300}\right)^{-m}$ and [M] is the concentration of air in molecules cm^{-3}.

- **Special rate expressions** are denoted by: special ("K = ...")

  For other types of reactions, the special formula for the calculation of k is given for each equation.

The small mechanism

NO2	=	1.000 O3P + 1.000 NO	phorat (1.000, 1);
O3	=	1.000 O1D	phorat (1.000,2);
O3	=	1.000 O3P	phorat (1.000,3);
HONO	=	1.000 HO + 1.000 NO	phorat (1.000, 4);
HNO3	=	1.000 HO + 1.000 NO2	phorat (1.000,5);
HNO4	=	0.650 HO2 + 0.650 NO2 + 0.350 HO + 0.350 NO3	phorat (1.000,6);
NO3	=	1.000 NO	phorat (1.000,7);
NO3	=	1.000 NO2 + 1.000 O3P	phorat (1.000,8);
H2O2	=	2.000 HO	phorat (1.000,9);
HCHO	=	1.000 CO	phorat (1.000, 10);
HCHO	=	2.000 HO2 + 1.000 CO	phorat (1.000, 11);
ALD	=	1.000 HO2 + 1.000 CO + 1.000 MO2	phorat (1.000, 12);
ALDR	=	2.000 HO2 + 2.000 CO	phorat (0.500,-17);
ALDR	=	1.000 CO + 1.000 HCHO	phorat (0.500,-18);
ALDR	=	2.000 CO	phorat (0.500,-24);
ALDR	=	1.000 HO2 + 1.000 CO + 1.000 ACO3	phorat (0.500, 19);
DCB	=	2.000 CO + 2.000 HO2 + 1.000 ALDR	phorat (1.000,20);
ONIT	=	1.000 NO2 + 0.999 HO2 + 0.001 MO2 + 0.201 ALD	phorat (1.000, 21);
CH4 + HO	=	1.000 MO2	thermal (4.48E-12, 1931.3);
ALK + HO	=	1.069 XO2 + 0.835 HO2 + 0.003 CO + 0.003 HO + 0.016 HCHO + 0.045 MO2 + 0.343 ALD + 0.006 ALDR + 0.117 XO2N	thermal (9.70E-12, 217.2);
OLE + HO	=	0.964 XO2 + 0.955 HO2 + 0.849 HCHO + 0.001 ACO3 + 0.637 ALD + 0.365 OLE + 0.026 XO2N	thermal (1.47E-11, -403.9);
ALD + HO	=	1.000 ACO3	thermal (5.55E-12, -331.0);
ALDR + HO	=	0.716 ACO3 + 0.284 HO2 + 1.095 CO	thermal (1.43E-11, 0.0);
HCHO + HO	=	1.000 HO2 + 1.000 CO	thermal (1.00E-11, 0.0);
PAN + HO	=	0.991 XO2 + 0.991 NO3 + 0.991 HCHO + 0.009 XO2N	thermal (4.00E-14, 0.0);
ONIT + HO	=	0.498 XO2 + 0.549 NO2 + 0.438 HO2 + 0.055 HCHO + 0.438 ONIT + 0.008 XO2N	thermal (5.31E-12, 260.0);
OLE + NO3	=	1.030 XO2 + 0.731 NO2 + 0.228 HO2 + 0.096 HCHO + 0.011 ACO3 + 0.239 ONIT + 0.697 ALD + 0.001 ALDR + 0.553 OLE + 0.030 XO2N	thermal (7.44E-13, -164.3);
ALD + NO3	=	1.000 ACO3 + 1.000 HNO3	thermal (1.40E-12, 1900.0);
ALDR + NO3	=	0.601 ACO3 + 0.399 HO2 + 1.133 CO + 1.000 HNO3	thermal (2.15E-12, 1900.0);
HCHO + NO3	=	1.000 HO2 + 1.000 CO + 1.000 HNO3	thermal (3.40E-13, 1900.0);
OLE + O3	=	0.342 HO2 + 0.353 CO + 0.324 HO + 0.005 H2O2 + 0.033 O3P + 0.172 XO2 + 0.683 HCHO + 0.060 MO2 + 0.056 ACO3+ 0.579 ALD + 0.042 ALDR + 0.295 OLE	thermal (8.50E-16, 886.4);
PAN	=	1.000 ACO3 + 1.000 NO2	troe-equil (9.70E-29, 5.6, 9.30E-12, 1.5, 1.16e28, 13954.);
XO2 + NO	=	1.000 NO2	thermal (4.00E-12, 0.0);
MO2 + NO	=	1.000 NO2 + 1.000 HO2 + 1.000 HCHO	thermal (4.20E-12, -180.0);
ACO3 + NO	=	1.000 NO2 + 0.001 HO2 + 0.001 CO+ 0.999 MO2	thermal (2.00E-11, 0.0);
XO2N + NO	=	1.000 ONIT	thermal (4.22E-12, -25.0);
ACO3 + NO2	=	1.000 PAN	troe (9.70E-29, 5.6, 9.30E-12, 1.5);
XO2 + NO3	=	1.000 NO2	thermal (1.20E-12, 0.0);
MO2 + NO3	=	1.000 NO2 + 1.000 HO2 + 1.000 HCHO	thermal (1.20E-12, 0.0);
ACO3 + NO3	=	1.000 NO2 + 0.001 HO2 + 0.001 CO + 0.999 MO2	thermal (4.00E-12, 0.0);
XO2N + NO3	=	0.975 HO2 + 0.307 XO2 + 0.001 HCHO + 0.025 MO2 + 0.701 ALD + 0.508 OLE + 1.000 NO2	thermal (1.20E-12, 0.0);
XO2 + HO2	=		thermal (1.66E-13,-1300.0);
MO2 + HO2	=		thermal (3.80E-13, -800.0);
ACO3 + HO2	=		thermal (1.15E-12, -550.0);
XO2N + HO2	=		thermal (1.65E-13,-1294.0);
ACO3 + HO2	=	1.000 O3 + 0.001 ALDR	thermal (3.86E-16,-2640.0);
XO2 + MO2	=	1.000 HO2 + 1.000 HCHO	thermal (7.34E-14, -939.7);
2 MO2	=	0.668 HO2 + 1.334 HCHO	thermal (9.10E-14, -416.0);
ACO3 + MO2	=	0.858 HO2 + 1.000 HCHO + 0.857 MO2	thermal (8.60E-12, 0.0);
XO2N + MO2	=	1.000 HO2 + 1.000 HCHO	thermal (4.96E-14, -890.3);
XO2 + ACO3	=	0.001 HO2 + 0.001 CO + 0.999 MO2	thermal (1.52E-12, -579.3);

2 ACO3	= 0.001 HO2 + 0.001 CO + 1.999 MO2	thermal (2.85E-12, -530.0);	
XO2N + ACO3	= 0.001 HO2 + 0.001 CO + 0.999 MO2	thermal (3.51E-12, -352.2);	
2 XO2	=	thermal (1.85E-14,-1514.4);	
XO2N + XO2	=	thermal (1.85E-14,-1322.6);	
2 XO2N	=	thermal (1.85E-14,-1322.6);	
O3P + O2	= 1.000 O3	special ("K = airc*6.e-34* (temp/300.)** (-2.3)");	
O3P + O3	=	thermal (8.00E-12, 2060.0);	
O1D + N2	= 1.000 O3P	thermal (1.80E-11, -110.0);	
O1D + O2	= 1.000 O3P	thermal (3.20E-11, -70.0);	
O1D + H2O	= 2.000 HO	thermal (2.20E-10, 0.0);	
O3 + HO	= 1.000 HO2	thermal (1.60E-12, 940.0);	
O3 + HO2	= 1.000 HO	thermal (1.10E-14, 500.0);	
HO + HO2	=	thermal (4.80E-11, -250.0);	
H2O2 + HO	= 1.000 HO2	thermal (2.90E-12, 160.0);	
2 HO2	= 1.000 H2O2	special ("K = 2.3d-13*exp (600./temp) + 1.7d-33*airc* exp (1000./temp)");	
2 HO2 + H2O	= 1.000 H2O2	special ("K = 3.22d-34*exp (2800./temp) + 2.38d-54*airc* exp (3200./temp)");	
O3P + NO	= 1.000 NO2	troe (9.E-32, 1.5, 3E-11, 0.);	
O3P + NO2	= 1.000 NO	thermal (6.50E-12, -120.0);	
O3P + NO2	= 1.000 NO3	troe (9.E-32, 2.0, 2.20E-11, 0.);	
HO + NO	= 1.000 HONO	troe (7.E-31, 2.6, 1.50E-11, 0.5);	
HO + NO2	= 1.000 HNO3	troe (2.60E-30, 3.2, 2.40E-11, 1.3);	
HO + NO3	= 1.000 NO2 + 1.000 HO2	thermal (2.20E-11, 0.0);	
HO2 + NO	= 1.000 NO2 + 1.000 HO	thermal (3.70E-12, -250.0);	
HO2 + NO2	= 1.000 HNO4	troe (1.80E-31, 3.2, 4.70E-12, 1.4);	
HNO4	= 1.000 HO2 + 1.000 NO2	troe-equil (1.80E-31, 3.2, 4.70E-12, 1.4, 4.76e26, 10900.);	
HO2 + NO3	= 0.300 HNO3 + 0.700 NO2 + 0.700 HO	thermal (3.50E-12, 0.0);	
HO + HONO	= 1.000 NO2	thermal (1.80E-11, 390.0);	
HO + HNO3	= 1.000 NO3	special ("k1=7.2d-15*exp (785./temp);k2=4.1d-16*exp (1440./temp); k3=1.9d-33*exp (725./temp)*airc; K = k1+k3/ (1.+k3/k2)");	
HO + HNO4	= 1.000 NO2	thermal (1.30E-12, -380.0);	
O3 + NO	= 1.000 NO2	thermal (2.00E-12, 1400.0);	
O3 + NO2	= 1.000 NO3	thermal (1.20E-13, 2450.0);	
2 NO + O2	= 2.000 NO2	thermal (3.30E-39, -530.0);	
NO3 + NO	= 2.000 NO2	thermal (1.50E-11, -170.0);	
NO3 + NO2	= 1.000 NO + 1.000 NO2	thermal (4.50E-14, 1260.0);	
NO3 + NO2	= 1.000 N2O5	troe (2.20E-30, 3.9, 1.50E-12, 0.7);	
N2O5	= 1.000 NO2 + 1.000 NO3	troe-equil (2.20E-30, 3.9, 1.50E-12, 0.7, 3.7E26, 11000.);	
2 NO3	= 2.000 NO2	thermal (8.50E-13, 2450.0);	
HO + SO2	= 1.000 HO2	troe (3E-31, 3.3, 1.50E-12, 0.0);	
CO + HO	= 1.000 HO2	special ("K = 1.5d-13* (1.+2.439e-20*airc)");	
ARO + HO	= 0.950 XO2 + 0.950 HO2 + 1.210 ALDR + 0.750 DCB + 0.050 XO2N	thermal (5.35E-12, -355.0);	
HO + DCB	= 0.500 ACO3 + 0.500 HO2 + 0.500 XO2 + 0.350 ALD + 0.350 OLE + 0.300 ALDR	thermal (2.80E-11, -175.0);	
DCB + NO3	= 0.500 ACO3 + 0.500 HO2 + 0.500 XO2 + 0.500 ALDR + 0.250 ALD + 0.500 NO2 + 0.500 HNO3	thermal (2.87E-13, 1000.0);	
DCB + O3	= 0.210 HO + 0.290 HO2 + 0.660 CO + 1.120 ALDR + 0.280 ACO3 + 0.160 ALD	thermal (2.00E-18, 0.0);	

The reduced mechanism

NO2	= 1.000 O3P + 1.000 NO	phorat (1.000, 1);	
O3	= 1.000 O1D	phorat (1.000, 2);	
O3	= 1.000 O3P	phorat (1.000, 3);	
HONO	= 1.000 HO + 1.000 NO	phorat (1.000, 4);	
HNO3	= 1.000 HO + 1.000 NO2	phorat (1.000, 5);	
HNO4	= 0.650 HO2 + 0.650 NO2 + 0.350 HO + 0.350 NO3	phorat (1.000, 6);	
NO3	= 1.000 NO	phorat (1.000, 7);	
NO3	= 1.000 NO2 + 1.000 O3P	phorat (1.000, 8);	
H2O2	= 2.000 HO	phorat (1.000, 9);	
HCHO	= 1.000 CO + 1.000 H2	phorat (1.000, 10);	
HCHO	= 2.000 HO2 + 1.000 CO	phorat (1.000, 11);	
ALD	= 1.000 HO2 + 1.000 CO + 1.000 MO2	phorat (1.000, 12);	
OP1	= 1.000 HO2 + 1.000 HO + 1.000 HCHO	phorat (1.000, 13);	
OP2	= 0.999 HO2 + 1.000 HO + 0.001 MO2 + 0.301 ALD + 0.699 KET	phorat (1.000, 13);	
PAA	= 1.000 HO + 1.000 MO2	phorat (1.000, 13);	
KET	= 0.172 HO2 + 0.172 XO2 + 0.828 MO2 + 1.000 ACO3 + 0.172 ALD	phorat (1.000, 16);	
GLY	= 2.000 HO2 + 2.000 CO	phorat (1.000, -17);	
GLY	= 1.000 CO + 1.000 HCHO	phorat (1.000, -18);	
GLY	= 2.000 CO + 1.000 H2	phorat (1.000, -24);	
MGLY	= 1.000 HO2 + 1.000 CO + 1.000 ACO3	phorat (1.000, 19);	
DCB	= 1.000 ACO3 + 1.000 HO2	phorat (1.000,20);	
ONIT	= 1.000 NO2 + 0.999 HO2 + 0.001 MO2 + 0.201 ALD + 0.799 KET	phorat (1.000, 21);	
MACR	= 1.000 HO2 + 1.000 CO + 1.000 HCHO + 1.000 ACO3	phorat (1.000, 22);	
HKET	= 0.500 HO2 + 0.500 HCHO + 0.500 MO2 + 1.000 ACO3	phorat (1.000, 16);	
HO + UDD	= 0.880 ALD + 0.120 KET + 1.000 HO2	thermal (2.70E-10, 0.0);	
CSL + NO3	= 1.000 HNO3 + 1.000 PHO	thermal (2.20E-11, 0.0);	
PHO + NO2	= 0.100 CSL + 1.000 ONIT	thermal (2.00E-11, 0.0);	
PHO + HO2	= 1.000 CSL	thermal (1.00E-11, 0.0);	
CH4 + HO	= 1.000 MO2	thermal (4.48E-12, 1931.3);	
ETH + HO	= 1.000 XO2 + 1.000 HO2 + 1.000 ALD	thermal (9.09E-12, 1062.3);	
HC3 + HO	= 0.599 XO2 + 0.842 HO2 + 0.036 CO + 0.036 HO + 0.036 HCHO + 0.083 MO2 + 0.036 ORA1 + 0.073 GLY + 0.497 ALD + 0.359 KET + 0.001 MGLY + 0.039 XO2N	thermal (5.54E-12, 271.9);	
HC5 + HO	= 1.091 XO2 + 0.881 HO2 + 0.012 HCHO + 0.026 MO2 + 0.342 ALD + 0.771 KET + 0.001 MGLY + 0.093 XO2N	thermal (7.86E-12, 149.1);	
HC8 + HO	= 1.374 XO2 + 0.737 HO2 + 0.002 HCHO + 0.001 MO2 + 0.307 ALD + 0.565 KET + 0.041 HKET + 0.262 XO2N	thermal (2.34E-11, 242.4);	
ETE + HO	= 1.000 XO2 + 1.000 HO2 + 1.600 HCHO + 0.200 ALD	thermal (1.96E-12, -438.0);	
OLT + HO	= 1.001 XO2 + 0.993 HO2 + 0.992 HCHO + 0.007 ACO3 + 0.941 ALD + 0.047 KET + 0.008 HKET	thermal (5.91E-12, -485.7);	
OLI + HO	= 1.001 XO2 + 1.000 HO2 + 1.712 ALD + 0.287 KET	thermal (1.42E-11, -479.7);	
DIEN + HO	= 0.971 XO2 + 0.971 HO2 + 0.767 HCHO + 0.971 MACR + 0.029 XO2N	thermal (1.48E-11, -448.0);	
ISO + HO	= 0.826 XO2 + 0.803 HO2 + 0.605 HCHO + 0.449 MACR + 0.354 OLT + 0.146 XO2N	thermal (2.54E-11, -410.0);	
API + HO	= 0.800 XO2 + 0.800 HO2 + 0.800 ALD + 0.800 KET + 0.200 XO2N	thermal (1.21E-11, -444.0);	
LIM + HO	= 0.652 XO2 + 0.650 HO2 + 0.280 HCHO + 0.370 MACR + 0.280 OLI + 0.350 XO2N	thermal (1.70E-10, 0.0);	
ALD + HO	= 1.000 ACO3	thermal (5.55E-12, -331.0);	
HCHO + HO	= 1.000 HO2 + 1.000 CO	thermal (1.00E-11, 0.0);	
KET + HO	= 1.224 XO2 + 0.668 HO2 + 0.001 HCHO + 0.332 ACO3 + 0.662 ALD + 0.338 MGLY	thermal (1.56E-12, 315.4);	
HKET + HO	= 0.033 XO2 + 1.000 HO2 + 1.000 MGLY	thermal (3.21E-12, 800.3);	
GLY + HO	= 0.400 XO2 + 1.000 HO2 + 1.600 CO	thermal (1.14E-11, 0.0);	
MGLY + HO	= 1.000 ACO3 + 1.000 CO	thermal (1.72E-11, 0.0);	
MACR + HO	= 0.510 ACO3 + 0.490 XO2 + 0.490 HO2 + 0.406 CO + 0.084 HCHO + 0.406 HKET + 0.084 MGLY	thermal (1.86E-11, -175.0);	
OP1 + HO	= 0.650 MO2 + 0.350 HO + 0.350 HCHO	thermal (2.93E-12, -190.0);	
OP2 + HO	= 0.464 XO2 + 0.408 HO2 + 0.591 HO + 0.056 HCHO + 0.005 OP2 + 0.316 ALD + 0.679 KET	thermal (3.40E-12, -190.0);	
PAA + HO	= 0.650 ACO3 + 0.350 XO2 + 0.350 HO + 0.350 HCHO	thermal (2.93E-12, -190.0);	
PAN + HO	= 1.000 XO2 + 1.000 NO3 + 1.000 HCHO	thermal (4.00E-14, 0.0);	
ONIT + HO	= 0.507 XO2 + 0.551 NO2 + 0.449 HO2 + 0.057 HCHO + 0.449 ONIT + 0.080 ALD + 0.471 KET	thermal (5.31E-12, 260.0);	

TPAN + HO	=	1.000 XO2 + 0.406 HO2 + 0.594 NO3 + 0.406 HCHO + 0.406 PAN + 0.594 HKET	thermal (3.25E-13, -500.0);
ETE + NO3	=	1.000 XO2 + 0.201 NO2 + 0.799 HO2 + 0.401 HCHO + 0.799 ONIT	thermal (2.94E-12, 2852.3);
OLT + NO3	=	1.228 XO2 + 0.237 NO2 + 0.741 HO2 + 0.237 HCHO + 0.022 ACO3 + 0.763 ONIT + 0.142 ALD + 0.100 KET	thermal (1.22E-13, 369.8);
OLI + NO3	=	1.176 XO2 + 0.470 NO2 + 0.530 HO2 + 0.530 ONIT + 0.685 ALD + 0.258 KET + 0.004 MGLY	thermal (8.64E-13, -450.0);
DIEN + NO3	=	0.981 XO2 + 0.613 NO2 + 0.368 HO2 + 0.193 CO + 0.031 HCHO + 0.754 MACR + 0.230 ONIT + 0.019 XO2N	thermal (2.87E-12, 1000.0);
ISO + NO3	=	0.934 XO2 + 0.843 NO2 + 0.071 HO2 + 0.106 HCHO + 0.014 ACO3 + 0.783 MACR + 0.085 ONIT + 0.070 OLT + 0.072 XO2N	thermal (4.00E-12, 446.0);
API + NO3	=	0.884 XO2 + 0.786 NO2 + 0.083 HO2 + 0.083 ONIT + 0.786 ALD + 0.786 KET + 0.130 XO2N	thermal (1.19E-12, -490.0);
LIM + NO3	=	0.900 XO2 + 0.778 NO2 + 0.093 HO2 + 0.025 HCHO + 0.774 MACR + 0.080 ONIT + 0.039 OLI + 0.129 XO2N	thermal (1.22E-11, 0.0);
ALD + NO3	=	1.000 ACO3 + 1.000 HNO3	thermal (1.40E-12, 1900.0);
HCHO + NO3	=	1.000 HO2 + 1.000 CO + 1.000 HNO3	thermal (3.40E-13, 1900.0);
GLY + NO3	=	0.400 XO2 + 1.000 HO2 + 1.600 CO + 1.000 HNO3	thermal (2.90E-12, 1900.0);
MGLY + NO3	=	1.000 ACO3 + 1.000 CO + 1.000 HNO3	thermal (1.40E-12, 1900.0);
MACR + NO3	=	0.200 ACO3 + 0.800 XO2 + 0.008 NO2 + 0.792 HO2 + 0.792 CO + 0.200 HNO3 + 0.008 HCHO + 0.792 ONIT + 0.008 MGLY	thermal (8.27E-15, 150.0);
TPAN + NO3	=	1.000 XO2 + 0.178 NO2 + 0.228 HO2 + 0.594 NO3 + 0.178 HCHO + 0.406 PAN + 0.594 ONIT	thermal (2.20E-14, 500.0);
ETE + O3	=	0.260 HO2 + 0.430 CO + 0.120 HO + 0.002 H2O2 + 0.130 H2 + 1.002 HCHO + 0.368 ORA1	thermal (9.14E-15, 2580.0);
OLT + O3	=	0.374 HO2 + 0.367 CO + 0.395 HO + 0.006 H2O2 + 0.051 H2 + 0.161 XO2 + 0.616 HCHO + 0.181 MO2 + 0.145 ORA1 + 0.557 ALD + 0.036 KET + 0.011 MGLY + 0.098 ORA2	thermal (4.39E-15, 1813.1);
OLI + O3	=	0.519 HO2 + 0.291 CO + 0.627 HO + 0.011 H2O2 + 0.437 XO2 + 0.010 HCHO + 0.193 MO2 + 0.029 ACO3 + 1.162 ALD + 0.158 KET + 0.114 MGLY + 0.144 ORA2	thermal (4.54E-15, 854.3);
DIEN + O3	=	0.554 HO2 + 0.682 CO + 0.372 HO + 0.005 H2O2 + 0.052 H2 + 0.015 XO2 + 0.090 ETE + 0.901 HCHO + 0.147 ORA1 + 0.015 GLY + 0.477 MACR + 0.119 OLT	thermal (6.00E-15, 1700.0);
ISO + O3	=	0.301 HO2 + 0.362 CO + 0.279 HO + 0.001 H2O2 + 0.053 H2 + 0.094 O3P + 0.142 XO2 + 0.893 HCHO + 0.029 MO2 + 0.151 ORA1 + 0.148 ACO3 + 0.388 MACR + 0.016 MGLY + 0.358 OLT	thermal (7.86E-15, 1913.0);
API + O3	=	0.510 HO2 + 0.140 CO + 0.852 HO + 0.021 H2O2 + 0.983 XO2 + 0.651 ALD + 0.457 KET + 0.210 MGLY + 0.069 ORA2	thermal (1.01E-15, 736.0);
LIM + O3	=	0.712 HO2 + 0.141 CO + 0.851 HO + 0.021 H2O2 + 0.001 H2 + 1.235 XO2 + 0.014 HCHO + 0.002 ORA1 + 0.847 MACR + 0.002 KET + 0.010 OLI + 0.136 OLT	thermal (2.00E-16, 0.0);
MACR + O3	=	0.288 HO2 + 0.522 CO + 0.072 HO + 0.001 H2O2 + 0.078 H2 + 0.401 HCHO + 0.221 ORA1 + 0.132 PAA + 0.132 ACO3 + 0.600 MGLY + 0.132 ORA2	thermal (1.36E-15, 2112.0);
TPAN + O3	=	0.700 NO2 + 0.078 HO2 + 0.129 CO + 0.036 HO + 0.001 H2O2 + 0.039 H2 + 0.701 HCHO + 0.110 ORA1 + 0.700 ACO3 + 0.300 PAN	thermal (2.46E-15, 1700.0);
PAN	=	1.000 ACO3 + 1.000 NO2	troe-equil (9.70E-29, 5.6, 9.30E-12, 1.5, 1.16e28, 13954.);
TPAN	=	1.000 ACO3 + 1.000 NO2	troe-equil (9.70E-29, 5.6, 9.30E-12, 1.5, 1.16e28, 13954.);
XO2 + NO	=	1.000 NO2	thermal (4.00E-12, 0.0);
MO2 + NO	=	1.000 NO2 + 1.000 HO2 + 1.000 HCHO	thermal (4.20E-12, -180.0);
ACO3 + NO	=	1.000 NO2 + 0.126 HCHO + 0.874 MO2 + 0.126 ACO3	thermal (2.00E-11, 0.0);
XO2N + NO	=	1.000 ONIT	thermal (4.68E-12, -48.2);
ACO3 + NO2	=	0.874 PAN + 0.126 TPAN	troe (9.70E-29, 5.6, 9.30E-12, 1.5);
XO2 + NO3	=	1.000 NO2	thermal (1.20E-12, 0.0);
MO2 + NO3	=	1.000 NO2 + 1.000 HO2 + 1.000 HCHO	thermal (1.20E-12, 0.0);
ACO3 + NO3	=	1.000 NO2 + 0.126 HCHO + 0.874 MO2 + 0.126 ACO3	thermal (4.00E-12, 0.0);
XO2N + NO3	=	0.971 HO2 + 0.584 XO2 + 0.131 HCHO + 0.029 MO2 + 0.165 MACR + 0.200 ALD + 0.656 KET + 0.002 HKET + 0.076 OLT + 1.000 NO2	thermal (1.20E-12, 0.0);
XO2 + HO2	=	1.000 OP2	thermal (1.66E-13,-1300.0);
MO2 + HO2	=	1.000 OP1	thermal (3.80E-13, -800.0);
ACO3 + HO2	=	0.874 PAA + 0.126 OP2	thermal (1.15E-12, -550.0);
XO2N + HO2	=	1.000 OP2	thermal (1.62E-13,-1285.7);
ACO3 + HO2	=	1.000 O3 + 0.126 OLT + 0.874 ORA2	thermal (3.86E-16,-2640.0);
XO2 + MO2	=	1.000 HO2 + 1.000 HCHO	thermal (4.99E-14,-1091.5);
2 MO2	=	0.668 HO2 + 1.334 HCHO	thermal (9.10E-14, -416.0);
ACO3 + MO2	=	0.806 HO2 + 1.072 HCHO + 0.735 MO2 + 0.072 ACO3 + 0.072 OLT + 0.122 ORA2	thermal (8.80E-12, 0.9);

XO2N + MO2	= 1.000 HO2 + 1.000 HCHO	thermal (7.32E-14, -839.3);	
XO2 + ACO3	= 0.126 HCHO + 0.874 MO2 + 0.126 ACO3	thermal (8.80E-13, -796.5);	
2 ACO3	= 0.256 HCHO + 1.744 MO2 + 0.256 ACO3	thermal (2.84E-12, -529.9);	
XO2N + ACO3	= 0.126 HCHO + 0.874 MO2 + 0.126 ACO3	thermal (2.45E-12, -464.2);	
2 XO2	=	thermal(9.77E-15,-1709.7);	
XO2N + XO2	=	thermal(3.60E-14,-1170.6);	
2 XO2N	=	thermal(3.60E-14,-1170.6);	
O3P + O2	= 1.000 O3	special ("K = airc*6.e-34* (temp/300.)** (-2.3)");	
O3P + O3	=	thermal(8.00E-12, 2060.0);	
O1D + N2	= 1.000 O3P	thermal (1.80E-11, -110.0);	
O1D + O2	= 1.000 O3P	thermal (3.20E-11, -70.0);	
O1D + H2O	= 2.000 HO	thermal (2.20E-10, 0.0);	
O3 + HO	= 1.000 HO2	thermal (1.60E-12, 940.0);	
O3 + HO2	= 1.000 HO	thermal (1.10E-14, 500.0);	
HO + HO2	=	thermal(4.80E-11, -250.0);	
H2O2 + HO	= 1.000 HO2	thermal (2.90E-12, 160.0);	
2 HO2	= 1.000 H2O2	special("K = 2.3d-13*exp (600./temp) + 1.7d-33*airc* exp (1000./temp)");	
2 HO2 + H2O	= 1.000 H2O2	special("K = 3.22d-34*exp (2800./temp) + 2.38d-54*airc* exp (3200./temp)");	
O3P + NO	= 1.000 NO2	troe (9.E-32, 1.5, 3E-11, 0.);	
O3P + NO2	= 1.000 NO	thermal (6.50E-12, -120.0);	
O3P + NO2	= 1.000 NO3	troe (9.E-32, 2.0, 2.20E-11, 0.);	
HO + NO	= 1.000 HONO	troe (7.E-31, 2.6, 1.50E-11, 0.5);	
HO + NO2	= 1.000 HNO3	troe (2.60E-30, 3.2, 2.40E-11, 1.3);	
HO + NO3	= 1.000 NO2 + 1.000 HO2	thermal (2.20E-11, 0.0);	
HO2 + NO	= 1.000 NO2 + 1.000 HO	thermal (3.70E-12, -250.0);	
HO2 + NO2	= 1.000 HNO4	troe (1.80E-31, 3.2, 4.70E-12, 1.4);	
HNO4	= 1.000 HO2 + 1.000 NO2	troe-equil(1.80E-31,3.2, 4.70E-12,1.4,4.76e26, 10900.);	
HO2 + NO3	= 0.300 HNO3 + 0.700 NO2 + 0.700 HO	thermal (3.50E-12, 0.0);	
HO + HONO	= 1.000 NO2	thermal (1.80E-11, 390.0);	
HO + HNO3	= 1.000 NO3	special("k1=7.2d-15*exp (785./temp); k2=4.1d-16*exp (1440./temp); k3=1.9d-33*exp (725./temp)*airc; K = k1+k3/ (1.+k3/k2)");	
HO + HNO4	= 1.000 NO2	thermal (1.30E-12, -380.0);	
O3 + NO	= 1.000 NO2	thermal (2.00E-12, 1400.0);	
O3 + NO2	= 1.000 NO3	thermal (1.20E-13, 2450.0);	
2 NO + O2	= 2.000 NO2	thermal (3.30E-39, -530.0);	
NO3 + NO	= 2.000 NO2	thermal (1.50E-11, -170.0);	
NO3 + NO2	= 1.000 NO + 1.000 NO2	thermal (4.50E-14, 1260.0);	
NO3 + NO2	= 1.000 N2O5	troe (2.20E-30, 3.9, 1.50E-12, 0.7);	
N2O5	= 1.000 NO2 + 1.000 NO3	troe-equil (2.20E-30, 3.9, 1.5E-12, .7, 3.7E26, 11000.);	
2 NO3	= 2.000 NO2	thermal (8.50E-13, 2450.0);	
HO + H2	= 1.000 HO2	thermal (5.50E-12, 2000.0);	
HO + SO2	= 1.000 SULF + 1.000 HO2	troe (3E-31, 3.3, 1.50E-12, 0.0);	
CO + HO	= 1.000 HO2	special("K=1.5d-13* (1.+2.439e-20*airc)");	
TOL + HO	= 0.960 XO2 + 0.960 HO2 + 1.080 GLY + 0.450 DCB + 0.050 XO2N + 0.590 MGLY + 0.020 CSL	thermal (1.81E-12, -355.0);	
XYL + HO	= 0.960 XO2 + 0.960 HO2 + 0.320 GLY + 0.850 DCB + 0.050 XO2N + 0.540 MGLY + 0.020 CSL	thermal (7.30E-12, -355.0);	
CSL + HO	= 0.850 GLY + 0.850 MGLY + 0.900 XO2 + 0.900 HO2 + 0.100 CSL	thermal (6.00E-11, 0.0);	
HO + DCB	= 0.500 ACO3 + 0.500 HO2 + 0.500 XO2 + 0.350 UDD + 0.150 GLY + 0.150 MGLY	thermal (2.80E-11, -175.0);	
DCB + NO3	= 0.500 ACO3 + 0.500 HO2 + 0.500 XO2 + 0.250 GLY + 0.250 ALD + 0.500 NO2 + 0.030 KET + 0.250 MGLY + 0.500 HNO3	thermal (2.87E-13, 1000.0);	
DCB + O3	= 0.210 HO + 0.290 HO2 + 0.660 CO + 0.500 GLY + 0.620 MGLY + 0.280 ACO3 + 0.160 ALD + 0.110 PAA + 0.110 ORA1 + 0.210 ORA2	thermal (2.00E-18, 0.0);	

The extended mechanism

NO2	= 1.000 O3P + 1.000 NO	phorat(1.000, 1);
O3	= 1.000 O1D	phorat(1.000,2);
O3	= 1.000 O3P	phorat(1.000,3);
HONO	= 1.000 HO + 1.000 NO	phorat(1.000, 4);
HNO3	= 1.000 HO + 1.000 NO2	phorat(1.000,5);
HNO4	= 0.650 HO2 + 0.650 NO2 + 0.350 HO + 0.350 NO3	phorat(1.000,6);
NO3	= 1.000 NO	phorat(1.000,7);
NO3	= 1.000 NO2 + 1.000 O3P	phorat(1.000,8);
H2O2	= 2.000 HO	phorat(1.000,9);
HCHO	= 1.000 CO + 1.000 H2	phorat(1.000, 10);
HCHO	= 2.000 HO2 + 1.000 CO	phorat(1.000, 11);
ALD6	= 2.000 HO2 + 1.000 CO + 1.822 XO2 + 0.003 HCHO + 0.003 ALD2 + 0.003 ALD3 + 0.003 ALD4 + 0.758 ALD5 + 0.003 KE3 + 0.237 KE6	phorat(1.000, 12);
ALD7	= 2.000 HO2 + 1.000 CO + 1.994 XO2 + 1.000 ALD6	phorat(1.000, 12);
ALD2	= 1.000 HO2 + 1.000 CO + 1.000 MO2	phorat(1.000, 12);
ALD3	= 1.963 HO2 + 1.000 CO + 1.000 XO2 + 0.963 ALD2 + 0.037 MO2 + 0.037 KE3	phorat(1.000, 12);
ALD4	= 1.929 HO2 + 1.000 CO + 1.112 XO2 + 0.011 HCHO + 0.006 ALD2 + 0.918 ALD3 + 0.071 KE3P + 0.005 ORA2	phorat(1.000, 12);
ALDI	= 1.999 HO2 + 1.000 CO + 1.000 XO2 + 0.001 ALD2 + 0.001 MO2 + 0.999 KE3	phorat(1.000, 12);
ALD5	= 1.999 HO2 + 1.000 CO + 1.734 XO2 + 0.316 HCHO + 0.682 ALD4 + 0.001 MO2 + 0.234 KE3 + 0.201 KE5	phorat(1.000, 12);
OP1	= 1.000 HO2 + 1.000 HO + 1.000 HCHO	phorat(1.000, 13);
OP2	= 0.999 HO2 + 1.000 HO + 0.001 ALD2 + 0.300 ALD3 + 0.001 MO2 + 0.699 KE3	phorat(1.000, 13);
PAA	= 1.000 HO + 1.000 MO2	phorat(1.000, 13);
ALD6	= 0.500 HO2 + 0.500 ALD4 + 0.500 ACO2 + 0.500 MO2 + 0.500 ACO5 + 0.500 ALD5	phorat(0.151, 16);
ALD7	= 0.500 HO2 + 0.504 XO2 + 0.496 HCHO + 0.496 ALD4 + 0.500 ACO2 + 0.500 MO2 + 0.500 ACO6 + 0.004 ALD5 + 0.500 ALD6	phorat(1.000, 16);
KE3	= 1.000 ACO2 + 1.000 MO2	phorat(1.000, 16);
KE4	= 0.500 HO2 + 0.500 XO2 + 0.430 ALD2 + 0.500 ACO2 + 0.430 ACO3 + 0.070 ACOI + 0.500 MO2 + 0.070 KE3	phorat(1.000, 16);
KE5	= 0.647 HO2 + 0.663 XO2 + 0.006 HCHO + 0.260 ALD2 + 0.270 ALD3 + 0.020 ALDI + 0.342 ACO2 + 0.252 ACO3 + 0.075 ACO4 + 0.053 ACOI + 0.353 MO2 + 0.278 ACO5 + 0.064 KE3 + 0.047 KE4	phorat(1.000, 16);
KE6	= 0.743 HO2 + 0.900 XO2 + 0.001 HCHO + 0.244 ALD2 + 0.243 ALD3 + 0.213 ALD4 + 0.257 ACO2 + 0.243 ACO3 + 0.090 ACO4 + 0.257 MO2 + 0.410 ACO5 + 0.001 KE3 + 0.043 KE5	phorat(1.000, 16);
KE7	= 0.841 HO2 + 1.112 XO2 + 0.196 ALD2 + 0.289 ALD3 + 0.196 ALD4 + 0.159 ACO2 + 0.196 ACO3 + 0.145 ACO4 + 0.159 MO2 + 0.341 ACO5 + 0.159 ACO6 + 0.159 ALD5	phorat(1.000, 16);
KE8	= 0.940 HO2 + 1.592 XO2 + 0.074 ALD2 + 0.148 ALD3 + 0.148 ALD4 + 0.060 ACO2 + 0.074 ACO3 + 0.074 ACO4 + 0.060 MO2 + 0.222 ACO5 + 0.148 ACO6 + 0.422 ACO7 + 0.148 ALD5 + 0.098 ALD6 + 0.324 ALD7	phorat(0.592, 16);
HKET	= 0.500 HO2 + 0.500 HCHO + 0.500 ACO2 + 0.500 MO2 + 0.500 ACO5	phorat(1.000, 16);
ALD4	= 0.289 HO2 + 0.289 HCHO + 0.211 ACO2 + 0.211 MO2 + 0.789 ACO5	phorat(0.071, 16);
GLY	= 2.000 HO2 + 2.000 CO	phorat(1.000, 17);
GLY	= 1.000 CO + 1.000 HCHO	phorat(1.000, 18);
MGLY	= 1.000 HO2 + 1.000 CO + 1.000 ACO2	phorat(1.000, 19);
DCB	= 1.000 TCO3 + 1.000 HO2	phorat(1.000, 20);
ONIT	= 1.000 NO2 + 0.999 HO2 + 0.001 ALD2 + 0.200 ALD3 + 0.001 MO2 + 0.799 KE3	phorat(1.000, 21);
MACR	= 1.000 HO2 + 1.000 CO + 1.000 HCHO + 1.000 ACO2	phorat(1.000, 22);
GLY	= 2.000 CO + 1.000 H2	phorat(1.000, 24);
CH4 + HO	= 1.000 MO2	thermal(4.48E-12, 1931.3);
ETH + HO	= 1.000 ETHP	thermal(9.09E-12, 1062.3);
HC3 + HO	= 0.585 HC3P + 0.380 HO2 + 0.036 CO + 0.036 HO + 0.010 HCHO + 0.334 ALD2 + 0.036 ORA1 + 0.036 GLY	thermal(5.56E-12, 273.0);
HC5 + HO	= 0.746 HC5P + 0.254 HO2 + 0.254 KE3	thermal(7.86E-12, 149.1);
HC8 + HO	= 0.938 HC8P + 0.062 HO2 + 0.002 HCHO + 0.013 ALD2 + 0.011 ALD3 + 0.023 HKET + 0.002 ALD6	thermal(2.32E-11, 220.8);
ETE + HO	= 1.000 ETEP	thermal(1.96E-12, -438.0);

OLT + HO	= 1.000 OLTP	thermal(5.93E-12, -489.5);
OLI + HO	= 1.000 OLIP	thermal(1.42E-11, -479.7);
DIEN + HO	= 1.000 ISOP	thermal(1.48E-11, -448.0);
ISO + HO	= 0.956 ISOP	thermal(2.54E-11, -410.0);
API + HO	= 1.000 APIP	thermal(1.21E-11, -444.0);
LIM + HO	= 1.000 LIMP	thermal(1.70E-10, 0.0);
ALD2 + HO	= 1.000 ACO2	thermal(5.55E-12, -331.0);
ALD3 + HO	= 0.943 ACO3 + 0.057 XO2 + 0.055 HO2 + 0.005 CO + 0.005 ALD2 + 0.025 ALD3 + 0.024 MGLY	thermal(8.41E-12, -286.2);
ALD4 + HO	= 0.703 ACO4 + 0.211 XO2 + 0.230 HO2 + 0.006 CO + 0.014 ALD2 + 0.006 ALD3 + 0.174 ALD4 + 0.008 GLY + 0.042 ACO5 + 0.044 MGLY + 0.001 ORA2 + 0.004 XO2N	thermal(2.08E-11, -185.5);
ALDI + HO	= 0.892 ACOI + 0.108 XO2 + 0.105 HO2 + 0.061 CO + 0.044 ALD3 + 0.061 KE3	thermal(9.35E-12, -271.4);
ALD5 + HO	= 0.788 ACO5 + 0.243 XO2 + 0.161 HO2 + 0.001 CO + 0.005 HCHO + 0.007 ALD2 + 0.069 ALD3 + 0.001 ALD4 + 0.001 GLY + 0.081 ALD5 + 0.055 KE3 + 0.017 MGLY + 0.010 XO2N	thermal(1.48E-11, -179.7);
ALD6 + HO	= 0.806 ACO6 + 0.255 XO2 + 0.134 HO2 + 0.014 CO + 0.002 HCHO + 0.005 ALD2 + 0.054 ALD3 + 0.012 ALD4 + 0.002 ACO2 + 0.001 KE5P + 0.004 ALD5 + 0.117 ALD6 + 0.010 KE3 + 0.013 KE4 + 0.013 KE6 + 0.059 MGLY + 0.016 XO2N	thermal(2.48E-11, -180.4);
ALD7 + HO	= 0.349 ACO7 + 0.113 XO2 + 0.611 HO2 + 0.054 ALD3 + 0.054 ALD4 + 0.010 ACO2 + 0.010 ALD5 + 0.547 ALD7 + 0.003 KE7 + 0.010 MGLY + 0.003 XO2N	thermal(3.59E-11, -152.6);
HCHO + HO	= 1.000 HO2 + 1.000 CO	thermal(1.00E-11, 0.0);
KE3 + HO	= 1.000 KE3P	thermal(3.21E-12, 800.3);
KE4 + HO	= 1.000 KE4P	thermal(2.58E-12, 191.0);
KE5 + HO	= 0.774 KE5P + 0.226 HO2 + 0.001 XO2 + 0.226 ALD5	thermal(1.66E-11, 239.8);
KE6 + HO	= 0.590 KE6P + 0.410 HO2 + 0.004 XO2 + 0.001 ALD2 + 0.002 ALD4 + 0.122 ALD6 + 0.001 KE3 + 0.286 KE6	thermal(2.07E-11, 187.1);
KE7 + HO	= 0.500 KE7P + 0.500 HO2 + 0.002 XO2 + 0.001 ALD2 + 0.001 ALD5 + 0.084 ALD7 + 0.415 KE7	thermal(2.49E-11, 139.7);
KE8 + HO	= 0.771 KE8P + 0.229 HO2 + 0.002 XO2 + 0.019 ALD7 + 0.210 KE8	thermal(3.67E-11, 167.6);
HKET + HO	= 0.033 XO2 + 1.000 HO2 + 1.000 MGLY	thermal(3.21E-12, 800.3);
GLY + HO	= 0.400 XO2 + 1.000 HO2 + 1.600 CO	thermal(1.14E-11, 0.0);
MGLY + HO	= 1.000 ACO2 + 1.000 CO	thermal(1.72E-11, 0.0);
MACR + HO	= 0.510 TCO3 + 0.490 XO2 + 0.490 HO2 + 0.406 CO + 0.084 HCHO + 0.406 HKET + 0.084 MGLY	thermal(1.86E-11, -175.0);
OP1 + HO	= 0.650 MO2 + 0.350 HO + 0.350 HCHO	thermal(2.93E-12, -190.0);
OP2 + HO	= 0.464 XO2 + 0.408 HO2 + 0.591 HO + 0.056 HCHO + 0.056 ALD2 + 0.259 ALD3 + 0.005 OP2 + 0.679 KE3	thermal(3.40E-12, -190.0);
PAA + HO	= 0.650 ACO2 + 0.350 XO2 + 0.350 HO + 0.350 HCHO	thermal(2.93E-12, -190.0);
PAN + HO	= 1.000 XO2 + 1.000 NO3 + 1.000 HCHO	thermal(4.00E-14, 0.0);
PPN + HO	= 1.000 XO2 + 0.791 HO2 + 0.209 NO3 + 0.209 ALD2 + 0.791 PPN	thermal(4.00E-14, 0.0);
PNBN + HO	= 1.000 XO2 + 0.864 HO2 + 0.043 NO3 + 0.093 ALD2 + 0.043 ALD3 + 0.001 PPN + 0.864 PNBN + 0.001 MO2	thermal(4.00E-14, 0.0);
ONIT + HO	= 0.507 XO2 + 0.551 NO2 + 0.449 HO2 + 0.057 HCHO + 0.057 ALD2 + 0.023 ALD3 + 0.449 ONIT + 0.471 KE3	thermal(5.31E-12, 260.0);
TPAN + HO	= 1.000 XO2 + 0.406 HO2 + 0.594 NO3 + 0.406 HCHO + 0.406 PAN + 0.594 HKET	thermal(3.25E-13, -500.0);
ETE + NO3	= 0.201 OLND + 0.799 OLNN	thermal(2.94E-12, 2852.3);
OLT + NO3	= 0.407 OLND + 0.593 OLNN	thermal(1.18E-13, 420.2);
OLI + NO3	= 0.551 OLND + 0.449 OLNN	thermal(8.64E-13, -450.0);
DIEN + NO3	= 0.026 OLND + 0.974 OLNN	thermal(1.72E-13, 161.4);
ISO + NO3	= 0.120 OLND + 0.880 OLNN	thermal(4.00E-12, 446.0);
API + NO3	= 0.905 OLND + 0.095 OLNN	thermal(1.19E-12, -490.0);
LIM + NO3	= 0.938 OLND + 0.062 OLNN	thermal(1.22E-11, 0.0);
ALD2 + NO3	= 1.000 ACO2 + 1.000 HNO3	thermal(1.40E-12, 1900.0);
ALD3 + NO3	= 1.000 ACO3 + 1.000 HNO3	thermal(2.30E-12, 1900.0);
ALD4 + NO3	= 1.000 ACO4 + 1.000 HNO3	thermal(2.27E-12, 1900.0);
ALDI + NO3	= 1.000 ACOI + 1.000 HNO3	thermal(1.40E-12, 1900.0);
ALD5 + NO3	= 1.000 ACO5 + 1.000 HNO3	thermal(2.04E-12, 1900.0);
ALD6 + NO3	= 1.000 ACO6 + 1.000 HNO3	thermal(3.53E-12, 1900.0);
ALD7 + NO3	= 1.000 ACO7 + 1.000 HNO3	thermal(2.34E-12, 1900.0);
HCHO + NO3	= 1.000 HO2 + 1.000 CO + 1.000 HNO3	thermal(3.40E-13, 1900.0);
GLY + NO3	= 0.400 XO2 + 1.000 HO2 + 1.600 CO + 1.000 HNO3	thermal(2.90E-12, 1900.0);
MGLY + NO3	= 1.000 ACO2 + 1.000 CO + 1.000 HNO3	thermal(1.40E-12, 1900.0);
MACR + NO3	= 0.200 TCO3 + 0.800 OLNN + 0.200 HNO3	thermal(8.27E-15, 150.0);
TPAN + NO3	= 1.000 XO2 + 0.178 NO2 + 0.228 HO2 + 0.594 NO3 + 0.178 HCHO + 0.178 PAN + 0.228 PPN + 0.594 ONIT	thermal(2.20E-14, 500.0);

ETE + O3	= 0.260 HO2 + 0.430 CO + 0.120 HO + 0.002 H2O2 + 0.130 H2 + 1.002 HCHO + 0.368 ORA1	thermal(9.14E-15, 2580.0);
OLT + O3	= 0.319 HO2 + 0.371 CO + 0.389 HO + 0.006 H2O2 + 0.051 H2 + 0.092 XO2 + 0.612 HCHO + 0.274 ALD2 + 0.066 ALD3 + 0.054 ALD4 + 0.005 ALDI + 0.135 MO2 + 0.146 ORA1 + 0.004 KE4P + 0.017 KE5P + 0.041 ALD5 + 0.003 KE3 + 0.016 KE5 + 0.120 MGLY + 0.099 ORA2	thermal(3.99E-15, 1784.3);
OLI + O3	= 0.402 HO2 + 0.291 CO + 0.627 HO + 0.011 H2O2 + 0.314 XO2 + 0.010 HCHO + 0.538 ALD2 + 0.213 ALD3 + 0.101 ALD4 + 0.193 MO2 + 0.029 ACO5 + 0.110 KE3P + 0.008 KE6P + 0.138 ALD5 + 0.052 ALD6 + 0.141 KE3 + 0.013 KE6 + 0.104 ORA2	thermal(4.54E-15, 854.3);
DIEN + O3	= 0.294 HO2 + 0.461 CO + 0.151 HO + 0.002 H2O2 + 0.120 H2 + 0.011 ETE + 0.113 HCHO + 0.341 ORA1 + 0.935 MACR + 0.015 OLT	thermal(5.44E-15, 1047.0);
ISO + O3	= 0.284 HO2 + 0.362 CO + 0.279 HO + 0.001 H2O2 + 0.053 H2 + 0.094 O3P + 0.126 XO2 + 0.893 HCHO + 0.148 ACO2 + 0.029 MO2 + 0.151 ORA1 + 0.016 KE3P + 0.388 MACR + 0.358 OLT	thermal(7.86E-15, 1913.0);
API + O3	= 0.300 HO2 + 0.140 CO + 0.852 HO + 0.021 H2O2 + 0.354 XO2 + 0.420 KE8P + 0.861 ALD7 + 0.070 KE8 + 0.069 ORA2	thermal(1.01E-15, 736.0);
LIM + O3	= 0.286 HO2 + 0.222 CO + 0.647 HO + 0.016 H2O2 + 0.037 H2 + 0.288 XO2 + 0.010 HCHO + 0.104 ORA1 + 0.297 KE7P + 0.007 KE8P + 0.608 MACR + 0.001 KE7 + 0.289 OLI + 0.098 OLT	thermal(2.00E-16, 0.0);
MACR + O3	= 0.288 HO2 + 0.522 CO + 0.072 HO + 0.001 H2O2 + 0.078 H2 + 0.401 HCHO + 0.132 ACO2 + 0.221 ORA1 + 0.132 PAA + 0.600 MGLY + 0.132 ORA2	thermal(1.36E-15, 2112.0);
TPAN + O3	= 0.700 NO2 + 0.078 HO2 + 0.129 CO + 0.036 HO + 0.001 H2O2 + 0.039 H2 + 0.701 HCHO + 0.700 ACO2 + 0.300 PAN + 0.110 ORA1	thermal(2.46E-15, 1700.0);
PAN	= 1.000 ACO2 + 1.000 NO2	troe-equil(9.70E-29, 5.6, 9.30E-12, 1.5, 1.16e28, 13954.);
PPN	= 1.000 ACO3 + 1.000 NO2	troe-equil(9.70E-29, 5.6, 9.30E-12, 1.5, 1.16e28, 13954.);
PNBN	= 1.000 ACO4 + 1.000 NO2	troe-equil(9.70E-29, 5.6, 9.30E-12, 1.5, 1.16e28, 13954.);
TPAN	= 1.000 TCO3 + 1.000 NO2	troe-equil(9.70E-29, 5.6, 9.30E-12, 1.5, 1.16e28, 13954.);
XO2 + NO	= 1.000 NO2	thermal(4.00E-12, 0.0);
OLNN + NO	= 0.961 NO2 + 0.961 HO2 + 0.522 MACR + 0.478 ONIT	thermal(4.00E-12, 0.0);
OLND + NO	= 1.777 NO2 + 0.034 HO2 + 0.034 XO2 + 0.346 HCHO + 0.422 ALD2 + 0.153 ALD3 + 0.088 ALD4 + 0.001 ALDI + 0.132 ACO2 + 0.013 ACO5 + 0.033 MACR + 0.201 ONIT + 0.031 ALD5 + 0.059 ALD6 + 0.001 ALD7 + 0.221 KE3 + 0.068 KE5 + 0.020 KE6 + 0.006 MGLY + 0.108 OLT	thermal(4.00E-12, 0.0);
MO2 + NO	= 1.000 NO2 + 1.000 HO2 + 1.000 HCHO	thermal(4.20E-12, -180.0);
ETHP + NO	= 1.000 NO2 + 1.000 HO2 + 1.000 ALD2	thermal(8.70E-12, 0.0);
HC3P + NO	= 0.932 NO2 + 0.789 HO2 + 0.100 XO2 + 0.051 HCHO + 0.144 ALD2 + 0.017 ALD3 + 0.080 ALD4 + 0.031 ALDI + 0.004 ACO3 + 0.120 MO2 + 0.063 GLY + 0.003 ACO5 + 0.016 KE4P + 0.068 ONIT + 0.002 ALD6 + 0.151 KE3 + 0.443 KE4 + 0.002 MGLY	thermal(4.17E-12, -6.3);
HC5P + NO	= 0.875 NO2 + 0.864 HO2 + 0.605 XO2 + 0.016 HCHO + 0.247 ALD2 + 0.053 ALD3 + 0.048 ALD4 + 0.007 ALDI + 0.011 MO2 + 0.125 ONIT + 0.066 ALD5 + 0.012 ALD6 + 0.283 KE3 + 0.091 KE4 + 0.172 KE5 + 0.131 KE6 + 0.015 KE8 + 0.002 MGLY	thermal(4.00E-12, 0.0);
HC8P + NO	= 0.726 NO2 + 0.720 HO2 + 0.730 XO2 + 0.001 HCHO + 0.028 ALD2 + 0.012 ALD3 + 0.011 ALD4 + 0.010 ALDI + 0.001 ACO2 + 0.002 MO2 + 0.002 ACO5 + 0.274 ONIT + 0.026 ALD5 + 0.054 ALD6 + 0.077 ALD7 + 0.039 KE3 + 0.012 KE4 + 0.019 KE5 + 0.034 KE6 + 0.144 KE7 + 0.280 KE8 + 0.001 MGLY	thermal(4.00E-12, 0.0);
ETEP + NO	= 1.000 NO2 + 1.000 HO2 + 1.600 HCHO + 0.200 ALD2	thermal(9.00E-12, 0.0);
OLTP + NO	= 1.000 NO2 + 0.832 HO2 + 0.001 XO2 + 0.831 HCHO + 0.612 ALD2 + 0.102 ALD3 + 0.055 ALD4 + 0.010 ALDI + 0.163 ACO2 + 0.005 HKET + 0.005 ACO5 + 0.087 ALD5 + 0.035 KE5 + 0.090 MGLY	thermal(4.00E-12, 0.0);
OLIP + NO	= 1.000 NO2 + 1.000 HO2 + 0.001 XO2 + 0.798 ALD2 + 0.303 ALD3 + 0.151 ALD4 + 0.057 ALD5 + 0.173 ALD6 + 0.265 KE3 + 0.022 KE6	thermal(4.00E-12, 0.0);
ISOP + NO	= 0.840 NO2 + 0.840 HO2 + 0.017 XO2 + 0.633 HCHO + 0.470 MACR + 0.160 ONIT + 0.370 OLT	thermal(4.00E-12, 0.0);
APIP + NO	= 0.800 NO2 + 0.800 HO2 + 0.200 ONIT + 0.800 ALD7	thermal(4.00E-12, 0.0);
LIMP + NO	= 0.650 NO2 + 0.650 HO2 + 0.001 XO2 + 0.331 HCHO + 0.319 MACR + 0.350 ONIT + 0.331 OLI	thermal(4.00E-12, 0.0);
ACO2 + NO	= 1.000 NO2 + 1.000 MO2	thermal(2.00E-11, 0.0);
ACO3 + NO	= 1.000 NO2 + 0.964 HO2 + 1.000 XO2 + 0.964 ALD2 + 0.036 MO2 + 0.036 KE3	thermal(2.00E-11, 0.0);
ACO4 + NO	= 1.000 NO2 + 0.901 HO2 + 1.017 XO2 + 0.007 HCHO + 0.006 ALD2 + 0.894 ALD3 + 0.099 KE3P + 0.002 ORA2	thermal(2.00E-11, 0.0);

ACOI + NO = 1.000 NO2 + 0.999 HO2 + 1.000 XO2 + 0.001 ALD2 + 0.001 MO2 + 0.999 KE3 thermal(2.00E-11, 0.0);

ACO5 + NO = 1.000 NO2 + 0.999 HO2 + 1.735 XO2 + 0.320 HCHO + 0.679 ALD4 + 0.001 MO2 + 0.237 KE3 + 0.203 KE5 thermal(2.00E-11, 0.0);

ACO6 + NO = 1.000 NO2 + 1.000 HO2 + 1.873 XO2 + 0.003 HCHO + 0.002 ALD2 + 0.002 ALD3 + 0.002 ALD4 + 0.771 ALD5 + 0.002 KE3 + 0.224 KE6 thermal(2.00E-11, 0.0);

ACO7 + NO = 1.000 NO2 + 1.000 HO2 + 1.994 XO2 + 1.000 ALD6 thermal(2.00E-11, 0.0);

KE3P + NO = 1.000 NO2 + 0.998 HO2 + 0.002 HCHO + 0.002 ACO2 + 0.998 MGLY thermal(4.00E-12, 0.0);

KE4P + NO = 1.000 NO2 + 0.516 HO2 + 0.300 XO2 + 0.346 ALD2 + 0.446 ALD4 + 0.484 ACO2 + 0.138 KE3 + 0.070 MGLY thermal(4.00E-12, 0.0);

KE5P + NO = 1.000 NO2 + 0.687 HO2 + 0.211 XO2 + 0.397 HCHO + 0.102 ALD2 + 0.081 ALD3 + 0.233 ALD4 + 0.006 ALDI + 0.119 ACO2 + 0.111 ACO3 + 0.015 ACOI + 0.007 ACO5 + 0.034 KE3P + 0.002 KE4P + 0.024 KE5P + 0.130 ALD5 + 0.067 KE3 + 0.032 KE4 + 0.312 KE5 + 0.012 MGLY thermal(4.00E-12, 0.0);

KE6P + NO = 1.000 NO2 + 0.781 HO2 + 0.205 XO2 + 0.233 HCHO + 0.316 ALD2 + 0.076 ALD3 + 0.381 ALD4 + 0.080 ACO2 + 0.076 ACO3 + 0.028 ACO4 + 0.034 ACO5 + 0.228 ALD5 + 0.063 ALD6 + 0.078 KE3 + 0.031 KE5 + 0.152 KE6 + 0.008 MGLY thermal(4.00E-12, 0.0);

KE7P + NO = 1.000 NO2 + 0.819 HO2 + 0.186 XO2 + 0.186 HCHO + 0.306 ALD2 + 0.238 ALD3 + 0.213 ALD4 + 0.033 ACO2 + 0.044 ACO3 + 0.034 ACO4 + 0.070 ACO5 + 0.303 ALD5 + 0.186 ALD6 + 0.040 ALD7 + 0.149 KE7 + 0.004 MGLY thermal(4.00E-12, 0.0);

KE8P + NO = 1.000 NO2 + 0.782 HO2 + 0.405 XO2 + 0.027 HCHO + 0.034 ALD2 + 0.039 ALD3 + 0.057 ALD4 + 0.004 ACO2 + 0.005 ACO3 + 0.004 ACO4 + 0.025 ACO5 + 0.053 ACO6 + 0.036 ACO7 + 0.003 KE5P + 0.035 KE6P + 0.053 KE7P + 0.079 ALD5 + 0.132 ALD6 + 0.250 ALD7 + 0.028 KE6 + 0.064 KE7 + 0.470 KE8 thermal(4.00E-12, 0.0);

TCO3 + NO = 1.000 NO2 + 1.000 HCHO + 1.000 ACO2 thermal(2.00E-11, 0.0);

XO2N + NO = 1.000 ONIT thermal(4.00E-12, 0.0);

ACO2 + NO2 = 1.000 PAN thermal(1.82E-12, -462.8);

ACO3 + NO2 = 1.000 PPN thermal(1.82E-12, -462.8);

ACO4 + NO2 = 1.000 PNBN thermal(1.82E-12, -462.8);

ACOI + NO2 = 1.000 PPN thermal(1.82E-12, -462.8);

ACO5 + NO2 = 1.000 PNBN thermal(1.82E-12, -462.8);

ACO6 + NO2 = 1.000 PNBN thermal(3.04E-12, -462.3);

ACO7 + NO2 = 1.000 PNBN thermal(1.82E-12, -462.8);

TCO3 + NO2 = 1.000 TPAN thermal(1.82E-12, -462.8);

XO2 + NO3 = 1.000 NO2 thermal(1.20E-12, 0.0);

OLNN + NO3 = 1.000 NO2 + 1.000 HO2 + 0.556 MACR + 0.444 ONIT thermal(1.20E-12, 0.0);

OLND + NO3 = 1.818 NO2 + 0.034 HO2 + 0.034 XO2 + 0.368 HCHO + 0.422 ALD2 + 0.153 ALD3 + 0.088 ALD4 + 0.001 ALDI + 0.135 ACO2 + 0.013 ACO5 + 0.038 MACR + 0.182 ONIT + 0.031 ALD5 + 0.059 ALD6 + 0.001 ALD7 + 0.221 KE3 + 0.068 KE5 + 0.020 KE6 + 0.006 MGLY + 0.122 OLT thermal(1.20E-12, 0.0);

MO2 + NO3 = 1.000 NO2 + 1.000 HO2 + 1.000 HCHO thermal(1.20E-12, 0.0);

ETHP + NO3 = 1.000 NO2 + 1.000 HO2 + 1.000 ALD2 thermal(1.20E-12, 0.0);

HC3P + NO3 = 1.000 NO2 + 0.843 HO2 + 0.108 XO2 + 0.051 HCHO + 0.154 ALD2 + 0.018 ALD3 + 0.083 ALD4 + 0.032 ALDI + 0.005 ACO3 + 0.132 MO2 + 0.063 GLY + 0.003 ACO5 + 0.016 KE4P + 0.002 ALD6 + 0.165 KE3 + 0.485 KE4 + 0.002 MGLY thermal(1.20E-12, 0.0);

HC5P + NO3 = 1.000 NO2 + 0.986 HO2 + 0.684 XO2 + 0.017 HCHO + 0.263 ALD2 + 0.061 ALD3 + 0.052 ALD4 + 0.010 ALDI + 0.014 MO2 + 0.074 ALD5 + 0.013 ALD6 + 0.304 KE3 + 0.103 KE4 + 0.204 KE5 + 0.163 KE6 + 0.017 KE8 + 0.002 MGLY thermal(1.20E-12, 0.0);

HC8P + NO3 = 1.000 NO2 + 0.993 HO2 + 0.984 XO2 + 0.001 HCHO + 0.034 ALD2 + 0.014 ALD3 + 0.014 ALD4 + 0.012 ALDI + 0.002 ACO2 + 0.002 MO2 + 0.003 ACO5 + 0.031 ALD5 + 0.065 ALD6 + 0.091 ALD7 + 0.047 KE3 + 0.015 KE4 + 0.024 KE5 + 0.046 KE6 + 0.203 KE7 + 0.428 KE8 + 0.001 MGLY thermal(1.20E-12, 0.0);

ETEP + NO3 = 1.000 NO2 + 1.000 HO2 + 1.600 HCHO + 0.200 ALD2 thermal(1.20E-12, 0.0);

OLTP + NO3 = 1.000 NO2 + 0.832 HO2 + 0.001 XO2 + 0.831 HCHO + 0.612 ALD2 + 0.102 ALD3 + 0.055 ALD4 + 0.010 ALDI + 0.163 ACO2 + 0.005 HKET + 0.005 ACO5 + 0.087 ALD5 + 0.035 KE5 + 0.090 MGLY thermal(1.20E-12, 0.0);

OLIP + NO3 = 1.000 NO2 + 1.000 HO2 + 0.001 XO2 + 0.798 ALD2 + 0.303 ALD3 + 0.151 ALD4 + 0.057 ALD5 + 0.173 ALD6 + 0.265 KE3 + 0.022 KE6 thermal(1.20E-12, 0.0);

ISOP + NO3 = 1.000 NO2 + 1.000 HO2 + 0.023 XO2 + 0.720 HCHO + 0.579 MACR + 0.420 OLT thermal(1.20E-12, 0.0);

APIP + NO3 = 1.000 NO2 + 1.000 HO2 + 1.000 ALD7 thermal(1.20E-12, 0.0);

LIMP + NO3 = 1.000 NO2 + 1.000 HO2 + 0.002 XO2 + 0.466 HCHO + 0.534 MACR + 0.466 OLI thermal(1.20E-12, 0.0);

ACO2 + NO3 = 1.000 NO2 + 1.000 MO2 thermal(4.00E-12, 0.0);

ACO3 + NO3 = 1.000 NO2 + 0.964 HO2 + 1.000 XO2 + 0.964 ALD2 + 0.036 MO2 + 0.036 KE3 thermal(4.00E-12, 0.0);

ACO4 + NO3	= 1.000 NO2 + 0.901 HO2 + 1.017 XO2 + 0.007 HCHO + 0.006 ALD2 + 0.894 ALD3 + 0.099 KE3P + 0.002 ORA2	thermal(4.00E-12, 0.0);
ACOI + NO3	= 1.000 NO2 + 0.999 HO2 + 1.000 XO2 + 0.001 ALD2 + 0.001 MO2 + 0.999 KE3	thermal(4.00E-12, 0.0);
ACO5 + NO3	= 1.000 NO2 + 0.999 HO2 + 1.735 XO2 + 0.320 HCHO + 0.679 ALD4 + 0.001 MO2 + 0.237 KE3 + 0.203 KE5	thermal(4.00E-12, 0.0);
ACO6 + NO3	= 1.000 NO2 + 1.000 HO2 + 1.873 XO2 + 0.003 HCHO + 0.002 ALD2 + 0.002 ALD3 + 0.002 ALD4 + 0.771 ALD5 + 0.002 KE3 + 0.224 KE6	thermal(4.00E-12, 0.0);
ACO7 + NO3	= 1.000 NO2 + 1.000 HO2 + 1.994 XO2 + 1.000 ALD6	thermal(4.00E-12, 0.0);
KE3P + NO3	= 1.000 NO2 + 0.998 HO2 + 0.002 HCHO + 0.002 ACO2 + 0.998 MGLY	thermal(1.20E-12, 0.0);
KE4P + NO3	= 1.000 NO2 + 0.516 HO2 + 0.300 XO2 + 0.346 ALD2 + 0.446 ALD4 + 0.484 ACO2 + 0.138 KE3 + 0.070 MGLY	thermal(1.20E-12, 0.0);
KE5P + NO3	= 1.000 NO2 + 0.687 HO2 + 0.211 XO2 + 0.397 HCHO + 0.102 ALD2 + 0.081 ALD3 + 0.233 ALD4 + 0.006 ALDI + 0.119 ACO2 + 0.111 ACO3 + 0.015 ACOI + 0.007 ACO5 + 0.034 KE3P + 0.002 KE4P + 0.024 KE5P + 0.130 ALD5 + 0.067 KE3 + 0.032 KE4 + 0.312 KE5 + 0.012 MGLY	thermal(1.20E-12, 0.0);
KE6P + NO3	= 1.000 NO2 + 0.781 HO2 + 0.205 XO2 + 0.233 HCHO + 0.316 ALD2 + 0.076 ALD3 + 0.381 ALD4 + 0.080 ACO2 + 0.076 ACO3 + 0.028 ACO4 + 0.034 ACO5 + 0.228 ALD5 + 0.063 ALD6 + 0.078 KE3 + 0.031 KE5 + 0.152 KE6 + 0.008 MGLY	thermal(1.20E-12, 0.0);
KE7P + NO3	= 1.000 NO2 + 0.819 HO2 + 0.186 XO2 + 0.186 HCHO + 0.306 ALD2 + 0.238 ALD3 + 0.213 ALD4 + 0.033 ACO2 + 0.044 ACO3 + 0.034 ACO4 + 0.070 ACO5 + 0.303 ALD5 + 0.186 ALD6 + 0.040 ALD7 + 0.149 KE7 + 0.004 MGLY	thermal(1.20E-12, 0.0);
KE8P + NO3	= 1.000 NO2 + 0.782 HO2 + 0.405 XO2 + 0.027 HCHO + 0.034 ALD2 + 0.039 ALD3 + 0.057 ALD4 + 0.004 ACO2 + 0.005 ACO3 + 0.004 ACO4 + 0.025 ACO5 + 0.053 ACO6 + 0.036 ACO7 + 0.003 KE5P + 0.035 KE6P + 0.053 KE7P + 0.079 ALD5 + 0.132 ALD6 + 0.250 ALD7 + 0.028 KE6 + 0.064 KE7 + 0.470 KE8	thermal(1.20E-12, 0.0);
TCO3 + NO3	= 1.000 NO2 + 1.000 HCHO + 1.000 ACO2	thermal(4.00E-12, 0.0);
XO2N + NO3	= 0.778 HO2 + 0.027 CO + 0.081 XO2 + 0.011 HCHO + 0.038 ALD2 + 0.423 ALD3 + 0.132 ALD4 + 0.011 ACO2 + 0.005 GLY + 0.045 ACO5 + 0.147 ACO6 + 0.006 KE5P + 0.137 ALD5 + 0.181 ALD6 + 0.001 ALD7 + 0.251 KE3 + 0.052 KE4 + 0.016 KE6 + 0.175 MGLY + 0.001 ORA2	thermal(1.20E-12, 0.0);
XO2 + HO2	=	thermal(1.66E-13,-1300.0);
OLNN + HO2	= 1.000 ONIT	thermal(1.66E-13,-1300.0);
OLND + HO2	= 1.000 ONIT	thermal(1.66E-13,-1300.0);
MO2 + HO2	= 1.000 OP1	thermal(3.80E-13, -800.0);
ETHP + HO2	= 1.000 OP2	thermal(7.50E-13, -700.0);
HC3P + HO2	= 1.000 OP2	thermal(1.66E-13,-1298.0);
HC5P + HO2	= 1.000 OP2	thermal(1.67E-13,-1300.1);
HC8P + HO2	= 1.000 OP2	thermal(1.69E-13,-1297.5);
ETEP + HO2	= 1.000 OP2	thermal(1.27E-13,-1300.0);
OLTP + HO2	= 1.000 OP2	thermal(1.66E-13,-1300.0);
OLIP + HO2	= 1.000 OP2	thermal(1.66E-13,-1300.0);
ISOP + HO2	= 1.000 OP2	thermal(1.66E-13,-1300.0);
APIP + HO2	= 1.000 OP2	thermal(1.66E-13,-1300.0);
LIMP + HO2	= 1.000 OP2	thermal(1.66E-13,-1300.0);
ACO2 + HO2	= 1.000 PAA	thermal(1.15E-12, -550.0);
ACO3 + HO2	= 1.000 OP2	thermal(1.15E-12, -550.0);
ACO4 + HO2	= 1.000 OP2	thermal(1.15E-12, -550.0);
ACOI + HO2	= 1.000 OP2	thermal(1.15E-12, -550.0);
ACO5 + HO2	= 1.000 OP2	thermal(1.15E-12, -550.0);
ACO6 + HO2	= 1.000 OP2	thermal(1.15E-12, -550.0);
ACO7 + HO2	= 1.000 OP2	thermal(1.15E-12, -550.0);
KE3P + HO2	= 1.000 OP2	thermal(1.15E-13,-1300.0);
KE4P + HO2	= 1.000 OP2	thermal(1.66E-13,-1300.0);
KE5P + HO2	= 1.000 OP2	thermal(1.66E-13,-1300.0);
KE6P + HO2	= 1.000 OP2	thermal(1.66E-13,-1300.0);
KE7P + HO2	= 1.000 OP2	thermal(1.66E-13,-1300.0);
KE8P + HO2	= 1.000 OP2	thermal(1.66E-13,-1300.0);
TCO3 + HO2	= 1.000 OP2	thermal(1.15E-12, -550.0);
XO2N + HO2	= 1.000 OP2	thermal(1.66E-13,-1300.0);
ACO2 + HO2	= 1.000 O3 + 1.000 ORA2	thermal(3.86E-16,-2640.0);
ACO3 + HO2	= 1.000 O3 + 1.000 ORA2	thermal(3.86E-16,-2640.0);
ACO4 + HO2	= 1.000 O3 + 1.000 ORA2	thermal(3.86E-16,-2640.0);
ACOI + HO2	= 1.000 O3 + 1.000 ORA2	thermal(3.86E-16,-2640.0);
ACO5 + HO2	= 1.000 O3 + 1.000 ORA2	thermal(3.86E-16,-2640.0);
ACO6 + HO2	= 1.000 O3 + 0.670 ALD6 + 0.330 ORA2	thermal(3.86E-16,-2640.0);

ACO7 + HO2 = 1.000 O3 + 1.000 ORA2 thermal(3.86E-16,-2640.0);

TCO3 + HO2 = 1.000 O3 + 1.000 OLT thermal(3.86E-16,-2640.0);

XO2 + MO2 = 1.000 HO2 + 1.000 HCHO thermal(3.87E-14,-1092.8);

OLNN + MO2 = 1.000 HO2 + 0.750 HCHO + 0.484 MACR + 0.516 ONIT thermal(4.89E-14,-1074.3);

OLND + MO2 = 0.424 NO2 + 0.529 HO2 + 0.029 XO2 + 0.961 HCHO + 0.189 ALD2 + 0.101 ALD3 + 0.065 ALD4 + 0.001 ALDI + 0.046 ACO2 + 0.001 ACO5 + 0.025 MACR + 0.576 ONIT + 0.028 ALD5 + 0.063 ALD6 + 0.062 KE3 + 0.038 KE5 + 0.002 KE6 + 0.015 MGLY + 0.009 OLT thermal(4.80E-14, -784.7);

2 MO2 = 0.668 HO2 + 1.334 HCHO thermal(9.10E-14, -416.0);

ETHP + MO2 = 1.000 HO2 + 0.750 HCHO + 0.750 ALD2 thermal(1.18E-13, -158.0);

HC3P + MO2 = 0.982 HO2 + 0.087 XO2 + 0.863 HCHO + 0.254 ALD2 + 0.021 ALD3 + 0.193 ALD4 + 0.066 ALDI + 0.009 ACO3 + 0.002 MO2 + 0.165 GLY + 0.005 ACO5 + 0.002 KE4P + 0.011 ALD6 + 0.004 KE3 + 0.010 KE4 + 0.012 MGLY thermal(2.58E-14, -837.8);

HC5P + MO2 = 0.993 HO2 + 0.297 XO2 + 0.813 HCHO + 0.075 ALD2 + 0.046 ALD3 + 0.156 ALD4 + 0.002 ALDI + 0.007 MO2 + 0.145 ALD5 + 0.058 ALD6 + 0.010 KE3 + 0.022 KE4 + 0.065 KE5 + 0.058 KE6 + 0.008 KE8 + 0.010 MGLY thermal(2.87E-14, -828.4);

HC8P + MO2 = 0.988 HO2 + 0.428 XO2 + 0.756 HCHO + 0.006 ALD2 + 0.009 ALD3 + 0.007 ALD4 + 0.001 ALDI + 0.003 ACO2 + 0.002 MO2 + 0.006 ACO5 + 0.042 ALD5 + 0.053 ALD6 + 0.150 ALD7 + 0.003 KE3 + 0.001 KE4 + 0.005 KE5 + 0.016 KE6 + 0.093 KE7 + 0.181 KE8 + 0.005 MGLY thermal(1.76E-14, -910.4);

ETEP + MO2 = 1.000 HO2 + 1.550 HCHO + 0.350 ALD2 thermal(1.71E-13, -708.0);

OLTP + MO2 = 0.980 HO2 + 0.001 XO2 + 1.230 HCHO + 0.232 ALD2 + 0.138 ALD3 + 0.107 ALD4 + 0.006 ALDI + 0.020 ACO2 + 0.017 HKET + 0.079 ALD5 + 0.018 ALD6 + 0.075 KE4 + 0.020 KE5 + 0.014 KE6 + 0.101 MGLY thermal(1.34E-13, -722.3);

OLIP + MO2 = 1.000 HO2 + 0.755 HCHO + 0.369 ALD2 + 0.158 ALD3 + 0.093 ALD4 + 0.027 ALD5 + 0.131 ALD6 + 0.063 KE3 + 0.059 KE4 + 0.046 KE5 + 0.063 KE6 + 0.079 KE8 thermal(5.15E-14, -866.1);

ISOP + MO2 = 1.000 HO2 + 0.012 XO2 + 1.104 HCHO + 0.543 MACR + 0.074 OLI + 0.383 OLT thermal(1.02E-13, -884.2);

APIP + MO2 = 1.000 HO2 + 0.783 HCHO + 0.500 ALD7 + 0.217 KE8 thermal(5.81E-14, -708.0);

LIMP + MO2 = 1.000 HO2 + 0.004 XO2 + 1.065 HCHO + 0.345 MACR + 0.446 OLI + 0.209 OLT thermal(7.39E-14, -708.0);

ACO2 + MO2 = 0.858 HO2 + 1.000 HCHO + 0.858 MO2 + 0.142 ORA2 thermal(8.60E-12, 0.0);

ACO3 + MO2 = 0.982 HO2 + 0.500 XO2 + 1.000 HCHO + 0.482 ALD2 + 0.018 MO2 + 0.018 KE3 + 0.500 ORA2 thermal(1.00E-11, 0.0);

ACO4 + MO2 = 0.951 HO2 + 0.509 XO2 + 1.004 HCHO + 0.003 ALD2 + 0.447 ALD3 + 0.049 KE3P + 0.501 ORA2 thermal(1.00E-11, 0.0);

ACOI + MO2 = 0.999 HO2 + 0.500 XO2 + 1.000 HCHO + 0.001 ALD2 + 0.001 MO2 + 0.499 KE3 + 0.500 ORA2 thermal(1.00E-11, 0.0);

ACO5 + MO2 = 0.999 HO2 + 0.868 XO2 + 1.160 HCHO + 0.339 ALD4 + 0.001 MO2 + 0.118 KE3 + 0.101 KE5 + 0.500 ORA2 thermal(1.00E-11, 0.0);

ACO6 + MO2 = 1.000 HO2 + 0.937 XO2 + 1.001 HCHO + 0.001 ALD2 + 0.001 ALD3 + 0.001 ALD4 + 0.386 ALD5 + 0.335 ALD6 + 0.001 KE3 + 0.112 KE6 + 0.165 ORA2 thermal(1.00E-11, 0.0);

ACO7 + MO2 = 1.000 HO2 + 0.997 XO2 + 1.000 HCHO + 0.500 ALD6 + 0.500 ORA2 thermal(1.00E-11, 0.0);

KE3P + MO2 = 0.999 HO2 + 0.751 HCHO + 0.001 ACO2 + 0.250 HKET + 0.749 MGLY thermal(3.53E-13, -708.0);

KE4P + MO2 = 0.930 HO2 + 0.251 XO2 + 0.753 HCHO + 0.063 ALD2 + 0.466 ALD4 + 0.070 ACO2 + 0.006 KE3 + 0.285 KE4 + 0.179 MGLY thermal(2.98E-14,-1047.4);

KE5P + MO2 = 0.883 HO2 + 0.187 XO2 + 0.912 HCHO + 0.057 ALD2 + 0.049 ALD3 + 0.141 ALD4 + 0.005 ALDI + 0.057 ACO2 + 0.046 ACO3 + 0.013 ACOI + 0.001 ACO5 + 0.001 KE3P + 0.282 ALD5 + 0.003 KE3 + 0.002 KE4 + 0.421 KE5 + 0.038 MGLY thermal(3.64E-14, -928.0);

KE6P + MO2 = 0.899 HO2 + 0.074 XO2 + 0.886 HCHO + 0.168 ALD2 + 0.040 ALD3 + 0.205 ALD4 + 0.027 ACO2 + 0.040 ACO3 + 0.015 ACO4 + 0.018 ACO5 + 0.128 ALD5 + 0.103 ALD6 + 0.045 KE3 + 0.001 KE5 + 0.474 KE6 + 0.014 MGLY thermal(8.79E-14, -812.4);

KE7P + MO2 = 0.902 HO2 + 0.051 XO2 + 0.856 HCHO + 0.166 ALD2 + 0.129 ALD3 + 0.115 ALD4 + 0.018 ACO2 + 0.024 ACO3 + 0.019 ACO4 + 0.038 ACO5 + 0.164 ALD5 + 0.106 ALD6 + 0.065 ALD7 + 0.487 KE7 + 0.007 MGLY thermal(1.15E-13, -753.1);

KE8P + MO2 = 0.869 HO2 + 0.077 XO2 + 0.787 HCHO + 0.040 ALD2 + 0.048 ALD3 + 0.071 ALD4 + 0.005 ACO2 + 0.006 ACO3 + 0.005 ACO4 + 0.030 ACO5 + 0.056 ACO6 + 0.023 ACO7 + 0.001 KE5P + 0.003 KE6P + 0.002 KE7P + 0.089 ALD5 + 0.104 ALD6 + 0.265 ALD7 + 0.002 KE6 + 0.006 KE7 + 0.560 KE8 + 0.002 MGLY thermal(4.43E-14, -786.3);

TCO3 + MO2 = 0.500 HO2 + 1.500 HCHO + 0.500 ACO2 + 0.500 OLT thermal(1.00E-11, 0.0);

XO2N + MO2 = 1.000 HO2 + 1.000 HCHO thermal(6.29E-14, -747.7);

XO2 + ACO2 = 1.000 MO2 thermal(6.82E-13, -803.3);

OLNN + ACO2 = 0.500 HO2 + 0.500 MO2 + 0.605 MACR + 0.395 ONIT + 0.500 ORA2 thermal(8.21E-13, -821.2);

OLND + ACO2 = 0.579 NO2 + 0.017 HO2 + 0.017 XO2 + 0.278 HCHO + 0.248 ALD2 + 0.092 ALD3 + 0.059 ALD4 + 0.001 ALDI + 0.066 ACO2 + 0.674 MO2 + 0.012 ACO5 + 0.019 MACR + 0.421 ONIT + 0.016 ALD5 + 0.029 ALD6 + 0.001 ALD7 + 0.188 KE3 + 0.064 KE5 + 0.019 KE6 + 0.005 MGLY + 0.119 OLT + 0.326 ORA2 thermal(6.22E-12, -148.9);

ETHP + ACO2 = 0.500 HO2 + 1.000 ALD2 + 0.500 MO2 + 0.500 ORA2 thermal(1.00E-11, 0.0);

HC3P + ACO2 = 0.424 HO2 + 0.054 XO2 + 0.031 HCHO + 0.129 ALD2 + 0.016 ALD3 + 0.085 ALD4 + 0.031 ALDI + 0.003 ACO3 + 0.696 MO2 + 0.062 GLY + 0.002 ACO5 + 0.016 KE4P + 0.004 ALD6 + 0.159 KE3 + 0.496 KE4 + 0.003 MGLY + 0.430 ORA2 thermal(5.18E-12, -204.8);

HC5P + ACO2 = 0.636 HO2 + 0.484 XO2 + 0.013 HCHO + 0.225 ALD2 + 0.055 ALD3 + 0.062 ALD4 + 0.004 ALDI + 0.652 MO2 + 0.087 ALD5 + 0.021 ALD6 + 0.274 KE3 + 0.104 KE4 + 0.207 KE5 + 0.157 KE6 + 0.018 KE8 + 0.003 MGLY + 0.356 ORA2 thermal(5.98E-12, -170.3);

HC8P + ACO2 = 0.592 HO2 + 0.651 XO2 + 0.001 HCHO + 0.031 ALD2 + 0.011 ALD3 + 0.010 ALD4 + 0.011 ALDI + 0.001 ACO2 + 0.598 MO2 + 0.001 ACO5 + 0.032 ALD5 + 0.056 ALD6 + 0.101 ALD7 + 0.043 KE3 + 0.014 KE4 + 0.024 KE5 + 0.046 KE6 + 0.199 KE7 + 0.436 KE8 + 0.001 MGLY + 0.404 ORA2 thermal(7.63E-12, -88.5);

ETEP + ACO2 = 0.500 HO2 + 0.800 HCHO + 0.600 ALD2 + 0.500 MO2 + 0.500 ORA2 thermal(9.49E-13, -765.0);

OLTP + ACO2 = 0.441 HO2 + 0.001 XO2 + 0.440 HCHO + 0.291 ALD2 + 0.157 ALD3 + 0.116 ALD4 + 0.005 ALDI + 0.066 ACO2 + 0.511 MO2 + 0.123 HKET + 0.004 ACO5 + 0.065 ALD5 + 0.021 ALD6 + 0.096 KE4 + 0.041 KE5 + 0.023 KE6 + 0.060 MGLY + 0.489 ORA2 thermal(4.61E-12, -292.5);

OLIP + ACO2 = 0.590 HO2 + 0.001 XO2 + 0.442 ALD2 + 0.170 ALD3 + 0.093 ALD4 + 0.590 MO2 + 0.028 ALD5 + 0.086 ALD6 + 0.222 KE3 + 0.124 KE4 + 0.091 KE5 + 0.102 KE6 + 0.115 KE8 + 0.410 ORA2 thermal(4.23E-12, -256.3);

ISOP + ACO2 = 0.578 HO2 + 0.012 XO2 + 0.432 HCHO + 0.578 MO2 + 0.660 MACR + 0.340 OLT + 0.422 ORA2 thermal(1.98E-12, -572.4);

APIP + ACO2 = 0.821 HO2 + 0.821 MO2 + 0.821 ALD7 + 0.179 KE8 + 0.179 ORA2 thermal(3.76E-12, -295.6);

LIMP + ACO2 = 0.818 HO2 + 0.002 XO2 + 0.409 HCHO + 0.818 MO2 + 0.502 MACR + 0.410 OLI + 0.089 OLT + 0.182 ORA2 thermal(4.69E-12, -250.8);

2 ACO2 = 2.000 MO2 thermal(2.80E-12, -530.0);

ACO3 + ACO2 = 0.964 HO2 + 1.000 XO2 + 0.964 ALD2 + 1.036 MO2 + 0.036 KE3 thermal(2.87E-12, -530.0);

ACO4 + ACO2 = 0.901 HO2 + 1.017 XO2 + 0.007 HCHO + 0.006 ALD2 + 0.894 ALD3 + 1.000 MO2 + 0.099 KE3P + 0.002 ORA2 thermal(2.87E-12, -530.0);

ACOI + ACO2 = 0.999 HO2 + 1.000 XO2 + 0.001 ALD2 + 1.001 MO2 + 0.999 KE3 thermal(2.87E-12, -530.0);

ACO5 + ACO2 = 0.999 HO2 + 1.735 XO2 + 0.320 HCHO + 0.679 ALD4 + 1.001 MO2 + 0.237 KE3 + 0.203 KE5 thermal(2.87E-12, -530.0);

ACO6 + ACO2 = 1.000 HO2 + 1.873 XO2 + 0.003 HCHO + 0.002 ALD2 + 0.002 ALD3 + 0.002 ALD4 + 1.000 MO2 + 0.771 ALD5 + 0.002 KE3 + 0.224 KE6 thermal(2.87E-12, -530.0);

ACO7 + ACO2 = 1.000 HO2 + 1.994 XO2 + 1.000 MO2 + 1.000 ALD6 thermal(2.87E-12, -530.0);

KE3P + ACO2 = 0.499 HO2 + 0.001 HCHO + 0.001 ACO2 + 0.500 MO2 + 0.999 MGLY + 0.500 ORA2 thermal(3.84E-13, -765.0);

KE4P + ACO2 = 0.277 HO2 + 0.161 XO2 + 0.159 ALD2 + 0.448 ALD4 + 0.286 ACO2 + 0.564 MO2 + 0.127 KE3 + 0.159 KE4 + 0.107 MGLY + 0.436 ORA2 thermal(2.98E-12, -386.0);

KE5P + ACO2 = 0.431 HO2 + 0.127 XO2 + 0.261 HCHO + 0.047 ALD2 + 0.038 ALD3 + 0.108 ALD4 + 0.003 ALDI + 0.070 ACO2 + 0.066 ACO3 + 0.007 ACOI + 0.634 MO2 + 0.007 ACO5 + 0.029 KE3P + 0.001 KE4P + 0.023 KE5P + 0.184 ALD5 + 0.062 KE3 + 0.030 KE4 + 0.486 KE5 + 0.019 MGLY + 0.366 ORA2 thermal(5.32E-12, -210.2);

KE6P + ACO2 = 0.397 HO2 + 0.115 XO2 + 0.115 HCHO + 0.149 ALD2 + 0.036 ALD3 + 0.181 ALD4 + 0.052 ACO2 + 0.036 ACO3 + 0.013 ACO4 + 0.515 MO2 + 0.016 ACO5 + 0.110 ALD5 + 0.111 ALD6 + 0.038 KE3 + 0.029 KE5 + 0.491 KE6 + 0.012 MGLY + 0.485 ORA2 thermal(1.61E-12, -560.7);

KE7P + ACO2 = 0.412 HO2 + 0.098 XO2 + 0.093 HCHO + 0.149 ALD2 + 0.116 ALD3 + 0.104 ALD4 + 0.016 ACO2 + 0.021 ACO3 + 0.017 ACO4 + 0.500 MO2 + 0.034 ACO5 + 0.148 ALD5 + 0.093 ALD6 + 0.069 ALD7 + 0.529 KE7 + 0.006 MGLY + 0.500 ORA2 thermal(1.19E-12, -653.9);

KE8P + ACO2 = 0.431 HO2 + 0.257 XO2 + 0.014 HCHO + 0.017 ALD2 + 0.020 ALD3 + 0.029 ALD4 + 0.002 ACO2 + 0.002 ACO3 + 0.002 ACO4 + 0.584 MO2 + 0.012 ACO5 + 0.031 ACO6 + 0.027 ACO7 + 0.002 KE5P + 0.027 KE6P + 0.047 KE7P + 0.040 ALD5 + 0.075 ALD6 + 0.180 ALD7 + 0.027 KE6 + 0.062 KE7 + 0.627 KE8 + 0.001 MGLY + 0.416 ORA2 thermal(4.41E-12, -251.9);

TCO3 + ACO2 = 1.000 HCHO + 1.000 ACO2 + 1.000 MO2 thermal(2.87E-12, -530.0);

XO2N + ACO2 = 1.000 MO2 thermal(3.85E-12, -294.6);

2 OLNN = 1.000 HO2 + 0.842 MACR + 1.158 ONIT thermal(3.19E-14,-1331.0);

OLND + OLNN = 0.397 NO2 + 0.526 HO2 + 0.026 XO2 + 0.179 HCHO + 0.219 ALD2 + 0.096 ALD3 + 0.051 ALD4 + 0.001 ALDI + 0.076 ACO2 + 0.001 ACO5 + 0.511 MACR + 1.120 ONIT + 0.026 ALD5 + 0.048 ALD6 + 0.057 KE3 + 0.031 KE5 + 0.002 KE6 + 0.012 MGLY + 0.009 OLT thermal(4.01E-14,-1029.6);

ACO3 + OLNN = 0.982 HO2 + 0.500 XO2 + 0.482 ALD2 + 0.018 MO2 + 0.605 MACR + 0.395 ONIT + 0.018 KE3 + 0.500 ORA2 thermal(3.09E-12, -397.3);

ACO4 + OLNN = 0.951 HO2 + 0.509 XO2 + 0.004 HCHO + 0.003 ALD2 + 0.447 ALD3 + 0.049 KE3P + 0.605 MACR + 0.395 ONIT + 0.501 ORA2 thermal(3.09E-12, -397.3);

ACOI + OLNN = 0.999 HO2 + 0.500 XO2 + 0.001 ALD2 + 0.001 MO2 + 0.605 MACR + 0.395 ONIT + 0.499 KE3 + 0.500 ORA2 thermal(3.09E-12, -397.3);

ACO5 + OLNN = 0.999 HO2 + 0.868 XO2 + 0.160 HCHO + 0.339 ALD4 + 0.001 MO2 + 0.605 MACR + 0.395 ONIT + 0.118 KE3 + 0.101 KE5 + 0.500 ORA2 thermal(3.09E-12, -397.3);

ACO6 + OLNN = 1.000 HO2 + 0.937 XO2 + 0.001 HCHO + 0.001 ALD2 + 0.001 ALD3 + 0.001 ALD4 + 0.605 MACR + 0.395 ONIT + 0.386 ALD5 + 0.335 ALD6 + 0.001 KE3 + 0.112 KE6 + 0.165 ORA2 thermal(3.09E-12, -397.3);

ACO7 + OLNN = 1.000 HO2 + 0.997 XO2 + 0.605 MACR + 0.395 ONIT + 0.500 ALD6 + 0.500 ORA2 thermal(3.09E-12, -397.4);

KE3P + OLNN = 0.999 HO2 + 0.001 HCHO + 0.001 ACO2 + 0.250 HKET + 0.487 MACR + 0.513 ONIT + 0.749 MGLY thermal(1.73E-13,-1000.0);

KE4P + OLNN = 0.864 HO2 + 0.212 XO2 + 0.129 ALD2 + 0.395 ALD4 + 0.136 ACO2 + 0.463 MACR + 0.537 ONIT + 0.007 KE3 + 0.318 KE4 + 0.151 MGLY thermal(3.27E-14,-1201.4);

KE5P + OLNN = 0.863 HO2 + 0.149 XO2 + 0.179 HCHO + 0.068 ALD2 + 0.058 ALD3 + 0.165 ALD4 + 0.005 ALDI + 0.065 ACO2 + 0.058 ACO3 + 0.011 ACOI + 0.001 ACO5 + 0.001 KE3P + 0.465 MACR + 0.535 ONIT + 0.214 ALD5 + 0.004 KE3 + 0.003 KE4 + 0.449 KE5 + 0.035 MGLY thermal(3.14E-14,-1133.5);

KE6P + OLNN = 0.898 HO2 + 0.073 XO2 + 0.137 HCHO + 0.169 ALD2 + 0.041 ALD3 + 0.205 ALD4 + 0.028 ACO2 + 0.041 ACO3 + 0.015 ACO4 + 0.018 ACO5 + 0.447 MACR + 0.553 ONIT + 0.129 ALD5 + 0.096 ALD6 + 0.043 KE3 + 0.002 KE5 + 0.480 KE6 + 0.015 MGLY thermal(4.42E-14,-1149.2);

KE7P + OLNN = 0.903 HO2 + 0.055 XO2 + 0.106 HCHO + 0.164 ALD2 + 0.128 ALD3 + 0.114 ALD4 + 0.017 ACO2 + 0.024 ACO3 + 0.018 ACO4 + 0.038 ACO5 + 0.434 MACR + 0.566 ONIT + 0.162 ALD5 + 0.106 ALD6 + 0.063 ALD7 + 0.491 KE7 + 0.007 MGLY thermal(5.00E-14,-1130.3);

KE8P + OLNN = 0.874 HO2 + 0.089 XO2 + 0.033 HCHO + 0.038 ALD2 + 0.045 ALD3 + 0.066 ALD4 + 0.004 ACO2 + 0.005 ACO3 + 0.005 ACO4 + 0.029 ACO5 + 0.053 ACO6 + 0.022 ACO7 + 0.001 KE5P + 0.004 KE6P + 0.003 KE7P + 0.445 MACR + 0.555 ONIT + 0.084 ALD5 + 0.099 ALD6 + 0.247 ALD7 + 0.003 KE6 + 0.008 KE7 + 0.584 KE8 + 0.002 MGLY thermal(2.08E-14,-1154.0);

2 OLND = 0.810 NO2 + 0.050 HO2 + 0.050 XO2 + 0.384 HCHO + 0.421 ALD2 + 0.185 ALD3 + 0.107 ALD4 + 0.002 ALDI + 0.139 ACO2 + 0.002 ACO5 + 0.049 MACR + 1.190 ONIT + 0.051 ALD5 + 0.101 ALD6 + 0.113 KE3 + 0.074 KE5 + 0.004 KE6 + 0.030 MGLY + 0.018 OLT thermal(5.11E-14, -944.6);

ACO3 + OLND = 0.579 NO2 + 0.665 HO2 + 0.690 XO2 + 0.279 HCHO + 0.897 ALD2 + 0.092 ALD3 + 0.059 ALD4 + 0.001 ALDI + 0.066 ACO2 + 0.025 MO2 + 0.012 ACO5 + 0.019 MACR + 0.421 ONIT + 0.016 ALD5 + 0.029 ALD6 + 0.001 ALD7 + 0.212 KE3 + 0.064 KE5 + 0.019 KE6 + 0.005 MGLY + 0.119 OLT + 0.327 ORA2 thermal(4.01E-12, -313.7);

ACO4 + OLND = 0.579 NO2 + 0.623 HO2 + 0.701 XO2 + 0.284 HCHO + 0.251 ALD2 + 0.694 ALD3 + 0.059 ALD4 + 0.001 ALDI + 0.066 ACO2 + 0.012 ACO5 + 0.067 KE3P + 0.019 MACR + 0.421 ONIT + 0.016 ALD5 + 0.029 ALD6 + 0.001 ALD7 + 0.188 KE3 + 0.064 KE5 + 0.019 KE6 + 0.005 MGLY + 0.119 OLT + 0.328 ORA2 thermal(4.01E-12, -313.7);

ACOI + OLND = 0.579 NO2 + 0.689 HO2 + 0.690 XO2 + 0.279 HCHO + 0.249 ALD2 + 0.092 ALD3 + 0.059 ALD4 + 0.001 ALDI + 0.066 ACO2 + 0.001 MO2 + 0.012 ACO5 + 0.019 MACR + 0.421 ONIT + 0.016 ALD5 + 0.029 ALD6 + 0.001 ALD7 + 0.860 KE3 + 0.064 KE5 + 0.019 KE6 + 0.005 MGLY + 0.119 OLT + 0.327 ORA2 thermal(4.01E-12, -313.7);

ACO5 + OLND = 0.579 NO2 + 0.689 HO2 + 1.185 XO2 + 0.494 HCHO + 0.248 ALD2 + 0.092 ALD3 + 0.516 ALD4 + 0.001 ALDI + 0.066 ACO2 + 0.001 MO2 + 0.012 ACO5 + 0.019 MACR + 0.421 ONIT + 0.016 ALD5 + 0.029 ALD6 + 0.001 ALD7 + 0.347 KE3 + 0.201 KE5 + 0.019 KE6 + 0.005 MGLY + 0.119 OLT + 0.327 ORA2 thermal(4.01E-12, -313.7);

ACO6 + OLND = 0.579 NO2 + 0.690 HO2 + 1.278 XO2 + 0.280 HCHO + 0.249 ALD2 + 0.094 ALD3 + 0.060 ALD4 + 0.001 ALDI + 0.066 ACO2 + 0.012 ACO5 + 0.019 MACR + 0.421 ONIT + 0.535 ALD5 + 0.248 ALD6 + 0.001 ALD7 + 0.189 KE3 + 0.064 KE5 + 0.170 KE6 + 0.005 MGLY + 0.119 OLT + 0.108 ORA2 thermal(4.01E-12, -313.7);

ACO7 + OLND = 0.579 NO2 + 0.690 HO2 + 1.359 XO2 + 0.279 HCHO + 0.248 ALD2 + 0.092 ALD3 + 0.059 ALD4 + 0.001 ALDI + 0.066 ACO2 + 0.012 ACO5 + 0.019 MACR + 0.421 ONIT + 0.016 ALD5 + 0.702 ALD6 + 0.001 ALD7 + 0.188 KE3 + 0.064 KE5 + 0.019 KE6 + 0.005 MGLY + 0.119 OLT + 0.327 ORA2 thermal(4.01E-12, -313.7);

KE3P + OLND = 0.395 NO2 + 0.529 HO2 + 0.030 XO2 + 0.153 HCHO + 0.216 ALD2 + 0.104 ALD3 + 0.059 ALD4 + 0.001 ALDI + 0.075 ACO2 + 0.237 HKET + 0.001 ACO5 + 0.030 MACR + 0.605 ONIT + 0.027 ALD5 + 0.059 ALD6 + 0.062 KE3 + 0.020 KE5 + 0.002 KE6 + 0.769 MGLY + 0.008 OLT thermal(1.63E-13,-1000.0);

KE4P + OLND = 0.404 NO2 + 0.408 HO2 + 0.249 XO2 + 0.187 HCHO + 0.323 ALD2 + 0.095 ALD3 + 0.464 ALD4 + 0.001 ALDI + 0.188 ACO2 + 0.001 ACO5 + 0.026 MACR + 0.596 ONIT + 0.026 ALD5 + 0.051 ALD6 + 0.064 KE3 + 0.297 KE4 + 0.034 KE5 + 0.002 KE6 + 0.188 MGLY + 0.009 OLT thermal(3.91E-14,-1137.4);

KE5P + OLND	= 0.401 NO2 + 0.409 HO2 + 0.214 XO2 + 0.340 HCHO + 0.272 ALD2 + 0.140 ALD3 + 0.190 ALD4 + 0.006 ALDI + 0.129 ACO2 + 0.047 ACO3 + 0.011 ACOI + 0.002 ACO5 + 0.001 KE3P + 0.025 MACR + 0.599 ONIT + 0.313 ALD5 + 0.049 ALD6 + 0.059 KE3 + 0.003 KE4 + 0.454 KE5 + 0.002 KE6 + 0.054 MGLY + 0.009 OLT	thermal(4.01E-14,-1049.9);
KE6P + OLND	= 0.396 NO2 + 0.426 HO2 + 0.109 XO2 + 0.327 HCHO + 0.382 ALD2 + 0.127 ALD3 + 0.242 ALD4 + 0.001 ALDI + 0.107 ACO2 + 0.039 ACO3 + 0.014 ACO4 + 0.018 ACO5 + 0.025 MACR + 0.604 ONIT + 0.149 ALD5 + 0.163 ALD6 + 0.096 KE3 + 0.040 KE5 + 0.470 KE6 + 0.032 MGLY + 0.009 OLT	thermal(6.04E-14,-1047.4);
KE7P + OLND	= 0.396 NO2 + 0.427 HO2 + 0.083 XO2 + 0.300 HCHO + 0.383 ALD2 + 0.213 ALD3 + 0.157 ALD4 + 0.001 ALDI + 0.097 ACO2 + 0.023 ACO3 + 0.018 ACO4 + 0.038 ACO5 + 0.025 MACR + 0.604 ONIT + 0.184 ALD5 + 0.146 ALD6 + 0.077 ALD7 + 0.052 KE3 + 0.039 KE5 + 0.002 KE6 + 0.483 KE7 + 0.024 MGLY + 0.009 OLT	thermal(6.90E-14,-1028.4);
KE8P + OLND	= 0.398 NO2 + 0.400 HO2 + 0.114 XO2 + 0.224 HCHO + 0.256 ALD2 + 0.135 ALD3 + 0.113 ALD4 + 0.001 ALDI + 0.082 ACO2 + 0.005 ACO3 + 0.005 ACO4 + 0.028 ACO5 + 0.052 ACO6 + 0.022 ACO7 + 0.001 KE5P + 0.004 KE6P + 0.003 KE7P + 0.026 MACR + 0.602 ONIT + 0.107 ALD5 + 0.142 ALD6 + 0.262 ALD7 + 0.053 KE3 + 0.037 KE5 + 0.005 KE6 + 0.007 KE7 + 0.572 KE8 + 0.017 MGLY + 0.009 OLT	thermal(2.77E-14,-1060.2);
2 XO2	=	thermal(7.20E-15,-1705.2);
XO2N + XO2	=	thermal(1.49E-14,-1200.7);
2 XO2N	=	thermal(1.49E-14,-1200.7);
O3P + O2	= 1.000 O3	special("K = airc*6.e-34* (temp/300.)**(-2.3)");
O3P + O3	=	thermal(8.00E-12, 2060.0);
O1D + N2	= 1.000 O3P	thermal(1.80E-11, -110.0);
O1D + O2	= 1.000 O3P	thermal(3.20E-11, -70.0);
O1D + H2O	= 2.000 HO	thermal(2.20E-10, 0.0);
O3 + HO	= 1.000 HO2	thermal(1.60E-12, 940.0);
O3 + HO2	= 1.000 HO	thermal(1.10E-14, 500.0);
HO + HO2	=	thermal(4.80E-11, -250.0);
H2O2 + HO	= 1.000 HO2	thermal(2.90E-12, 160.0);
2 HO2	= 1.000 H2O2	special("K = 2.3d-13* exp(600./temp) + 1.7d-33* airc*exp(1000./temp)");
2 HO2 + H2O	= 1.000 H2O2	special("K = 3.22d-34* exp(2800./temp) + 2.38d-54 *airc*exp(3200./temp)");
O3P + NO	= 1.000 NO2	troe(9.E-32, 1.5, 3E-11, 0.);
O3P + NO2	= 1.000 NO	thermal(6.50E-12, -120.0);
O3P + NO2	= 1.000 NO3	troe(9.E-32, 2.0, 2.20E-11, 0.);
HO + NO	= 1.000 HONO	troe(7.E-31, 2.6, 1.50E-11, 0.5);
HO + NO2	= 1.000 HNO3	troe(2.60E-30, 3.2, 2.40E-11, 1.3);
HO + NO3	= 1.000 NO2 + 1.000 HO2	thermal(2.20E-11, 0.0);
HO2 + NO	= 1.000 NO2 + 1.000 HO	thermal(3.70E-12, -250.0);
HO2 + NO2	= 1.000 HNO4	troe(1.80E-31, 3.2, 4.70E-12, 1.4);
HNO4	= 1.000 HO2 + 1.000 NO2	troe-equil(1.80E-31, 3.2, 4.70E-12, 1.4, 4.76e26, 10900.);
HO2 + NO3	= 0.300 HNO3 + 0.700 NO2 + 0.700 HO	thermal(3.50E-12, 0.0);
HO + HONO	= 1.000 NO2	thermal(1.80E-11, 390.0);
HO + HNO3	= 1.000 NO3	special("k1=7.2d-15*exp(785. /temp);k2=4.1d-16* exp(1440./temp); k3=1.9d-33* exp(725./temp)*airc; K = k1+k3/(1.+k3/k2)");
HO + HNO4	= 1.000 NO2	thermal(1.30E-12, -380.0);
O3 + NO	= 1.000 NO2	thermal(2.00E-12, 1400.0);
O3 + NO2	= 1.000 NO3	thermal(1.20E-13, 2450.0);
2 NO + O2	= 2.000 NO2	thermal(3.30E-39, -530.0);
NO3 + NO	= 2.000 NO2	thermal(1.50E-11, -170.0);
NO3 + NO2	= 1.000 NO + 1.000 NO2	thermal(4.50E-14, 1260.0);
NO3 + NO2	= 1.000 N2O5	troe(2.20E-30, 3.9, 1.50E-12, 0.7);
N2O5	= 1.000 NO2 + 1.000 NO3	troe-equil(2.20E-30, 3.9, 1.50E-12, 0.7, 3.7E26, 11000.);
2 NO3	= 2.000 NO2	thermal(8.50E-13, 2450.0);
HO + H2	= 1.000 HO2	thermal(5.50E-12, 2000.0);

HO + SO2	= 1.000 SULF + 1.000 HO2	troe(3E-31, 3.3, 1.50E-12, 0.0);
CO + HO	= 1.000 HO2	special("K=1.5d-13*(1.+2.439 e-20*airc)");
TOL + HO	= 0.900 ADDT + 0.100 XO2 + 0.100 HO2	thermal(1.81E-12, -355.0);
XYL + HO	= 0.900 ADDX + 0.100 XO2 + 0.100 HO2	thermal(7.30E-12, -355.0);
CSL + HO	= 0.850 ADDC + 0.100 PHO + 0.050 HO2 + 0.050 XO2	thermal(6.00E-11, 0.0);
HO + DCB	= 0.500 TCO3 + 0.500 HO2 + 0.500 XO2 + 0.350 UDD + 0.150 GLY + 0.150 MGLY	thermal(2.80E-11, -175.0);
HO + UDD	= 0.880 ALD5 + 0.120 KE3 + 1.000 HO2	thermal(2.70E-10, 0.0);
DCB + NO3	= 0.500 TCO3 + 0.500 HO2 + 0.500 XO2 + 0.250 GLY + 0.250 ALD5 + 0.500 NO2 + 0.030 KE3 + 0.250 MGLY + 0.500 HNO3	thermal(2.87E-13, 1000.0);
CSL + NO3	= 1.000 HNO3 + 1.000 PHO	thermal(2.20E-11, 0.0);
DCB + O3	= 0.210 HO + 0.290 HO2 + 0.660 CO + 0.500 GLY + 0.620 MGLY + 0.280 ACO2 + 0.160 ALD5 + 0.110 PAA + 0.110 ORA1 + 0.210 ORA2	thermal(2.00E-18, 0.0);
PHO + NO2	= 0.100 CSL + 1.000 ONIT	thermal(2.00E-11, 0.0);
PHO + HO2	= 1.000 CSL	thermal(1.00E-11, 0.0);
ADDT + NO2	= 1.000 CSL + 1.000 HONO	thermal(3.60E-11, 0.0);
ADDT + O2	= 0.980 TOLP + 0.020 CSL + 0.020 HO2	thermal(1.66E-17,-1044.0);
ADDT + O3	= 1.000 CSL + 1.000 HO	thermal(5.00E-11, 0.0);
ADDX + NO2	= 1.000 CSL + 1.000 HONO	thermal(3.60E-11, 0.0);
ADDX + O2	= 0.980 XYLP + 0.020 CSL + 0.020 HO2	thermal(1.66E-17,-1044.0);
ADDX + O3	= 1.000 CSL + 1.000 HO	thermal(1.00E-11, 0.0);
ADDC + NO2	= 1.000 CSL + 1.000 HONO	thermal(3.60E-11, 0.0);
ADDC + O2	= 0.980 CSLP + 0.020 CSL + 0.020 HO2	thermal(1.66E-17,-1044.0);
ADDC + O3	= 1.000 CSL + 1.000 HO	thermal(5.00E-11, 0.0);
TOLP + NO	= 0.950 NO2 + 0.950 HO2 + 1.200 GLY + 0.500 DCB + 0.050 ONIT + 0.650 MGLY	thermal(4.00E-12, 0.0);
XYLP + NO	= 0.950 NO2 + 0.950 HO2 + 0.350 GLY + 0.950 DCB + 0.050 ONIT + 0.600 MGLY	thermal(4.00E-12, 0.0);
CSLP + NO	= 1.000 GLY + 1.000 MGLY + 1.000 NO2 + 1.000 HO2	thermal(4.00E-12, 0.0);
TOLP + HO2	= 1.000 OP2	thermal(3.75E-13, -980.0);
XYLP + HO2	= 1.000 OP2	thermal(3.75E-13, -980.0);
CSLP + HO2	= 1.000 OP2	thermal(3.75E-13, -980.0);
TOLP + MO2	= 1.000 HCHO + 1.000 HO2 + 0.650 GLY + 1.000 DCB + 0.350 MGLY	thermal(3.56E-14, -708.0);
XYLP + MO2	= 1.000 HCHO + 1.000 HO2 + 0.370 GLY + 1.000 DCB + 0.630 MGLY	thermal(3.56E-14, -708.0);
CSLP + MO2	= 1.000 GLY + 1.000 MGLY + 2.000 HO2 + 1.000 HCHO	thermal(3.56E-14, -708.0);
TOLP + ACO2	= 1.000 MO2 + 1.000 HO2 + 1.000 DCB + 0.650 GLY + 0.350 MGLY	thermal(7.40E-13, -765.0);
XYLP + ACO2	= 1.000 MO2 + 1.000 HO2 + 1.000 DCB + 0.370 GLY + 0.630 MGLY	thermal(7.40E-13, -765.0);
CSLP + ACO2	= 1.000 GLY + 1.000 MGLY + 1.000 HO2 + 1.000 MO2	thermal(7.40E-13, -765.0);
TOLP + NO3	= 1.000 NO2 + 1.000 HO2 + 0.500 DCB + 1.300 GLY + 0.700 MGLY	thermal(1.20E-12, 0.0);
XYLP + NO3	= 1.000 NO2 + 1.000 HO2 + 1.000 DCB + 0.740 GLY + 1.260 MGLY	thermal(1.20E-12, 0.0);
CSLP + NO3	= 1.000 GLY + 1.000 MGLY + 1.000 NO2 + 1.000 HO2	thermal(1.20E-12, 0.0);

Martin JUNIER
Swiss citizen
Born on 9th May 1971
Married, one child

Professional experience

since 1998	PhD student at the modelling group of the Soil and Air Pollution Laboratory (LPAS) of the Swiss Federal Institute of technology (EPFL). My tasks are the development and application of a 3D mesoscale air pollution model.

Education

1998	Degree in Environmental engineering, EPFL.
since 1998	Continuing education at EPFL: UNIX administration, C programming, Book-keeping, management and finance.

Computer knowledge

Operating systems	Very good user knowledge of UNIX (Solaris), MacOS (9 - X) and Windows.
Programming	Excellent skills in Fortran 77, shell programming, basic knowledge of C, HTML, CSS.

Languages

French	Mother tongue
English	Good oral and written skills
German	Good understanding

Spare time activities

Rowing	In charge of the training of adult beginners in Lausanne-Sports rowing club. Webmaster of the official site (membres.lycos.fr/lsaviron). Instructor for the University Sports.
Photography	Taking and printing pictures (film and digital, black and white and colour).

Publications

Junier M., Clappier A., Roulet Y.-A., van den Bergh H., Cuvelier C., Thunis P., 2001, Numerical Simulation of the links between Air Pollution, Aerosols and Solar Radiation. Proceedings from the EUROTRAC-2 symposium 2000, Springer-Verlag Berlin, Heidelberg.

Junier M., Kirchner F., Clappier A., van den Bergh H., 2004, The chemical mechanism generation program CHEMATA, part II: Comparison of four chemical mechanisms for mesoscale calculation of atmospheric pollution, *submitted to Atmospheric Environment.*

Martilli A., Roulet Y.-A., Junier M., Kirchner F., Rotach M., Clappier A., 2003, On the impact of urban surface exchange parameterisations on air quality simulations: the Athens case, Atmospheric Environment, Vol. 37, pp. 4217–4231.

Roulet Y.-A., Kirchner F., Junier M., Martilli A., Clappier A., Jiménez R., Calpini B., van den Bergh H., 2000, Modellierung des Auswirkungen einer Tunneleröffnung auf die Luftqualität im Kanton Obwalden, Project report, EPFL-LPAS Lausanne.

Sathya V., Russell A. G.,Perego S., Junier M., Clappier A., van den Bergh H., 2003, Photochemical grid model uncertainty estimates derived from Monte-Carlo analysis of a mesoscale meteorological model, *accepted in Atmospheric Environment.*

Sathya V., Russel A. G., Perego S., Maignan M., Junier M., Clappier A., van den Bergh H., Uncertainties in photochemical grid modelling of ozone, the impact of uncertainties in meteorological inputs. Proceedings of the 2nd international symposium on non CO_2 green house gases (NCGG-2).